

**Aus dem Institut für Klinische Neuroimmunologie
der Ludwig-Maximilians-Universität München
Direktoren: Prof. Dr. Hohlfeld, Prof. Dr. Kerschensteiner**

**Visualizing the stimulation of
encephalitogenic T cells
in Gut Associated Lymphoid Tissue as a
trigger of autoimmunity**

**Dissertation
zum Erwerb des Doktorgrades der Naturwissenschaften
an der Medizinischen Fakultät
der Ludwig-Maximilians-Universität München**

**vorgelegt von
Ping Fang
aus
Changchun, China
2018**

Mit Genehmigung der Medizinischen Fakultät der Ludwig-Maximilians-Universität München

Betreuer: Priv. Doz. Dr. Naoto Kawakami

Mitgutachter: **Prof. Dr. Svetlana Sirko**
Klinikum der Universität München, Physiologisches Institut

Prof. Dr. Rainer Haas
Klinikum der Universität München,
Max von Pettenkofer Institut für
Hygiene und Medizinische Mikrobiologie

Prof. Dr. Peter Nelson
Klinikum der Universität München,
München Medizinische Klinik und Poliklinik IV

Dekan: **Prof. Dr. med. dent. Reinhard HICKEL**

Tag der mündlichen Prüfung: 28.11.2018

Eidesstattliche Versicherung

Ping Fang

Name, Vorname

Ich erkläre hiermit an Eides statt,
dass ich die vorliegende Dissertation mit dem Thema

Visualizing the stimulation of encephalitogenic T cells in Gut Associated Lymphoid Tissue as a trigger of autoimmunity

selbständig verfasst, mich außer der angegebenen keiner weiteren Hilfsmittel bedient und alle Erkenntnisse, die aus dem Schrifttum ganz oder annähernd übernommen sind, als solche kenntlich gemacht und nach ihrer Herkunft unter Bezeichnung der Fundstelle einzeln nachgewiesen habe. Ich erkläre des Weiteren, dass die hier vorgelegte Dissertation nicht in gleicher oder in ähnlicher Form bei einer anderen Stelle zur Erlangung eines akademischen Grades eingereicht wurde.

München, 28.11.2018

Ort, Datum

Ping Fang

Unterschrift Doktorandin

TABLE OF CONTENTS

SUMMARY	1
ZUSAMMENFASSUNG	3
INTRODUCTION	5
1.1 Multiple Sclerosis	5
1.2 Experimental Autoimmune Encephalomyelitis.....	8
1.2.1 Spontaneous EAE Mouse Model.....	9
1.3 Intestinal Immune System and Encephalomyelitis	10
1.3.1 Gut Associated Lymphoid Tissue	10
1.3.2 Distribution of Lymphocytes in the Small Intestine	13
1.3.3 Intestinal Th17 Cells	14
1.3.4 CD44 ⁺ CD4 ⁺ T cells and Encephalomyelitis.....	15
1.3.5 Gut Microbiota and Encephalomyelitis	16
1.4 Calcium Dependent T cell Imaging.....	17
1.4.1 Calcium Fluctuation during T cell Activation	17
1.4.2 Twitch2b Calcium Sensor	18
1.4.3 NFAT-GFP Sensor	19
OBJECTIVES	21
MATERIAL AND METHODS	22
2.1 Material	22
2.2 Methods.....	27
RESULTS	36
3.1 Retroviral Transduction of T cells	36
3.2 MOG specific T cells in the GALT.....	39
3.3 Phenotypes of Encephalitogenic T Cells from the Mesenteric Lymph	51
3.4 The Influence of Microbiota on Encephalitogenic T Cells.....	56
3.5 The Mechanism of MOG Specific T cell Stimulation in Lamina Propria	60

3.6	Intravital Imaging of T cells in the Lamina Propria of the Colon.....	64
3.7	Transduction of Cultured B Cells with Activation Sensor	65
DISCUSSION		67
4.1	Calcium Signaling of MOG Specific T Cells in LP	67
4.2	Influence of Microbiota on T cell Activation and EAE Incidence	72
4.3	Phenotypes of T cells Emigrating from the GALT	73
REFERENCES.....		77
ABBREVIATIONS.....		87
CURRICULUM VITAE.....		90
ACKNOWLEDGMENTS		92

SUMMARY

Autoantigen-specific encephalitogenic T cells exist in the healthy immune repertoire. In case of CNS autoimmunity, such as multiple sclerosis (MS), cells penetrate into the central nervous system (CNS), where they get activated by local antigen presenting cells, and induce inflammation. However, the triggering mechanisms that provoke CNS infiltration of pre-existing autoreactive T cells are largely unknown.

Recent studies have shown evidence that microbiota induce proliferation of encephalitogenic T cells in gut associated lymphatic tissues (GALT) before CNS infiltration in the spontaneous experimental autoimmune encephalomyelitis (EAE), an animal model of MS. In this study, the activation and subsequent behaviour of encephalitogenic T cells in the GALT are investigated. Myelin oligodendrocyte glycoprotein (MOG) specific T cells from transgenic mice are retrovirally transduced with FRET-based calcium activation sensors and adoptively transferred to recipient mice. T cells in the lamina propria and Peyer's patches are imaged *in vivo* with two-photon microscopy and the calcium fluctuation is quantified to detect T cell activation. Moreover, migrating T cells in the efferent lymphatic vessels of GALT were analysed in order to elucidate phenotypic changes due to *in vivo* stimulation.

Intravital imaging reveals that encephalitogenic T cells, but not polyclonal T cells, display continuous calcium signaling in the lamina propria. In contrast, encephalitogenic T cells in the Peyer's patch show only brief calcium signaling. The continuous calcium signaling is diminished by administration of anti-MHC class II blocking antibody. This observation suggests that the calcium signaling of encephalitogenic T cells is mediated by antigen presenting cells. Additionally, the role of commensal microbiota is highlighted through the fact encephalitogenic T cells do not show continuous calcium signaling in germ free mice, which suggests the influence of microbiota.

The increased number of IL17A and IFN γ producing T cells were detected in efferent lymph from mesenteric lymph nodes, further suggests the stimulation of T cells in the GALT. This phenotype, in addition to the enhanced number of CD44⁺ encephalitogenic T cells, suggests

that microbiota induced stimulation in the GALT influences the migration of encephalitogenic T cells in CNS autoimmunity.

In summary, the following study reveals pre-existing encephalitogenic T cells are capable of being stimulated in the lamina propria of ileum. The stimulation is dependent upon an intact gut microbiota compartment and may enhance migration of encephalitogenic T cells.

ZUSAMMENFASSUNG

Autoantigen-spezifische enzephalitogene T-Zellen gehören zum Repertoire des gesunden Immunsystems. Bisherige Erkenntnisse legen nahe, dass diese Zellen ins Zentrale Nervensystem (ZNS) einwandern, wo sie von lokalen Antigen-präsentierenden Zellen aktiviert werden und Entzündungen auslösen, die in Autoimmunerkrankungen wie der Multiplen Sklerose (MS) resultieren. Dennoch ist der Mechanismus, wie die ZNS-Infiltration der bereits bestehenden autoreaktiven T-Zellen ausgelöst wird, weitgehend unbekannt. Neueste Studien zeigen mithilfe der spontanen experimentellen autoimmunen Enzephalomyelitis (EAE), einem Tiermodell für MS, dass Mikrobiota die Proliferation von enzephalitogenen T-Zellen im Darm-assoziierten lymphatischen Gewebe (GALT) auslösen und eine darauffolgende Einwanderung ins ZNS stattfindet.

In der vorliegenden Arbeit wurden das Verhalten und die Aktivierung von enzephalitogenen T-Zellen im GALT untersucht. Mithilfe eines FRET-basierten Calcium-sensitiven Proteins wurde die T-Zell-Aktivierung im Zwei-Photonen-Mikroskop beobachtet. MOG-spezifische T-Zellen von transgenen Mäusen wurden retroviral mit Aktivierungssensoren transduziert und in Empfänger-Mäuse injiziert. Die T-Zellen wurden in der Lamina Propria und in den Peyer-Plaques *in vivo* mikroskopiert und deren Calcium-Schwankungen ausgewertet. Des Weiteren wurden T-Zellen aus den efferenten lymphatischen Gefäßen des GALT analysiert, um phänotypische Veränderungen von auswandernden T-Zellen zu bestimmen.

Die Zwei-Photonen-Mikroskopie ergab, dass enzephalitogene, nicht jedoch polyklonale T-Zellen in der Lamina propria kontinuierliche Calcium-Signalgebung aufweisen. Im Gegensatz dazu zeigen T-Zellen in den Peyer-Plaques nur kurze Calcium-Signale. Die kontinuierlich hohen Calcium-Levels konnten durch die Verabreichung von MHC-II-blockierenden Antikörpern reduziert werden. Diese Beobachtung deutet darauf hin, dass die Calcium-Signalgebung durch Antigen-präsentierende Zellen ausgelöst wird. Dass die enzephalitogenen T-Zellen ebenfalls keine anhaltend erhöhten Calcium-Levels in keimfreien Mäusen zeigten, deutet auf den Einfluss der Mikrobiota hin.

Dass eine erhöhte Anzahl an IL17A- und IFN γ -prduzierenden T-Zellen in der efferenten Lymphe der mesenterischen Lymphknoten detektiert wurde, weist auf die Stimulation von T-Zellen im GALT hin. Zusammen mit der erhöhten Expression von CD44 an der Oberfläche von enzephalitogenen T-Zellen deuten diese Erkenntnisse darauf hin, dass die Auslösbarkeit der Migration von selbstreaktiven T-Zellen ins ZNS im GALT initiiert wird.

Diese Arbeit zeigt, dass bereits existierende enzephalitogene T-Zellen in der Lamina propria des Ileums durch Mikrobiota stimuliert werden und dass dies die Migrationsfähigkeit der T-Zellen erhöht.

INTRODUCTION

1.1 Multiple Sclerosis

Multiple sclerosis (MS) is the most frequent chronic autoimmune disease in the central nervous system (CNS), which is characterized by demyelination, axonal damage and neurodegeneration, accompanying local inflammation (Patejdl and Zettl 2017). There are approximately 2.5 million people worldwide afflicted with MS (Flachenecker and Stuke 2008). The disease is fairly common in white caucasians of northern European ancestry. The prevalence in the Nordic region, the British Isles and Canada is ≥ 220 in 100,000 (Rivera 2017). In the United States, at least 350,000 individuals are affected by MS (Sospedra and Martin 2005). The prevalence of MS in Asia has been low but keeps increasing (Eskandarieh, Heydarpour et al. 2016). By 2007, the prevalence rate of MS in Shanghai, China, has been reported to be 1.39 in 100,000 (Cheng, Miao et al. 2007). The disease affects women about twice as often as men. The average age of disease onset is 30-years-old. 25 years after diagnosis, approximately 50% of patients require permanent use of a wheelchair (Dendrou, Fugger et al. 2015). Therefore, MS has posed a major personal and socioeconomic burden.

MS has variable clinical courses which include the relapsing remitting form of multiple sclerosis (RRMS), primary progressive multiple sclerosis (PPMS) and secondary progressive multiple sclerosis (SPMS) (Correale, Gaitan et al. 2017, Patejdl and Zettl 2017). About 15% of MS patients show remaining progression of the disease, which is named PPMS (Lublin and Reingold 1996). However, even most of patients can completely or partially recover from the clinical symptoms, after 10-15 years from the onset, the disease can deteriorate progressively and recur, defined as SPMS (Correale, Gaitan et al. 2017). Patients with MS can present different clinical symptoms including motor impairment, visual disturbance, cognitive impairment and etc.. The variation in clinical manifestations correlates with spatiotemporal dissemination of lesion sites in the CNS (Dendrou, Fugger et al. 2015). MS lesions have been found both in the cerebral cortex and the deep grey matter of the brain (Kidd, Barkhof et al. 1999, Vercellino, Masera et al. 2009). There are three forms of cortical lesions in MS: cortico-subcortical lesions, small intra-cortical lesions and subpial lesions (Bo, Vedeler et al. 2003). For the demyelinating lesions in the deep grey matter, nuclei are

affected not only by focal plaques of demyelination, but also by diffuse neuronal loss in the absence of demyelinated lesions (Cifelli, Arridge et al. 2002, Lassmann 2014).

Although the pathological mechanisms of MS are not fully clarified, it has been widely recognized that brain autoreactive T cells play a critical role during the development of disease (Wekerle 2017). Even the CNS has immunological privilege that can prevent the infiltration of most peripheral immune cells, it is not without any exception. Once autoimmune T cells that pre-exist in the periphery, are stimulated, some of them are able to cross the blood brain barrier (BBB) and infiltrate into CNS. These autoreactive T cells which scan the CNS and eventually respond to the local antigenic tissue, initiate a cascade of inflammatory events including the recruitment of monocytes and B cells (Wekerle 2017). There are different subsets of autoimmune T cells possibly mediating the progression of MS, among which CD4⁺ T cells have been concerned as a key player for years. Several studies indirectly support the involvement of CD4⁺ T cells in MS pathogenesis. First, autoreactive CD4⁺ T cells exist in both MS patients and healthy donors (Sospedra and Martin 2005, Pilli, Zou et al. 2017). The autoreactive T cells recognize myelin basic protein (MBP) (Pette, Fujita et al. 1990, Valli, Sette et al. 1993), myelin associated glycoprotein (MAG) (Andersson, Yu et al. 2002) and MOG (Zhang, Markovic-Plese et al. 1994) through HLA binding (Blum, Wearsch et al. 2013). Second, myelin-reactive CD4⁺ T cells in MS patients are functionally different from those in healthy controls, with higher expression of IFN γ and IL17 (Olsson, Sun et al. 1992, Pelfrey, Rudick et al. 2000). Third, genomic studies showed that many MS-associated genes, such as HLA-DRB1*1501, are involved in the activation and regulation of CD4⁺ T cells (Sawcer, Franklin et al. 2014).

Additionally, experimental autoimmune encephalomyelitis (EAE), which is a T cell mediated disease model, has been established to study the pathology of MS. In a transgenic mouse model, EAE is spontaneously developed due to the expression of a human myelin-antigen-specific T cell receptor (TCR) together with the matching human HLA class II molecule (Madsen, Andersson et al. 1999, Ellmerich, Mycko et al. 2005). CD4⁺ T cells can be differentiated to different subtypes according to their cytokine profile. Among them, IFN γ producing Th1 cells have been considered as encephalitogenic T cells (Ando, Clayton et al. 1989, Merrill, Kono et al. 1992). IL17 producing Th17 cells are firstly described as a new lineage of T helper cell lineages in 2005 (Park, Li et al. 2005). Later, Th17 cells are detected

in active areas of MS lesions (Tzartos, Friese et al. 2008). Recently, Th17 cells have been identified as a pathogenic effector in CNS autoimmune disease (Zepp, Wu et al. 2011, Sie, Korn et al. 2014). BBB endothelial cells have been demonstrated to express IL17 and IL22 receptors in MS lesions, and BBB tight junctions can be disrupted by IL17 and IL22 both *in vitro* and *in vivo* (Kebir, Kreymborg et al. 2007). Th17 cells can infiltrate into the CNS to damage neurons and recruit more CD4⁺ lymphocytes (Kebir, Kreymborg et al. 2007). Studies of EAE provide more evidence about the pathogenic role of Th17 cells in CNS autoimmune inflammation. Th17 cells increase significantly in the presence of IL23 in the spinal cord during EAE induction (Hirota, Duarte et al. 2011). Administration of anti-IL17 blocking antibody after immunization reduced the EAE incidence in mice (Park, Li et al. 2005). Furthermore, mice adoptively transferred Th17 polarized MOG-specific CD4⁺ T cells can develop EAE, which indicates Th17 cells involve in the pathogenesis of CNS autoimmune inflammation (Jager, Dardalhon et al. 2009). However, how Th17 cells mediate CNS autoimmune inflammation is still being investigated. Taken together, these results indicate that Th17 cells significantly contribute to EAE/MS pathogenesis.

Up to date, therapeutic strategies for MS mainly include anti-inflammation, neuroprotection and repair-promoting. Anti-inflammatory strategies, such as applying IFN β 1, fingolimod, anti- α 4 integrin and anti-CD20 antibody, rather benefit the patients of younger age, shorter disease duration and ongoing inflammatory lesion activity (Ontaneda, Thompson et al. 2017). The efficacy of most anti-inflammatory strategies has been demonstrated in RRMS and recently in SPMS. For example, IFN β 1-targeted therapies were applied to several clinical trials of SPMS. However, only two trials showed positive results while others were negative (Li, Zhao et al. 2001, Cohen, Cutter et al. 2002, Andersen, Elovaara et al. 2004, Panitch, Miller et al. 2004, Wolinsky, Narayana et al. 2007). An analysis latterly figured out that participants with recent relapse activity are more likely to be benefited from the IFN β 1 treatment (Kappos, Weinschenker et al. 2004). Neuroprotective strategies, including the application of simvastatin, phenytoin, cannabinoids and vitamin, also show varying results on the disease course. For example, phenytoin, a repurposed sodium-channel blocker, can protect axons from inflammatory injury in acute optic neuritis. Treatment with phenytoin within two weeks after onset shows a 30% reduction of retinal nerve fiber layer loss compared with placebo (Raftopoulos, Hickman et al. 2016). In contrast, another sodium

channel blocker, lamotrigine, provides negative results on rescuing cerebral volume loss in SPMS (Kapoor, Furby et al. 2010). The disparity may be due to a 'pseudo-atrophy' effect observed in the first year of lamotrigine study, which may obscure potential benefits (Ontaneda, Thompson et al. 2017). Nowadays, repair-promoting strategy is also highly noticed in MS treatment. For example, LINGO-1 expressed in the oligodendrocytes and neurons impedes remyelination (Mi, Pepinsky et al. 2013). Anti-LINGO-1 blocking antibody can promote remyelination in acute optic neuritis (Cadavid, Balcer et al. 2017). However, treatment of RRMS and SPMS with anti-LINGO-1 blocking antibody does not improve the disability of the patients (Clinicaltrials.gov identifier NCT01864148). Recently, as a potential therapy for progressive MS, cell-based repair-promotion draws attention. Windrem and colleagues find that hypomyelinating shiverer mice remyelinate and recover from clinical phenotype after neonatal transplantation of glial progenitor cells isolated from fetal human brain (Windrem, Schanz et al. 2008). Mesenchymal stem cells are also a promising candidate for repair-promotion, since they exhibit numerous immunomodulatory and tissue-protective properties in animal model of MS (Cohen 2013). However, future trials need to provide more definitive evidence concerning safety and efficacy. Moreover, important methodological questions still remain, including the preferred source, optimal cell production protocols and dosing schedules as well as routes of administration. (Ontaneda, Thompson et al. 2017).

1.2 Experimental Autoimmune Encephalomyelitis

There is a complex interaction between immunopathological and neuropathological mechanisms involved in MS that is impossible to be fully illuminated by any single clinical trial. Therefore, EAE has primarily served as an animal model of human MS. Although none of the existing EAE models perfectly reflects the entire MS pathology, each variant of EAE resembles some pathological features of MS. EAE was first described by Rivers and colleagues over 80 years ago to understand the pathogenesis of the post-vaccinal encephalomyelitis (Rivers, Sprunt et al. 1933) and is increasingly used for studying pathogenesis and therapeutics of autoimmune diseases. Moreover, immunology and

neurobiology based interventions in EAE have been evaluated to explore novel therapies of MS (Krishnamoorthy and Wekerle 2009, Constantinescu, Farooqi et al. 2011).

There are several methods to establish EAE animal models. Immunization with CNS homogenates or myelin proteins such MBP, proteolipid protein (PLP) and MOG, through the auxiliary of Complete Freund's Adjuvant (CFA), has been used intensively as the active EAE induction (Pender, Tabi et al. 1995, Storch, Stefferl et al. 1998, Stromnes and Goverman 2006). An important difference between active EAE and human MS is that autoreactive T cells in active EAE models are primed and activated by identified antigens whereas triggers of human MS are still unclear (Constantinescu, Farooqi et al. 2011). Alternatively, EAE can be induced by adoptive transfer of *in vitro* activated encephalitogenic T cells (Ben-Nun, Wekerle et al. 1981). Adoptive transfer EAE is appropriate to study the role of brain autoreactive T cells in CNS inflammation (Kawakami, Lassmann et al. 2004, Bartholomaeus, Kawakami et al. 2009). However, it is still insufficient to study the spontaneity of the disease (Gold, Lington et al. 2006). More recently, spontaneous EAE models have been developed with transgenic mice. Transgenic mice expressing MBP or MOG specific TCRs, develop EAE in the absence of identified antigen sensitization (Goverman, Woods et al. 1993, Krishnamoorthy, Saxena et al. 2009). Therefore, spontaneous EAE models are more suitable for investigating the triggers of human MS.

1.2.1 Spontaneous EAE Mouse Model

Spontaneous EAE models have great advantages to investigate the natural triggering of autoimmunity compared with traditional induced EAE models. Neither myelin antigen immunization nor external encephalitogenic T cells but pre-existing endogenous encephalitogenic T cells are required for the EAE induction. The transgenic 2D2 mouse line expresses a TCR reactive to MOG 35-55. 2D2 mice develop optic neuritis with an incident rate of 35%, and EAE in 4% of the mice without immunization with myelin antigen (Table 1.2.1 adopted from (Bettelli, Pagany et al. 2003)). Splenocytes from 2D2 mice rather resemble the Th1 cell phenotype by expressing high levels of IFN γ when they are *in vitro* activated by MOG 35-55 peptides (Bettelli, Pagany et al. 2003). Later, the 2D2 mice are crossed to transgenic mice with MOG specific Ig heavy chain knock-in B cells (Krishnamoorthy, Lassmann et al. 2006). The double transgenic offspring, named OSE mouse,

shows higher EAE incidence which is up to 60% (Bettelli, Baeten et al. 2006, Krishnamoorthy, Lassmann et al. 2006).

	Clinical		Histological	
	EAE	Optic neuritis	EAE	Optic neuritis
Group A	4%		100%	100%
Mice with EAE	(<i>n</i> = 72) ^a	ND	(<i>n</i> = 3)	(<i>n</i> = 3)
Group B	0%	35%	0%	47%
Mice without EAE	(<i>n</i> = 69)	(<i>n</i> = 37) ^b	(<i>n</i> = 15) ^c	(<i>n</i> = 15) ^c

Table 1.2.1 Spontaneous autoimmune diseases in 2D2 TCR transgenic mice. ^a72 TCR transgenic mice were tracked for EAE. ^bAmong transgenic mice without EAE, 37 displayed clinical signs of optic neuritis. ^c15 transgenic mice were investigated by histology. Group A: mice that presented spontaneous clinical EAE (*n*=3); Group B: mice that never presented signs of EAE. Adopted from (Bettelli, Pagany et al. 2003).

TCR1640 mice, expressing TCR specific for MOG 92-106 on SJL/J background, can also develop spontaneous EAE without antigen immunization. However, different from 2D2 mice which shows chronic EAE, TCR1640 mice are described to present relapsing remitting EAE at a high frequency without genetic modification of B cells (Pollinger, Krishnamoorthy et al. 2009). In EAE presented TCR1640 mice, there is a significant expansion of MOG reactive B cells from the endogenous compartment. Histological analysis shows the deposition of anti-MOG Ig and infiltration of B cells into spinal cord of the ailing TCR1640 mice (Pollinger, Krishnamoorthy et al. 2009).

1.3 Intestinal Immune System and Encephalomyelitis

1.3.1 Gut Associated Lymphoid Tissue

The gut contains the small and the large intestine forming a continuous tube that a single layer of columnar epithelium lines internally. The small intestine begins at the pylorus,

successively constituted by duodenum, jejunum and ileum then terminating at the ileocaecal valve. The large intestine is divided to four segments, with the proximal colon close to caecum, the transverse colon, the distal colon and ends at the anus (Mowat and Agace 2014). The small intestine is anatomically characterized by finger-like projections extended in to lumen, known as villi. In the intestinal mucosa, lamina propria is the loosely packed connective tissue between epithelium and muscularis mucosa, containing blood supply, lymph drainage and nervous provision. Large number and variety of immune cells, such as T cells, B cells and innate immune cells, distribute and patrol throughout the lamina propria, where majority of immunological events happens (Mowat and Agace 2014, Faria, Reis et al. 2017).

Other well characterized lymphoid structures in the GALT include Peyer's patches, caecal patches and colonic patches. Peyer's patches, comprised of B cell lymphoid follicles and clear T cell zones as similar as lymph node (Cornes 1965), mainly distribute in the ileum of the small intestine. In contrast to lymph nodes, Peyer's patches are not encapsulated, which indicates possible responses to luminal antigen. Additionally, Peyer's patches and colonic patches are the main source of intestine-homing IgA plasma blasts and important sites of T cell priming (Perry and Sharp 1988, Masahata, Umemoto et al. 2014). Some smaller lymphoid aggregates like cryptopatches and isolated lymphoid follicles which are only microscopically visible, also play important roles in gut immune events. Distinct from Peyer's patches, isolated lymphoid aggregates primarily consist of B cells, which are implicated as essential sites of T cell independent IgA generation (Tsuji, Suzuki et al. 2008, Mowat and Agace 2014). These isolated lymphoid aggregates correlate with the increased microbiota in the intestine to maintain intestinal homeostasis (Bouskra, Brezillon et al. 2008).

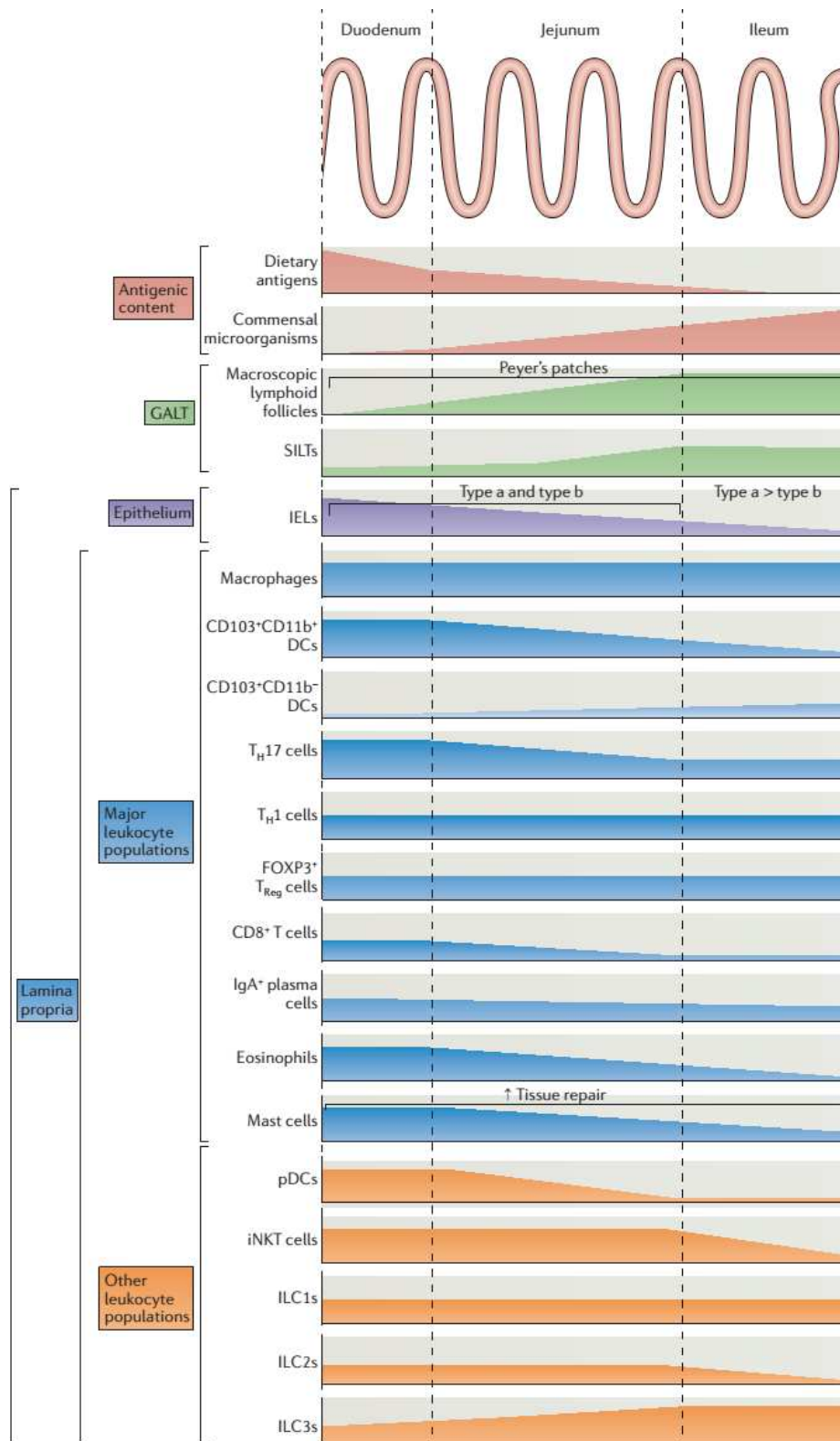


Figure 1.3.1 The immune organs and cells varies along the small intestine. The figure characterized regional specialization in the mouse intestine, indicating the variation of antigens (red graphs), GALT (green graphs) and leukocyte populations (blue and orange graphs) in frequency along the small intestine. DC, dendritic cell; FOXP3, forkhead box P3; IEL, intraepithelial lymphocyte; ILC, innate lymphoid cell; iNKT, invariant natural killer T; pDC, plasmacytoid DC; SILT, solitary isolated lymphoid tissue; TH, T helper. (Adopted from Mowat et al, 2014)

1.3.2 Distribution of Lymphocytes in the Small Intestine

The Lamina propria and the epithelial layer are the most essential effector sites of the intestinal immune system. The lamina propria contains both CD4⁺ and CD8⁺ T cells. The variety of intestinal CD4⁺ T cells includes IL10⁺T regulatory, IFN γ ⁺Th1, IL4⁺Th2 and IL17⁺Th17 subsets (Ivanov, McKenzie et al. 2006, Veenbergen and Samsom 2012, Mowat and Agace 2014). Th1 and Th2 cells exist throughout the intestine of human without significant variation (Wolff, Leung et al. 2012). Th17 cells have been found in the lamina propria of the jejunum, ileum, caecum and colon, which show a higher proportion in the ileum and colon of humans (Denning, Norris et al. 2011, Sathaliyawala, Kubota et al. 2013). T regulatory cells (Tregs) which express both CD4 and Foxp3 also comprise a high proportion of T cells in the lamina propria, maintaining the immunological tolerance to the microbiota and dietary antigens (Bilate and Lafaille 2012). Moreover, the lamina propria contains a great number of IgA and IgM producing plasma cells depending on the presence of GALT microbiota. T cells existing in the epithelium can be divided into two subsets. Besides conventional T cells mainly expressing an $\alpha\beta$ TCR and CD8 $\alpha\beta$ heterodimer or CD4, unconventional T cells in the epithelial layer express CD8 $\alpha\alpha$ homodimers and either a $\gamma\delta$ TCR or an $\alpha\beta$ TCR (Hayday and Gibbons 2008, Cheroutre, Lambomez et al. 2011).

There are not only lymphocytes, but also a variety of innate immune cells in the intestine. A plenty group 3 innate lymphoid cells (ILC3s) detected in the small intestine express effector cytokines and MHC class II molecules in response to gut microbiota, regulating the homeostasis of intestinal Th17 cells (Lecuyer, Rakotobe et al. 2014, Longman, Diehl et al. 2014). In lamina propria, there are abundant macrophages producing large amount of cytokines such as IL10 and IL1 β to regulate the activity of T cells (Takeda, Clausen et al. 1999, Shaw, Kamada et al. 2012). Four subsets of mouse intestinal dendritic cells have been described, including CD103⁺CD11b⁺, CD103⁺CD11b⁻, CD103⁻CD11b⁺ and CD103⁻CD11b⁻. Among them, CD103⁺CD11b⁺ dendritic cells mainly exist in the small intestine, which are associated with the presence of Th17 cells through the expression of IL6 (Denning, Norris et al. 2011). Figure 1.3.1 shows the distribution of main subsets of immune cells in the small intestine.

1.3.3 Intestinal Th17 Cells

Th17 cells are a prominent T cell subset in the lamina propria of the small intestine, expressing IL17A, IL17F and IL22 to stimulate intestinal epitheliums to produce mucin and antimicrobial proteins (Weaver, Elson et al. 2013). They also mediate the high-affinity secretory IgA response of B cells, during the bacteria invasion and colonization (Honda and Littman 2016). On the other hand, intestinal Th17 cells also play a pathogenic role in aggravating autoimmune diseases by secreting cytokines such as the granulocyte macrophage colony-stimulating factor (GM-CSF) which is induced by IL23 from DCs (El-Behi, Ciric et al. 2011). It has been well characterized that the differentiation of Th17 cells requires the expression of the orphan nuclear receptor ROR γ t with combination of IL6 and TGF- β (Ivanov, McKenzie et al. 2006). There are several studies investigating the impacts of environmental factors on intestinal Th17 cells. High salt diet increases the frequency of Th17 cells in the lamina propria accompanied with more severe EAE in mice (Kleinewietfeld, Manzel et al. 2013, Wu, Yosef et al. 2013). The induction of Th17 cells is due to the upregulation of serine/threonine-protein kinase Sgk1 (SGK1) which phosphorylates and deactivates fork head box protein O1 to aggravate the ROR γ t-mediated transcription of IL17A and IL23 receptor (Kleinewietfeld, Manzel et al. 2013). Long chain fatty acids can enhance the expression of IL17A and IFN γ in T cells of the lamina propria by the P38 phosphorylation and worsen the EAE development (Haghikia, Jorg et al. 2015). Among the environmental factors, microbiota play as the most pivotal role on the induction of Th17 cell in the small intestine. Adhesion of segmented filamentous bacteria (SFB) to the intestinal epithelium has been related to the accumulation of Th17 cells (Atarashi, Tanoue et al. 2015). SFB can upregulate genes of three isoforms of serum amyloid A in the small intestinal epithelial cells, in response of which CX3CR1⁺ myeloid cells produce IL23, IL6 and TGF- β to activate ILC3s, enhancing the differentiation of Th17 cells (Atarashi, Tanoue et al. 2015, Honda and Littman 2016). Expression of IL17A in ROR γ t⁺ cells can also be directly stimulated by epithelium-secreted serum amyloid A induced by SFB colonization (Sano, Huang et al. 2015). Similar induction of Th17 cells has been observed in the monocolonization of *C. rodentium* in germ free mice. Th17 cells proliferate rather than Th1 cells upon the physical interaction between the bacteria and epithelial cells. Once the bacteria damage the epithelial layer and intrude, massive expression of IFN γ overwhelms IL17A (Atarashi, Tanoue

et al. 2015). Figure 1.3.2 shows the details about induction and differentiation of Th17 cell in the small intestine.

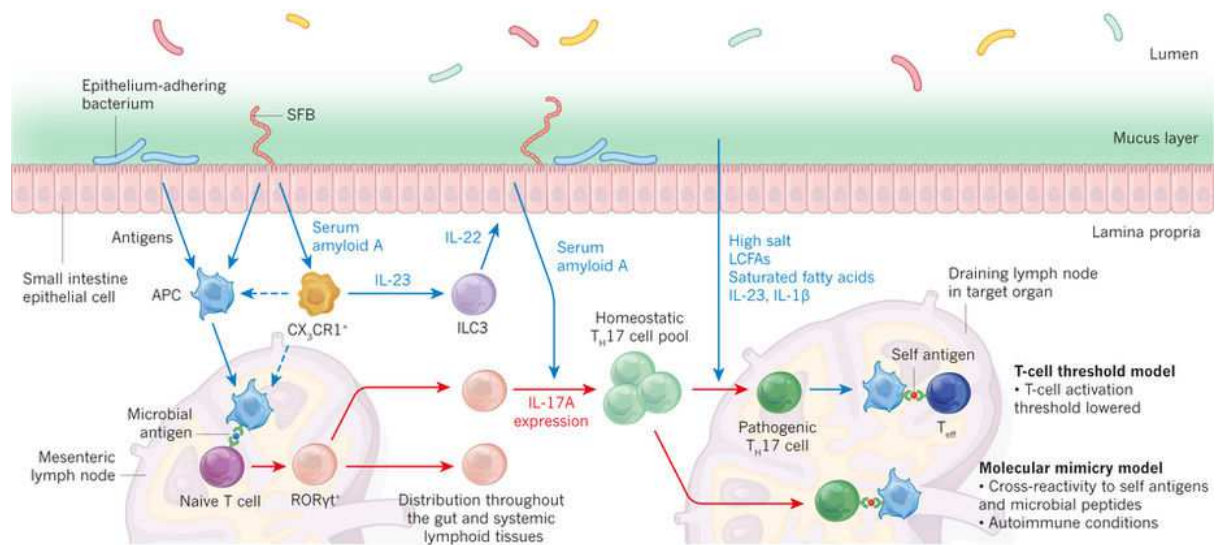


Figure 1.3.2 Microbiota-mediated induction of Th17 cells and the autoimmunity of Th17 cells in the GALT. Adopted from (Honda and Littman 2016)

1.3.4 CD44⁺CD4⁺ T cells and Encephalomyelitis

CD44 is a family of cell surface glycoproteins. It is considered as an adhesion molecule that mediates the lymphocyte homing, extravasation and binding to the extracellular matrix (Camp, Scheynius et al. 1993, DeGrendele, Estess et al. 1996, DeGrendele, Estess et al. 1997). CD44 is widely used as a marker of antigen-experienced T cells and also an activation marker implicated in migration (Firan, Dhillon et al. 2006, Alvarez-Sanchez, Cruz-Chamorro et al. 2015). The most acknowledged function of CD44 is recruiting T cells to inflamed sites (Winkler, Foster et al. 2012).

Recently, CD44 has been reported as an associated factor of EAE development. It has been shown that CD44⁺ activated MBP specific T cells possess the ability to infiltrate into the brain of naïve mice (Brocke, Piercy et al. 1999). Both blocking antibody and genetic deletion of CD44 can attenuate active EAE in a dose-dependent manner (Brocke, Piercy et al. 1999, Guan, Nagarkatti et al. 2011). Lack of the molecule impairs Th1/Th17 polarization (Guan, Nagarkatti et al. 2011). Taken together, increased CD44⁺CD4⁺ T cells might imply a higher

risk of CNS inflammation although the mechanism is still unclear. On the other hand, CD44 may play a crucial role in alteration of gut microbiome and their metabolism to mediate the progress of EAE. CD44 deficient mice exhibit a significant alteration in bacterial 16S ribosomal RNA gene sequencing compared with wildtype mice (Chitralla, Guan et al. 2017). Fecal transfer from CD44 deficient naïve mice to EAE-induced recipients can lead to amelioration of the disease (Chitralla, Guan et al. 2017). How CD44 alters the gut bacteria still needs to be further studied. However, until now, there is no direct evidence to relate intestinal CD44⁺CD4⁺ T cells to the incidence of EAE.

1.3.5 Gut Microbiota and Encephalomyelitis

Although the triggers of T cell stimulation in MS and EAE are still indefinite, more and more studies draw our attention to the microbiota in the gut. Several studies utilizing the 16S ribosomal RNA sequencing have introduced the alterations of the microbiome in MS patients compared with healthy controls, as well as in the MS patients on disease modifying treatment compared with untreated patients (Chen, Chia et al. 2016, Jangi, Gandhi et al. 2016). Vitamin D deficiency, smoking and obesity, which are factors involved in MS development (Thompson, Baranzini et al. 2018), can also modify the gut microbiome composition (Biedermann, Zeitz et al. 2013, Ridaura, Faith et al. 2013, Bashir, Prietl et al. 2016), raising the question of association between gut microbiota and MS.

More compelling evidence show the influence of gut microbiota on encephalitogenic T cells. In an active EAE model, reduction of bacteria in the gut by oral antibiotic treatment attenuates the severity of the disease by alleviation in the global level of pre-inflammation (Ochoa-Reparaz, Mielcarz et al. 2009). Another study shows that Gut-CNS immune responses during EAE can be aggravated by intestinal microbiota (Lee, Menezes et al. 2011). Oral antibiotic administration decreases IL17A and IFN γ producing CD4⁺ T cells significantly in the spinal cord and the lamina propria of the small intestine at the peak of EAE (Lee, Menezes et al. 2011). Additionally, the colonization of SFB to germ free restores Th1 and Th17 cells during EAE in both the lamina propria of the ileum and the spinal cord (Ivanov, Atarashi et al. 2009).

Spontaneous EAE mouse models provide further evidence that gut microbiota play a crucial role in EAE pathogenesis. Transgenic mice that express MBP specific TCR develop

spontaneous EAE in the conventional area where some avirulent organisms exist. When these transgenic mice are located in the specific pathogen free (SPF) condition, the occurrence of EAE decreases significantly (Goverman, Woods et al. 1993). Later, more details are clarified in TCR1640 mice which have been introduced as another spontaneous EAE model. The TCR1640 mice develop spontaneous EAE with an incidence up to 80% when they are kept under SPF condition. Interestingly, when the transgenic mice are housed in the germ free environment, EAE incidence is dramatically decreased (Berer, Mues et al. 2011). The decreased incidence is associated with reduced proliferation of IL17⁺CD4⁺ MOG specific T cells in the lamina propria and Peyer's patches of germ free mice (Berer, Mues et al. 2011). Another study of MS twins also verifies the influence of microbiota on the disease incidence. Monozygotic twin pairs assembled in this study are clinically discordant for MS. In each pair, one twin has clinically definite MS whereas the co-twin is unaffected. Germ free TCR1640 mice colonized microbiota from MS-twin samples display significantly higher incidence of EAE compared with those colonized microbiota from healthy-twin samples (Berer, Gerdes et al. 2017). This study provides evidence that MS-derived microbiota can precipitate an MS-like autoimmune disease in a spontaneous mouse model. In summary, these studies have drawn attention to the impact of microbiota in the GALT on triggering MS/EAE. However, mechanisms and the species of microbiota initiating EAE have not been fully understood.

1.4 Calcium Dependent T cell Imaging

1.4.1 Calcium Fluctuation during T cell Activation

Antigen recognition through TCR engages a variety of signaling cascades, including activation of several protein tyrosine kinases, which start the phosphorylation of adaptor proteins. This induces the recruitment and activation of the phospholipase PLC γ 1. In parallel, activation of T cells through binding G-protein-coupled chemokine receptors lead to the activation of PLC β . Then, both PLC β and PLC γ 1 mediate the hydrolysis of the membrane phospholipid phosphatidylinositol-4,5-bisphosphate(PtdIns(4,5)P₂) to inositol-1,4,5-trisphosphate (IP₃) and diacylglycerol (DAG) (Fracchia, Pai et al. 2013). IP₃ can bind to its

receptor on the membrane of the endoplasmic reticulum (ER), triggering the release of calcium ions to the cytosol (Feske 2007). Identifying the reduction of calcium ions in the ER, stromal interaction molecule 1 (STIM1) on the ER activates calcium-release-activated calcium (CRAC) channels within the plasma membrane, causing the rapid increase of intracellular Ca^{2+} . Enzymes like calcineurin can be activated in turn by the conformational change of calmodulin (CaM) upon binding of cytosolic calcium (Feske 2007, Fracchia, Pai et al. 2013). Calcineurin dephosphorylates transcription factors such as nuclear factor of activated T cells (NFAT), NF- κ B and AP-1 which results in the nuclear translocation of transcription complexes and the expression of activation-regulated genes in T cells (Feske, Giltane et al. 2001).

1.4.2 Twitch2b Calcium Sensor

Twitch2b is a fluorescence resonance energy transfer (FRET)-based biosensor which can identify the activation of T cells via the display of the cytosolic calcium level fluctuation. The FRET pair of Twitch2b is composed of the cpVenus^{CD}, a variant of yellow fluorescent protein (YFP), and the mCerulean3, a variant of the cyan fluorescent protein (CFP) (Thestrup, Litzlbauer et al. 2014). The two variants of fluorescent proteins are connected by a Troponin C (TnC) variant which provides a high affinity calcium binding motif (Fig. 1.4.1) (Thestrup, Litzlbauer et al. 2014). Twitch2b emits more CFP emission than YFP in lower calcium environment. However, in high calcium environment, CFP emission is decreased and YFP emission is increased due to conformational changes of Twitch2b as results of calcium binding to TnC domain and a subsequent energy transfer from CFP to YFP. (Fig. 1.4.1 A) (Thestrup, Litzlbauer et al. 2014).

Twitch2b possesses several advantages for the intravital imaging of T cells. Compared with calcium indicator dyes, the Twitch2b sensor is a genetically encoded calcium indicator that can be stably integrated in the genome of target cells, whereas functional calcium indicator dyes such as indo-1 can be easily lost during the proliferation of cells. In addition, such calcium indicators will be exhausted from T cells within a short time (Sommer, Bischof et al. 1994, Mues, Bartholomaeus et al. 2013). Furthermore, since T cells can change location in the three dimensional tissue with high mobility, their brightness changes ceaselessly depending on the z-depth of T cells. Therefore, a ratiometric calcium indicator is necessary to normalize

this effect (Thestrup, Litzlbauer et al. 2014). GCaMPs, a different kind of genetic activation sensors (Tian, Hires et al. 2009), are not designed for ratiometric measurements, since: 1) the signal intensity of GCaMPs changes without a spectral shift when calcium concentration changes; 2) the peak fluorescence intensity varies with expression levels (Cho, Swanson et al. 2017). Compared with GCaMPs, FRET-based ratiometric imaging with the Twitch2b sensor is reliable to analyse the activation of lymphocytes, since: 1) it is less affected by changes in the optical path length; 2) the excitation light wavelength is fixed 3) it is less impacted by expression levels among cells (Thestrup, Litzlbauer et al. 2014). By calculating the ratio of YFP divided by CFP as well as the duration of calcium signaling, activation of T cells can be identified in real time (Mues, Bartholomäus et al. 2013, Kyratsous, Bauer et al. 2017). Compared with Twitch1 and TN-XXL, predecessors of Twitch2b (Mank, Santos et al. 2008), Twitch2b is more efficient to bind the cytosolic calcium so that the detection of calcium influx is more sensitive and faster. The FRET changes in Twitch2b are optimized after a functional screen, which has been highly improved compared with TN-XXL (figure 1.4.1B). Furthermore, the brightness of Twitch2b is highly improved allowing better identification of expressing cells during *in vivo* imaging (Thestrup, Litzlbauer et al. 2014).

1.4.3 NFAT-GFP Sensor

As it was described previously, elevation of cytosolic calcium is the central event when lymphocytes get activated via cell surface receptors and activate calcineurin. Cytosolic NFAT is dephosphorylated by the activated calcineurin and then translocate into nucleus to bind genomic DNA, inducing the expression of many activation genes in cells. Based on this mechanism, the location of NFAT in the cell can be utilized to identify the activation status of lymphocytes. For the NFAT-GFP sensor, the DNA binding domain has been mostly removed to eliminate the influence on the cell status. GFP is fused to the C-terminal of truncated NFAT to show the subcellular localization. This NFAT-GFP sensor has been successfully used to visualize the activation of T cells in the spinal cord of the rat transfer EAE model (Lodygin, Odoardi et al. 2013, Pesic, Bartholomäus et al. 2013). Importantly, NFAT-GFP and Twitch detect different levels of activation in the cells. Whereas Twitch detects antigen independent weak stimulation, only saturated calcium signaling induce NFAT-GFP translocation, which is often induced by antigen dependent stimulation

(Kyratsous, Bauer et al. 2017). Therefore, the combination of the Twitch and the NFAT-GFP sensor provide a detailed view of T cell activation.

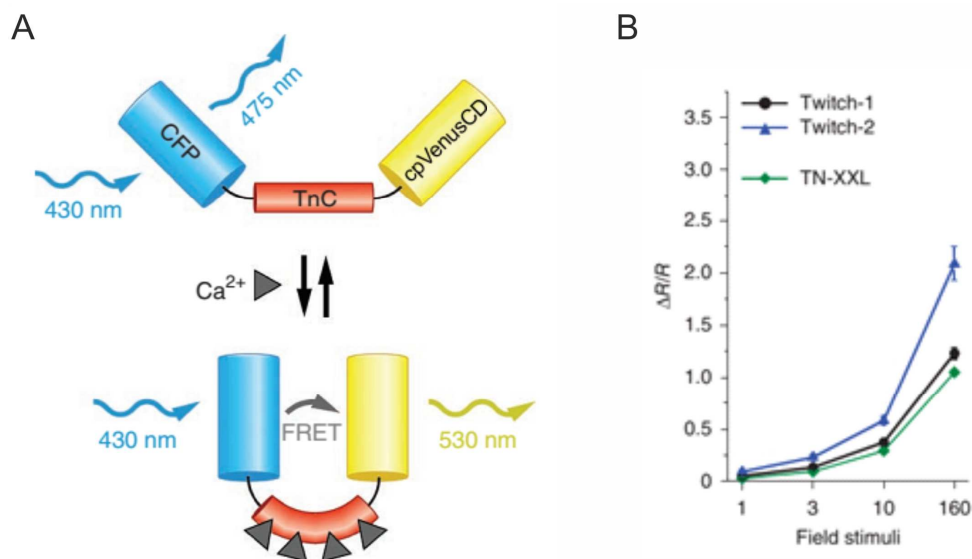


Figure 1.4.1 Functional characterization of Twitch2b. (A) A schematic of Twitch2b, containing donor fluorophore mCerulean3 CFP, cpVenusCD acceptor and calcium-sensitive domain TnC, before (upper) and after (lower) binding of calcium. (B) Alteration in fluorescence ratio of selected Twitch variants in response to short-field stimuli eliciting 1–160 action potentials. Response of TN-XXL was taken as comparison. Error bars, mean \pm s.e.m. (n= 60–204). Modified from (Mues, Bartholomaeus et al. 2013, Thestrup, Litzlbauer et al. 2014)

OBJECTIVES

The one of pivotal events to induce CNS inflammation in the EAE is stimulation of pre-existing autoreactive T cells in the peripheral tissue. I hypothesize that this priming occurs in the GALT. By combining two-photon intravital imaging, fluorescent protein-based activation sensors and well established animal model, T cells stimulation in GALT is explored in details in this study.

The first aim of this project is to confirm whether encephalitogenic T cells are stimulated in the GALT and to identify the location of the immune-reactive events. A new intravital imaging approach needs to be established under the influence of intestinal peristalsis to obtain stable movies. By using this method, the calcium signaling and the velocity of intestinal T cells must be analysed. To analyse the consequences of T cell stimulation in the GALT, phenotypes of encephalitogenic T cells are analysed in the efferent mesenteric lymph.

The second aim of this project is to investigate how T cells get stimulation in GALT. By administration of functional blocking antibodies, the molecular mechanism of calcium signaling in T cells can be clarified. Special attention is paid whether the activation of T cells in the GALT depends on antigen or not.

The last aim of this project is to discuss the impact of microbiota on the activation of encephalitogenic T cells, since gut microbiota exerts large effects on immune cell differentiation and polarization. By transferring the activation sensor labelled T cells to recipients housed in germ-free condition, the impact of microbiota involving in T cell activation is possible to be illustrated.

MATERIAL AND METHODS

2.1 Material

2.1.1 Reagents, Medium and Buffer

Name	Constituent	Amount	Company
TCM	DMEM	1 L	Sigma
	L-glutamine	2 mM	Sigma
	Penicillin/Streptomycin	100 IU/ml, 100 µg/ml	Sigma
	L-asparagine	0.036 g/L	Sigma
	Sodium-Pyruvate	1 mM	Sigma
	Non-essential amino acids	10 ml/L	Sigma
	2-Mercaptoethanol	4 µl/L	Merck
EH	DMEM	97.5% Vol	Sigma
	HEPES, 1M	2.5% Vol	Sigma
TCM+FCS	TCM	90% Vol	-
	Fetal calf serum	10% Vol	Biochrom
ACK buffer	NH ₄ Cl	150 mM	Sigma
	KHCO ₃	1 mM	Sigma
	EDTA	0.1 mM	Merck
	H ₂ O	500 ml	-
RPMI	RPMI 1640	1 L	Sigma
	L-glutamine	2 mM	Sigma
	Penicillin/Streptomycin	100 IU/ml, 100 µg/ml	Sigma
	L-asparagine	0.036 g/L	Sigma
	Sodium-Pyruvate	1 mM	Sigma
	Non-essential amino acids	10 ml/L	Sigma
	2-Mercaptoethanol	4 µl/L	Merck
RPMI+FCS	TCM	90% Vol	-

MATERIAL AND METHODS

	Fetal calf serum	10% Vol	Biochrom
PBS(pH 7.4)	Na ₂ HPO ₄	10 mM	Sigma
	KH ₂ PO ₄	1.8 mM	Sigma
	NaCl	140 mM	VWR international
	KCl	2.7 mM	VWR international
	H ₂ O	1 L	-
FACS buffer	Rat serum	1% Vol	-
	PBS	99% Vol	-
	EDTA	1 mM	Merck
	Sodium azide	0.05 % Vol	Sigma
Freezing medium	Horse serum	50% Vol	Gibco
	EH	40% Vol	-
	DMSO	10% Vol	Sigma
2x BES (pH 6.95)	N,N-bis(2-hydroxyethyl)-2-aminoethanesulfonic acid	50 mM	Sigma
	NaCl	280 mM	VWR international
	Na ₂ HPO ₄	1.5 mM	Merck
CaCl₂ buffer	CaCl ₂	2.5 M	Sigma
	H ₂ O	50 ml	-
4x Retro/PEG (pH 7.4)	50% PEG6000	320 ml	Sigma
	NaCl, 5M	40 ml	Sigma
	HEPES, 1M	20 ml	Sigma
	H ₂ O	120 ml	-
B220 buffer	Ca ²⁺ and Mg ²⁺ free PBS (pH7.4)	500 ml	Sigma
	BSA	0.1 % Vol	Sigma
	EDTA	2mM	Merck

Table2.1.1a List of cell culture media, buffers and reagents used in this study.

Name	Constituent	Amount	Company
LB medium	Tryptone	10 g	Sigma
	Yeast extract	5 g	Sigma
	NaCl	5 g	VWR international
	H ₂ O	1 L	-
LB agar plate	Tryptone	10 g	Sigma
	Yeast extract	5 g	Sigma
	NaCl	5 g	VWR international
	Bacto Agar	15 g	Merck
	Ampicillin	100 µg/L	Sigma
	H ₂ O	1L	-
TAE (pH 8.0)	Tris-HCl	40 mM	Sigma
	Acetic acid	40 mM	Sigma
	EDTA	1 mM	Merck
	H ₂ O	1L	-
Mouse tail lysis buffer	Tris	100 mM	Sigma
	NaCl	120 mM	VWR international
	EDTA	5 mM	Merck
	Tween 20	0.5% Vol	Sigma
	Proteinase K	1mg/ml	Genaxxon
	H ₂ O	50 ml	-
DNA loading dye	R0611		Thermo Scientific
DNA ladder	1kb GeneRuler		Thermo Scientific

Table 2.1.1b List of bacteria growth media, buffers and reagents of DNA works used in this study.

2.1.2 Cytokines

Name	Store concentration	Working concentration	Company
IL2	10 µg/ml	10 ng/ml	Peprotech
IL4	20 µg/ml	1 ng/ml	Peprotech

IL21	20 µg/ml	10 ng/ ml	Peprotech
------	----------	-----------	-----------

Table 2.1.2 List of cytokines used in this study

2.1.3 Antibodies

Antibody Clone, Isotype	Host and specificity company	Applications
CD3e 500A2, IgG	Golden Syrian Hamster anti mouse Thermo Fisher	Cell culture
CD3 17A2, IgG2bκ	Rat anti mouse Thermo Fisher	Flow cytometry
CD28 37.51, IgG	Golden Syrian Hamster anti mouse Thermo Fisher	Cell culture
TCRβ H57-597, IgG	Armenian Hamster anti mouse Thermo Fisher	Flow cytometry
CD19 1D3, IgG2aκ	Rat anti mouse BD	Flow cytometry
CD4 GK1.5, IgG2bκ	Rat anti mouse Thermo Fisher	Flow cytometry
CD69 H1.2F3, IgG	Armenian Hamster anti mouse Thermo Fisher	Flow cytometry
IgG1 A85-1, IgG1κ	Rat anti mouse BD	Flow cytometry
IgM II/41, IgG2aκ	Rat anti mouse Thermo Fisher	Flow cytometry
CD138 281-2 IgG2aκ	Rat anti mouse BD	Flow cytometry
Vα3.2 TCR RR3-16, IgG2bκ	Rat anti mouse Thermo Fisher	Flow cytometry
Vβ11 TCR RR3-15, IgG2bκ	Rat anti mouse Thermo Fisher	Flow cytometry
CD25 PC61.5, IgG1λ	Rat anti mouse Thermo Fisher	Flow cytometry
CD44 IM7, IgG2bκ	Rat anti mouse Biolegend	Flow cytometry
IFNγ XMG1.2, IgG1κ	Rat anti mouse Thermo Fisher	Flow cytometry
IL17A TC11-18H10, IgG1κ	Rat anti mouse Biolegend	Flow cytometry
MHC class II M5/114.115.2, IgG2bκ	Rat anti mouse Biolegend	Functional blocking
APC IgG	Donkey anti Rat Jackson Laboratory	Histology

Ep-CAM G8.8, IgG2a	Rat anti mouse Santa Cruz	Histology
-----------------------	------------------------------	-----------

Table 2.1.3 List of antibodies used in this study

2.1.4 Plasmids

Name	Provider
pMSCV- Δ neo-Twitch2B	Thestrup <i>et al.</i> , 2014
pMSCV- Δ NFAT-GFP	Modified from Pesic <i>et al.</i> , 2013
pCL-Eco	Mues <i>et al.</i> , 2013

Table 2.1.4 List of plasmids used in this study

2.1.5 PCR Primers

Recognition	Sequence 5'->3'	Expected size
TCR V α 3.2	CCC GGG CAA GGC TCA GCC ATG CTC CTG	675 bp
	GCG GCC GCA ATT CCC AGA GAC ATC CCT CC	
TCR V α 8.3	CTC CAT AAG AGC AGC AGC TCC	700 bp
	CGT CTG TTT CCC ATT CTA AAC TGT ACC	
TCR V β 4	CAA TCT CTG CTT TTG ATG GCT CAA AC	600 bp
	CTG GAT ATA AAG TCC ACG CAG CC	
Internal positive control	CTA GGC CAC AGA ATT GAA AGA TCT	324 bp
	GTA GGT GGA AAT TCT AGC ATC ATC C	

Table 2.1.5 List of PCR primers used in this study

Oligonucleotide primers were designed with Snap Gene Viewer Version 2.8.3. All DNA oligonucleotides were synthesized by Metabion and reconstituted in sterile, deionised water to give a stock solution of 100 μ M. All the primers used in this study have been listed in Table 2.1.5.

2.1.6 Animals

C57BL/6 mice, SJL/J mice, 2D2 mice and TCR1640 mice were obtained from Charles River, kept and bred in the animal facility of Max Planck Institute of Biochemistry or Biomedical center, LMU. All the animal experiments were conducted according to Bavarian state regulations of animal experimentation and approved by the appropriate authorities.

Lymphocytes obtained from mice

Mice were sacrificed and lymphoid tissues were dissected. Single cell suspensions were obtained by dissociating tissues through 40 µm cell strainers (BD). Cells were collected by centrifugation at 400 g and 4 °C for 5 min for further treatment and analysis.

Adoptive transfer of lymphocytes

Labelled Lymphocytes were re-suspended in 200 µl EH medium and injected to each recipient intraperitoneally.

2.2 Methods

2.2.1 DNA Work

DNA transformation to bacteria

5-alpha Competent E. coli cells (NEB) were thawed on ice. 1µl containing approximately 50 ng plasmid DNA was added to the competent cell and stirred lightly with the pipette tip. The mixture was placed on ice for 30 min then heated at 42 °C for 30 sec. Afterwards, 500 µl SOC medium (Sigma) was added to the mixture and mixed well. The sample was rotated at 250 rpm in 37 °C for 1 hour. After the rotation, the sample was diluted serially in SOC medium and spread 50 µl onto LB plates, which contains 100 µg/ml ampicillin. LB agar plates were incubated in 37 °C overnight. At the second day, the single colony showed on the plate was selected for following experiments.

Plasmid purification

DNA plasmids were purified by NucleoBond Xtra Midi or Maxi EF Kit (Macherey-Nagel) following the manufacture's instruction. DNA plasmids were eluted by endotoxin free stiller H₂O and quantitated by Nanodrop ND-2000 (Peqlab).

Mouse tail DNA purification

Mouse tail biopsies were digested in 500 µl mouse tail buffer with 1 mg/ml Proteinase K overnight at 56 °C. After incubation, the sample was centrifuged at 16000 g and 4 °C for 5 min. The supernatant was transferred to a new Eppendorf tube and heated at 95 °C for 10 min to deactivate proteinase K. After cooling down, 350 µl of isopropanol was added to the supernatant and mixed gently. The mixture was incubated at room temperature for 10 min and then centrifuged at 16000 g and 4 °C for 10 min. The supernatant was decanted and DNA pellet can be observed. The pellet was washed with 1 ml 70% ethanol and centrifuge at 16000 g and 4 °C for 5 min. supernatant was removed, the pellet was dried at 56 °C for 10 min and dissolved in 500 µl H₂O.

DNA amplification

DNA was amplified by polymerase chain reaction (PCR) using DreamTaq green PCR master mix (Thermo fisher Scientific). PCR was run by T3-Thermocycler (Biometra) according to the instruction of manufacturers.

Agarose gel electrophoresis

Agarose gel containing 1% agarose in TAE buffer and 1x gelred (Biotium) was used to divide different DNA segments. DNA segments in analytical gels were visualized in the Geldoc XR system (Bio-Rad) with long wavelength UV light (312 nm).

2.2.2 Cell Culture

Name of cell lines	Provider	Origin
40LB	Krishnamoorthy lab, MPI	Nojima <i>et al.</i> , 2011
HEK	Kerschensteiner lab, LMU	ATCC® CRL-1573
Phoenix	Götz lab, LMU	ATCC® CRL-3215

Freezing and thawing of cell lines

For preparation of long-term stocks, 10 million cells were harvested and suspended with 1 ml freezing medium in a cryotube. Cell stocks were frozen in a Cryo 1 °C freezing container (Thermo Fisher Scientific) at -80 °C and subsequently stored in liquid nitrogen. For thawing, cell stocks were incubated in 37°C, then washed with 10 ml EH medium to remove DMSO. After washing, cells are cultured in 10 ml TCM+10%FCS.

Cultivation of cell lines

Cell lines were cultivated with TMC+10%FCS medium in 10 cm tissue culture dishes (Corning) in a humidified incubator (New Brunswick) at 37 °C and 10% CO₂. Semi-adherent cells, such as Phoenix cells and HEK cells, were harvested by flushing off the cell culture dish; whereas adherent cells, such as 40LB cells, were treated by Trypsin-EDTA (Sigma) for 5 min at 37 °C and then flushed off. Cells were enumerated by a hemocytometer (Neubauer) and pelleted by centrifugation at 400 g and 4 °C for 5 min. Cells were subcultured by diluting in fresh TCM+10%FCS medium at ratios from 1:3 to 1:5.

Irradiation of cell lines

40LB Cells were suspended in 20 ml EH medium and exposed to 120 Gy r-radiation source. After irradiation, cells were re-suspended in TCM+10%FCS and cultivated as description above.

Calcium phosphate transfection of phoenix cells

1.5 Million Phoenix cells were plated to 10 cm culture dish in 10 ml TCM+10%FCS and incubated overnight in a humidified incubator at 37 °C and 10% CO₂. Next day, 25 µM chloroquine (Sigma-Aldrich) was added to cells. To prepare transfection complex to each dish of cells, 12 µg pMSCV plasmid and 3.5 µg pCL-Eco plasmid were dissolved in 450 µl H₂O mixed with 50 µl 2.5 M CaCl₂, adding 500 µl 2x BES dropwise during vortexing. The transfection complex was incubated at 37 °C for 20 min to form calcium phosphate-DNA co-precipitate then applied onto phoenix cells dropwise. After overnight incubation, culture medium was replaced by fresh TCM+10%FCS to detoxify cells from calcium phosphate and chloroquine.

PEI transfection of HEK cells

1.5 Million HEK cells were plated to 10 cm culture dish in 10 ml TCM+10%FCS and incubated overnight in a humidified incubator at 37 °C and 10% CO₂. To prepare transfection complex to each dish of cells, prepare buffer A: 12 µg pMSCV plasmid and 3.5 µg pCL-Eco plasmid were dissolved in 500 µl TCM and buffer B: 20 µl PEI Max (2 mg/ml) was mixed with 500 µl TCM. After incubation for 5 min, buffer A and buffer B were mixed by vortex. The transfection complex was incubated at room temperature for 20 min then applied onto HEK cells dropwise. After overnight incubation, culture medium was replaced by fresh TCM+10%FCS to detoxify cells

Retrovirus collection

The supernatant of transfected cells was collect 48 hr and 72 hr after transfection and filtrated with 0.45 µm filter. There were two methods to prepare the concentrated retrovirus stock. First, the supernatant was concentrated with an Amicon Ultra 15 ml centrifugal filter (cut-off: 100 KDa, Millipore) at 4000 g and 4 °C for 20 min. Alternatively, the supernatant was mixed with 4x Retro/PEG solution as the ratio 1:3 and stored at 4 °C overnight. At the second day, the mixture was centrifuged 1500 g for 30 min at 4 °C to obtain virus pellet. After centrifugation, remove supernatant and re-suspend the virus pellet with certain volume of TCM medium. The concentrated virus was stored at -80 °C until use.

Primary culture and Spin-down retroviral transduction of primary T cells

Splenocytes and lymph node cells were prepared from C57BL/6 mice, SJL mice, 2D2 mice and TCR1640 mice. Splenocytes were treated with ACK for 3 min on ice to removed erythrocytes. The cells were cultivated at 37 °C and 5% CO₂ in RPMI+10%FCS medium, 20 millions of cells per well in 6-well tissue cultured plate (corning) and stimulated with 0.5 µg/ml anti-CD3e and 0.5 µg/ml anti-CD28 antibodies. Recombinant murine IL2 was applied to cells as 10 ng/ml at the second day. T cells were purified either before the primary culturing or 2 days after the culturing. The purification of T cells was followed the instruction of Dynabeads™ Mouse Pan B kit (Thermo Fisher Scientific). Two days after the stimulation, retroviral transduction was performed for T cells. Obtained T cells were re-suspended in RPMI+10%FCS medium containing 8 µg/ml polybrene (Sigma) and 10 ng/ml IL2, mixed with retroviral stock as 5:1 and applied to 12-well no tissue cultured plate (Corning) as 2 million in each well with 500 µl medium. The cells were spinning down at 2000 g in room temperature for 90 min. After centrifugation, 800 µl RPMI+10%FCS medium containing 10 ng/ml IL2 was applied to each well of plate. The cells were incubated in a humidified incubator overnight at 37 °C and 5% CO₂ then analyzed the transduction efficiency by flow cytometry. T cells were harvested and counted at the same day of analysis. Number of transduced T cells was calculated by the transduction efficiency. 10 Million transduced T cells were intravenously transferred to each of the recipients.

Primary B cell culture

One day before B cell cultivation, 40LB cells, as feeder cell, were irradiated as described above and plated as 80% confluence in 10 cm tissue cultured dishes. Splenocytes obtained from mice were treated with ACK buffer for 3 min to remove erythrocytes. B cells were purified as the instruction of mouse B cell isolation kit (Stemcell Technologies) and applied to each dish of 40LB cells as 8×10^5 cells with 40 ml RPMI+10%FCS containing 1 ng/ml recombinant murine IL4. The medium was refreshed at the second day with 1 ng/ml IL4 in RPMI+10%FCS. After 2-days cultivation, B cells were further cultured on irradiated 40LB cells in fresh

RPMI+10%FCS containing 10 ng/ml recombinant murine IL21 (Nojima, Haniuda et al. 2011).

Retroviral transduction of primary B cells

At the second day of cultivated in IL21 containing medium, the stimulated B cells were harvested for retroviral transduction. B cells were re-suspended in RPMI+10%FCS medium containing 8 µg/ml polybrene and 10 ng/ml IL21, mixed with retroviral stock as 5:1 and applied to 12-well no tissue cultured plate (Corning) as 2 million in each well with 500 µl medium. Cells were centrifuged at 2000 g for 90 mins in RT. After centrifugation, 800 µl RPMI+10%FCS medium containing 10 ng/ml IL21 was added to each well of plate. The cells were incubated in a humidified incubator overnight at 37 °C and 5% CO₂ then analyzed the transduction efficiency by flow cytometry.

Cell labeling with carboxy-fluorescein diacetate succinimidyl ester (CFSE)

20 Millions of lymphocytes were suspended in 5 ml PBS containing 1% FCS and 2 µM CFSE (Life technologies) and incubated at 37 °C for 15 min. The falcon tube containing cells was filled to 50 ml by cold EH+10%HS medium and incubated on ice for 5 min to stop the labeling reaction. Cells were collected by 300 g centrifugation at 4 °C for 5 min and washed with cold PBS for once. Then cells were re-suspended in EH medium and ready to transfer to the recipients.

2.2.4 Intravital Imaging for the Small Intestine

Two-photon microscopy

Time-lapse two-photon laser-scanning microscopy was performed using a SP2 confocal microscope (Leica) equipped with a 10 W Millennia/Tsunami laser (Newport Spectra Physics). Excitation wavelength was tuned to 835nm for Twitch2b sensor or 880 nm for NFAT sensor and routed through a 25x water-immersion objective (N.A. 0.95, Leica). Imaging was done with 2x zoom and 25-35 µm z-stacks were acquired with 2-3 µm step size. Acquisition rate was 25.219 s time interval, with images line-averaged twice. Fluorescent signals were detected

using non-descanned photomultiplier tube detectors (Hamamatsu) equipped with 475/50 (CFP), 525/50 (GFP), 537/26 (FRET) and 630/69 (Tetramethylrhodamine) band-pass filters (Semrock). To control the blood flow, 100 μ g tetramethylrhodamine (molecular weight: 2 MDa) (Invitrogen) was intravenously injected to each mouse.

Administration of antibodies

During the intravital imaging, 100 μ g blocking antibodies mixed with 100 μ g tetramethylrhodamine-dextran conjugates (molecular weight: 2 MDa) was intravenously injected to each mouse. Tetramethylrhodamine was used to confirm that the antibody was successfully transferred.

Image analysis

Time-lapse images were acquired using Leica LCS software (Leica), and subsequently processed and analyzed by ImageJ (NIH). To obtain two-dimensional movies, a Gaussian blur filter was applied, the contrast was adjusted by linear rescaling, and maximum intensity z-projections were made. Ratiometric pseudocolor pictures were generated by dividing the FRET by the CFP channel and applying a fire lookup table. For analysis, cell shape at each time point was manually outlined in the maximum projection picture, and average signal intensities of all pixels within this area were calculated. Motility parameters and cell trajectories were calculated from the obtained position coordinates using ImageJ.

2.2.5 Histology

Tissue section

Fresh organs from mice were fixed in 4% PFA overnight and immersed in 35 % sucrose overnight. Tissues were embedded in Tissue-Tec O.C.T. Compound (Sakura), and 20 μ m sections were cut on a CM3050 S Cryocutter (Leica). The sections were stored at -20 °C until use for immunohistochemistry.

Fluorescence immunohistochemistry

Tissue sections were thawed, fixed in 4% PFA for 30 min, and blocked with 1% bovine serum albumin in PBS for 1 h at room temperature. This buffer was used for all further steps. Incubation with primary antibody (dilution 1:100) was done at 4 °C overnight, and with secondary antibody (dilution 1:400) for 1-3 h at room temperature. The sections were washed three times, each for 10 min, in between. Slides were embedded in Fluoromount-G medium (eBioscience). Images were acquired on an SP8X WLL upright confocal microscope (Leica). Individual images were assembled through maximum projection in each channel and then overlaid by ImageJ.

2.2.6 Lymphatic Cannulation

30 min prior to cannulation, 200 µl olive oil was administered by oral gavage to identify mesenteric lymphatic vessels that are located just upstream of the thoracic duct (Druzd, Matveeva et al. 2017). Mice were anesthetized by intraperitoneal injection of fentanyl/midazolam/medetomidine (50 µg/kg, 5mg/kg and 500 µg/kg bodyweight, respectively) and lymph was drawn via a fine bore polythene tubing (Warner Instruments) that had previously been flushed with PBS containing EDTA. Volume of lymphatic solution was recorded and cell numbers were determined together with defined amount of FITC conjugated beads by flow cytometry.

2.2.7 Flow Cytometry

Purification of lymphocytes from peripheral blood

200 µl Blood and 25 µl optiprep (Sigma) were mixed together in an Eppendorf tube. 500 µl PBS was applied carefully on top of the mixture. The gradient solution was centrifuged at 2000 g for 30 min at room temperature, with mild acceleration and no breaking deceleration. The lymphocytes were collected from interface.

Surface staining

Lymphocytes obtained from lymph solution or blood were transferred into 96-well V-bottom plates (Nunc) and washed with 100 μ l FACS buffer by centrifuging at 400 g for 5 min at 4 °C. Antibodies were diluted as 1:200 in the FACS buffer and applied 50 μ l per well. After 30 min incubation on ice, cells were washed twice with FACS buffer. Lastly, cells were suspended in 100 μ l PBS and 100 μ l FITC conjugated beads were added to the cells to re-suspend. Every washing step required a centrifugation at 400 g for 5 min at 4°C.

Intracellular staining

For intracellular staining, cells were stimulated by PMA (10 μ g/ml)/ionomycin (1 μ M) (Sigma) for 2 hr and then incubated in 5 μ g/ml Brefeldin A (Sigma) for another 2 hr. Then, cells were fixed in 2 % PFA for 20 min on ice. Cells were washed in PBS after fixation and then were permeabilized by incubation with permeabilization buffer (Thermo Fisher) on ice for 15 min. The primary antibodies for IFN γ and IL17A were diluted as 1:200 in the permeabilization buffer and added 50 μ l to each well of cells. Cells were incubated on ice for 30min. After washing twice with permeabilization buffer, cells were resuspended in 100 μ l PBS plus 100 μ l FITC conjugated beads.

All samples were measured by FACS VERSE (BD) and data analysis was performed by FlowJo software (FlowJo LLC).

2.2.8 Statistical Analysis

The statistical evaluation was performed using Prism software (GraphPad). Test used, as well as the resulting p value is specified for each experiment separately in the figure legends. Significance was indicated according to the p-value as the following: NS: no significant, * $p < 0.05$, ** $p < 0.01$, *** $p < 0.001$.

RESULTS

3.1 Retroviral Transduction of T cells

3.1.1 Optimization of Retroviral Transduction of Mouse T cells

To visualize the real-time activation of T cells *in vivo* by two-photon microscopy, T cells were genetically labelled to express one of two activation sensors. Twitch2b and NFAT-GFP expressing transgenic mice are not yet available. Therefore, this study utilizes retroviral gene transfer. Previously, by co-culturing with retrovirus producing GP+E86 cells packaged retrovirus, rat T cell lines were successfully transduced with NFAT-GFP or Twitch and used to visualize real-time activation (Pesic, Bartholomaeus et al. 2013, Kyratsous, Bauer et al. 2017). Unfortunately, this method does not work well for mouse T cells. For mouse T cells, the exposure to high titer retrovirus results in efficient transduction (Mues, Bartholomaeus et al. 2013). This latter method was further optimized as follows: Retrovirus containing activation sensors were packaged by transfecting retrovirus plasmid, pMSCV, and packaging plasmid, pCL-Eco, to packaging cells, such as Phoenix cells and HEK cells. Initially, different transfection methods were evaluated. PEI transfection, but not calcium phosphate transfection, of HEK cells allowed for the greatest results. The produced retroviral supernatant was subsequently further concentrated to enhance transduction efficiency. Retrovirus was concentrated by the Amicon centrifugal filter, as this method presented a higher transduction efficiency than precipitation by PEG (Fig.3.1.1).

In addition, the way in which T cells are cultured *in vitro* also affected the efficiency of retroviral transduction. Therefore, different protocols were explored to maximize retroviral transduction. To this end, T cells were purified at different time points, either before T cell stimulation with anti-CD3/CD28 antibodies or after stimulation, just before retroviral transduction. The best result was obtained when T cells are purified before their stimulation (Fig.3.1.1). Combining these methods provided highly efficient transduction, around 12%. Therefore, this protocol was applied to all the retroviral transduction cultures in this study.

3.1.2 Retroviral Transduction of T Cells with NFAT-GFP

In the present work, primary cultured T cells were purified after harvested from spleen and lymph nodes of wildtype or MOG specific TCR transgenic mice, 2D2 and TCR1640 mice. Following stimulation with anti-CD3/CD28 antibodies for 2 days, spin-down transduction was performed as described in the methods section. 24 hrs after transduction, transduction efficiency was confirmed by flow cytometry. Both polyclonal and 2D2 T cells are successfully labelled with NFAT-GFP sensors (Fig. 3.1.2).

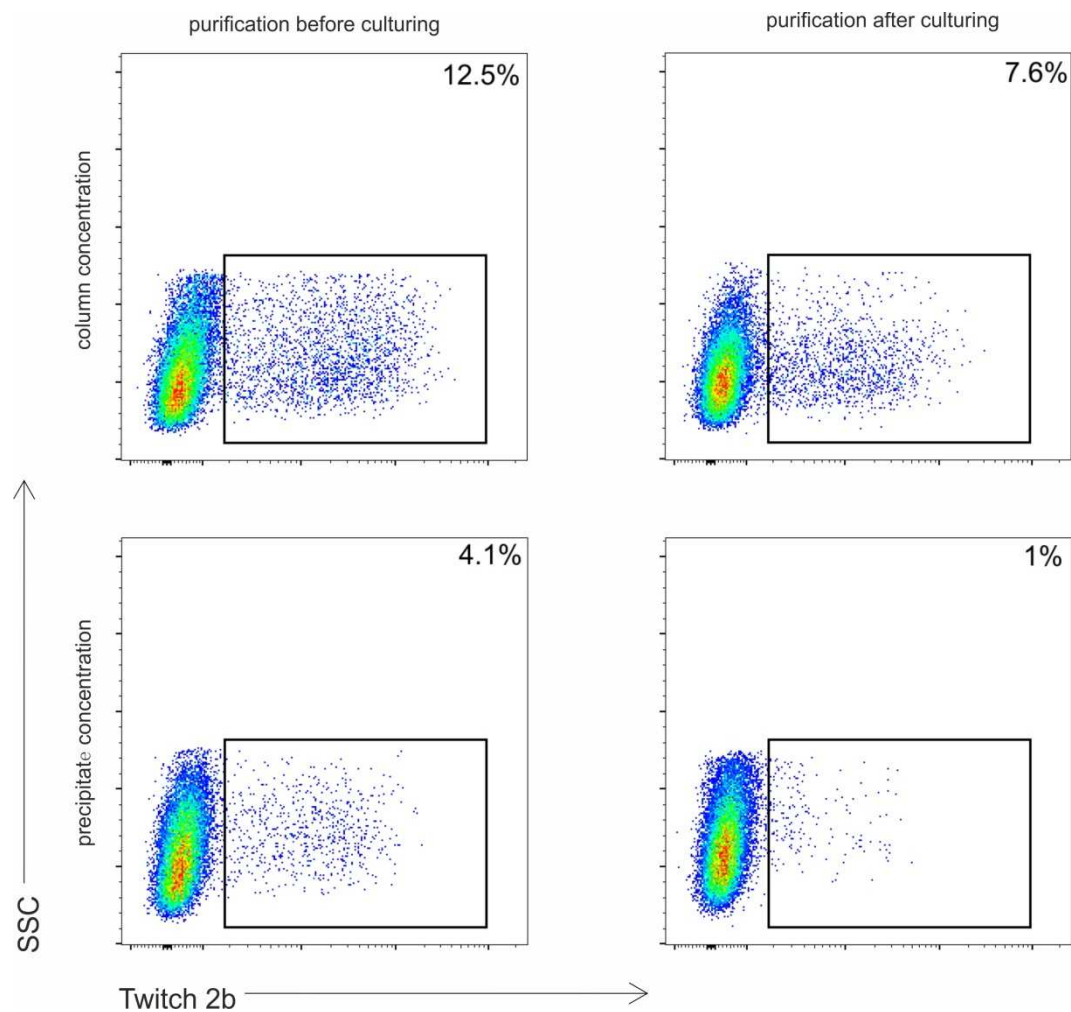


Figure 3.1.1 Retroviral transduction efficiency of polyclonal T cells from SJL/J mice under different conditions. T cells were purified before or after culturing. Twitch2b coding retrovirus was concentrated by centrifugal column or by PEG precipitation. Expression of Twitch2b was analysed 24 hr after transduction. Representative results from 2 independent experiments.

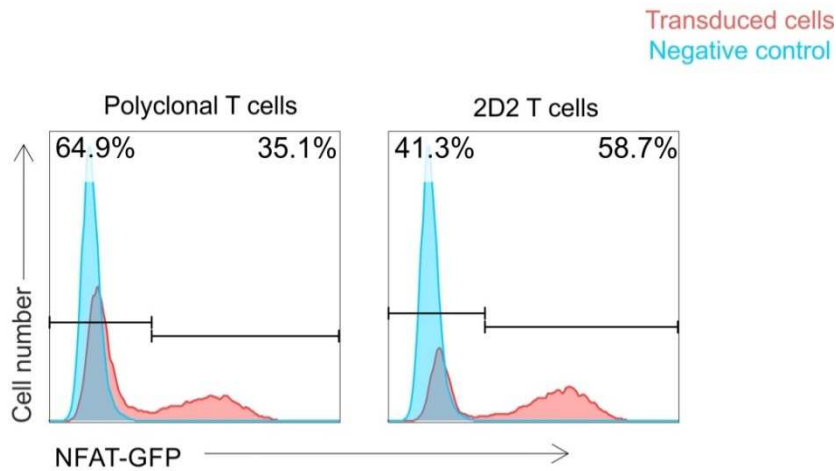


Figure 3.1.2 Representative flow cytometry histograms of NFAT-GFP expression in T cells. Polyclonal T cells or 2D2 T cells were transduced by NFAT-GFP coding retrovirus. Expression of NFAT-GFP was analysed 24 hr after transduction.

3.1.3 Retroviral Transduction of T Cells with Twitch2b

As described above, the Twitch2b sensor delineates the status of T cell activation, through visualization of intracellular calcium levels by two photon microscopy (Mues, Bartholomaus et al. 2013, Thestrup, Litzlbauer et al. 2014). For this reason, primary cultured mouse T cells were genetically labelled by the Twitch2b sensor in the same manner as previously described for the NFAT-GFP sensor. Transduction efficiency was analysed by flow cytometry 24 hrs after the transduction (Fig. 3.1.3).

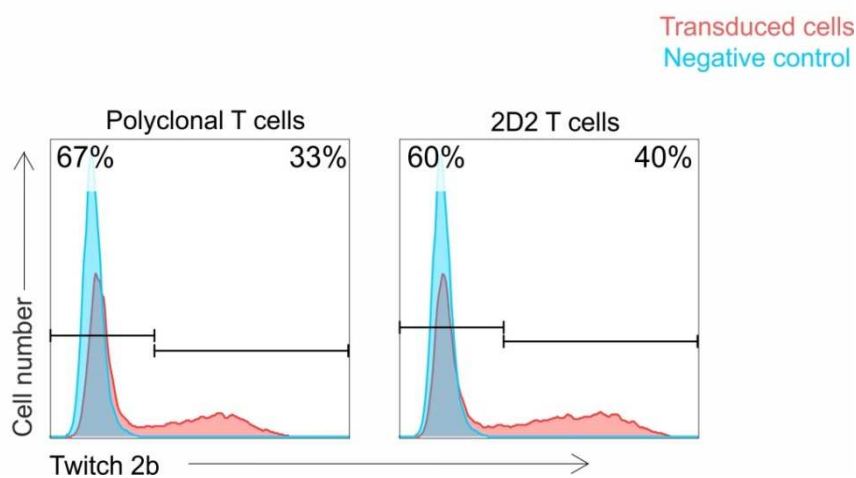


Figure 3.1.3 Representative flow cytometry histograms of Twitch2b expression in T cells. Polyclonal or 2D2 T cells were transduced with Twitch2b coding retrovirus. Expression of Twitch2b was analysed 24 hr after transduction.

3.2 MOG specific T cells in the GALT

3.2.1 GALT Infiltration of T cells

To determine the appropriate time point for intravital imaging of transferred T cells in the GALT, lymphocytes labelled with CFSE were transferred to mice in order to explore the kinetics of GALT cell infiltration. Mesenteric lymph nodes and Peyer's patches were dissected from recipients at different time points after adoptive transfer. The spleen was used as a positive control, as it is known that adoptively transferred T cells migrate efficiently there. Since a mixed population of lymphocytes was used for the adoptive transfer, infiltrating CFSE-labelled lymphocytes were subsequently stained with anti-CD3 and CD19 antibodies to identify T cells and B cells respectively. Phenotype was determined by flow cytometry analysis and the number of cells was quantified by adding a defined number of FITC beads as described in method section.

The number of T cells in Peyer's patches was stable from 24 hr to 7 days after injection, whereas the number in the mesenteric lymph nodes increased up to 48 hrs until it became stable at 7 days after injection (Fig. 3.2.1 A). Based on these results, the third day after injection was selected as the time point of imaging T cells in GALT for the following experiments.

The number of B cells continued to increase in both Peyer's patches and mesenteric lymph nodes from 3 hrs to 7 days after cell transfer (Fig. 3.2.1 B). Therefore, intravital imaging of B cells in the GALT could be performed at the earliest 7 days after the cells transfer.

The total number of CFSE labelled lymphocytes infiltrating the GALT was also quantified. Generally, the number of lymphocytes constantly increased with time in the Peyer's patches and mesenteric lymph nodes (Fig. 3.2.1 C).

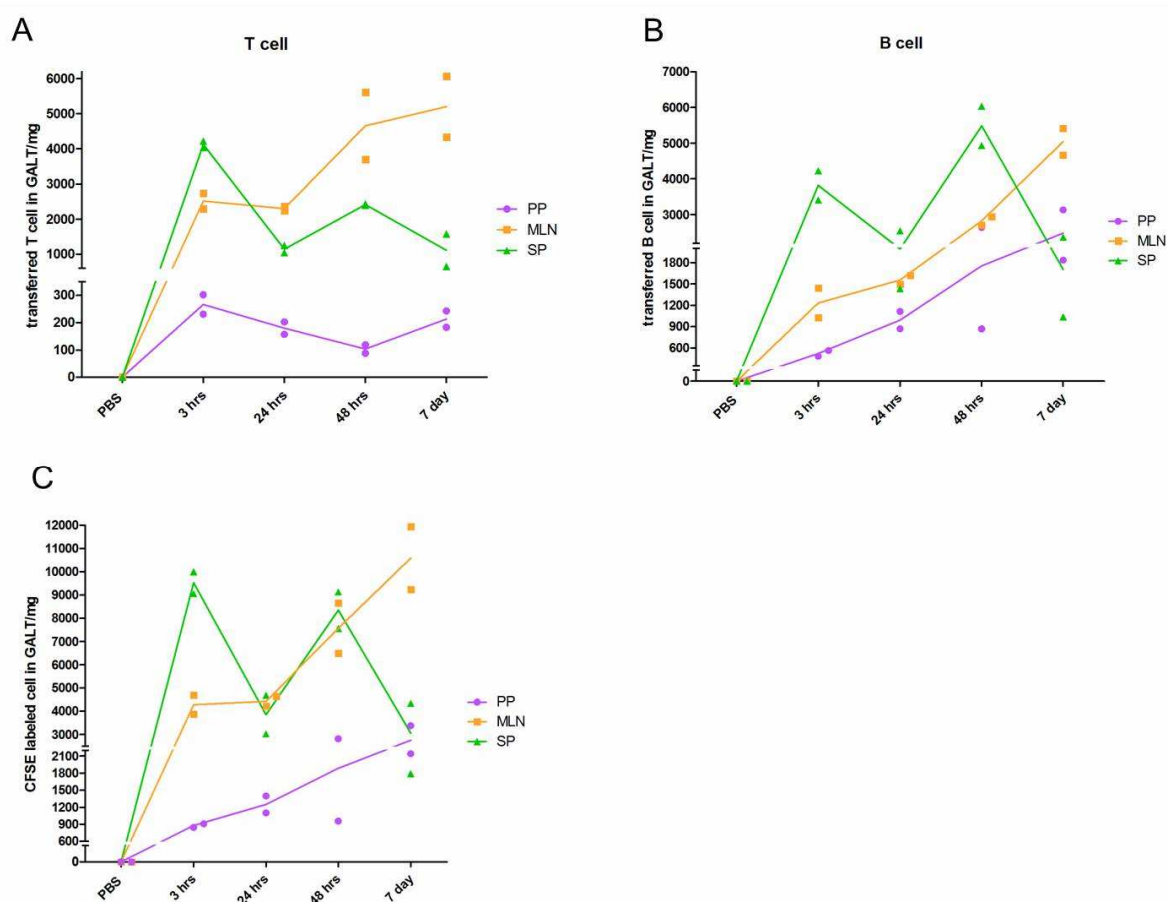


Figure 3.2.1 Kinetics of GALT infiltrating lymphocytes. Dynamics of transferred T cells (A), B cells (B) and total lymphocytes (C) in the Peyer's patch (PP), mesenteric lymph node (MLN) and spleen (SP) were analyzed 3 hr, 24 hr, 48 hr and 7 days after i.v. injection. Each time point/group contains two animals. Results are representative of 3 independent experiments.

3.2.2 Establishment of Surgical Setup for Imaging Intestine

Applying intravital imaging in the intestine is difficult as intestinal peristalsis greatly interferes with the stability of the visual field. To overcome this challenge, a special surgical setup was established in this study. Mice were anaesthetized by intraperitoneal injection of fentanyl/midazolam/medetomidine (50 $\mu\text{g}/\text{kg}$, 5 mg/kg , and 500 $\mu\text{g}/\text{kg}$ bodyweight, respectively), orotracheally intubated, and ventilated with 1% isoflurane. Mice were placed on a custom-made microscope stage and the body temperature was regulated by a heated pad and thermo-sensor (37 $^{\circ}\text{C}$). Electrocardiograms were recorded and physiological parameters, such as concentrations of inspiratory and expiratory gases, and ventilation pressure were constantly monitored during imaging. The small

intestine was exposed as showing in figure 3.2.2, which was coated with agarose, stabilized by tissue adhesive glue (3M Animal Care Products), and a cover slip mounted with gentle pressure (Fig. 3.2.2 A). This setup was for imaging the PP from the intestinal wall side. For imaging the lamina propria, the lumen side of the ileum was exposed by a cautery pen-created incision in order to prevent bleeding. Intestinal contents were removed carefully by tutofusin (Baxter) rinsing. The lamina propria was stabilized on top of tutofusin buffer rinsed tissue paper through surrounding the exposed area with tissue adhesive glue and carefully mounting a cover slip. This surgical setup ensures the preservation of both the morphology and blood flow of the lamina propria (Fig. 3.2.2 B). In addition, this setup is also suitable for imaging Peyer's patch from lumen side.

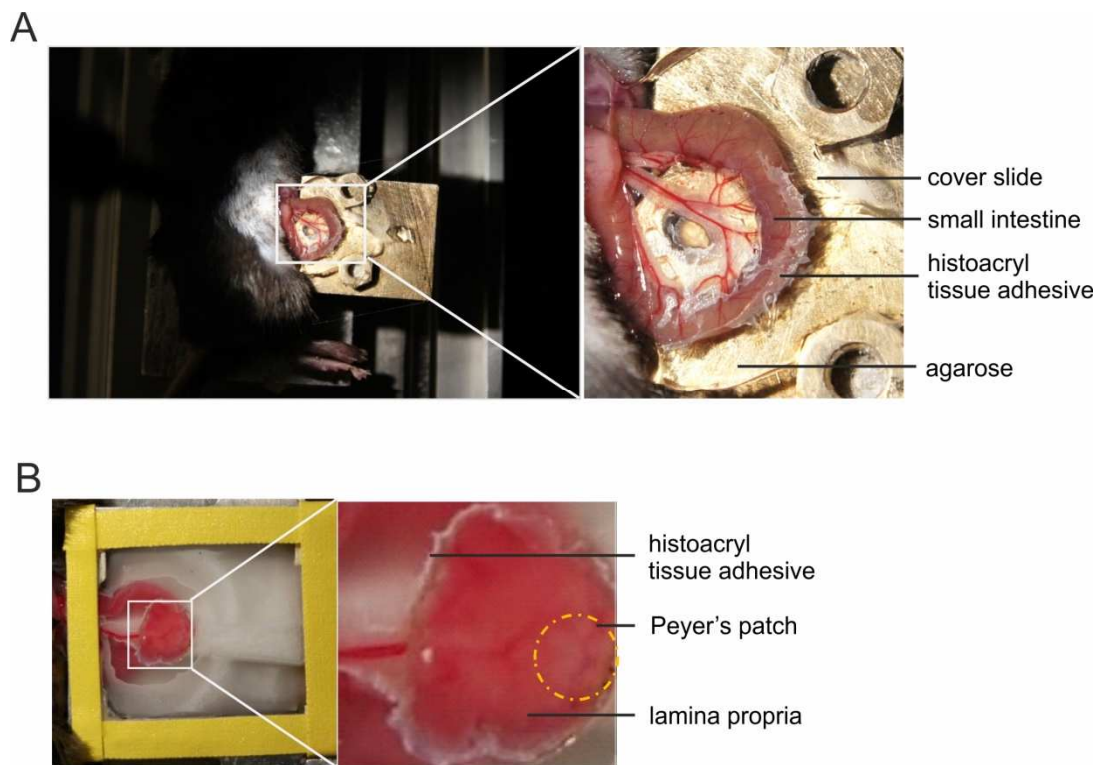


Figure 3.2.2 Surgical setup for intravital imaging of Peyer's patches and lamina propria. A. The surgical setup for imaging Peyer's patches from the intestinal wall side. The intestine was surrounded by agarose and stabilized by tissue adhesive glue. **B.** The surgical window for imaging both the lamina propria and Peyer's patches from the lumen side. Tissue adhesion was applied at the periphery of the exposed tissue to allow for stabilization without disturbing the central area. The pressure used to mount the coverslip on the tissue was regulated by adjusting the height of the coverslip.

3.2.3 Intravital Imaging of MOG Specific T Cells in the Lamina Propria

Twitch2b labelled 2D2 T cells were intravenously transferred to wildtype C57BL/6 mice. In parallel, Twitch2b labelled polyclonal T cells from C57BL/6 mice were transferred to the littermates in order to evaluate the importance of antigen specificity. Intravital imaging of the lamina propria was performed 3 days after the adoptive transfer.

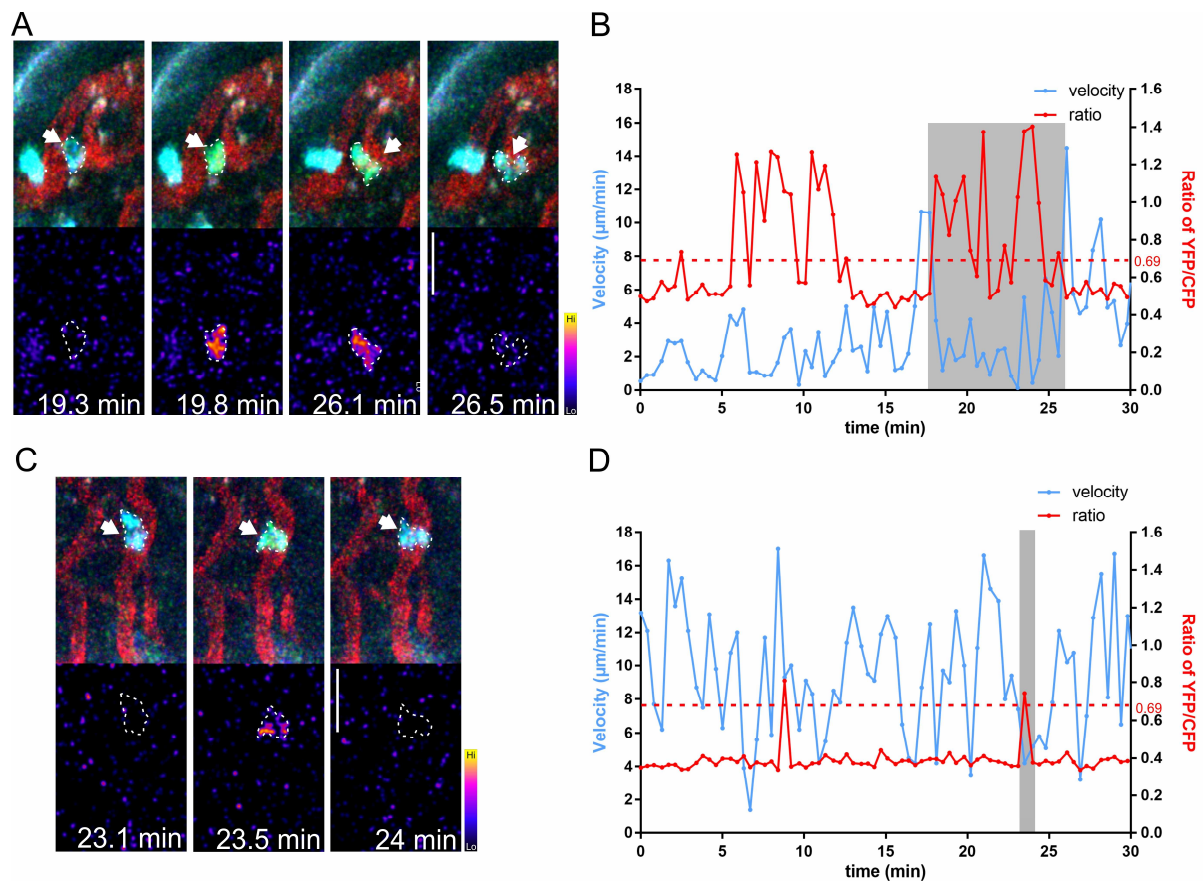


Figure 3.2.3 Calcium imaging of T cells in the lamina propria. A and C. Series of pictures shows long calcium signaling in a 2D2 T cell (A) and short calcium signaling in a polyclonal T cell (C). The cell of interest is indicated with arrows in fluorescent overlay pictures (upper) and outlined in pseudocolour ratio images (lower). Blood vessels labelled in red with Rhodamine; T cells labelled in blue/green with Twitch2b; Scale bar, 20 μm . **B and D.** Time course tracking of a representative 2D2 T cell showing long calcium signaling (A) and a polyclonal T cell showing short lasting calcium signaling (D). Intracellular calcium fluctuation (red line) and velocity (blue line). Gray shadow indicates the time window shown A and C.

The Twitch2b sensor depicts cytosolic calcium levels through quantifying the ratio of YFP/CFP fluorescence. Therefore, in order to define calcium signals, it is necessary to set a threshold for YFP/CFP. In the present study, the threshold was defined as a ratio of 0.69 which is a threshold that 95% of the polyclonal T cells in the lamina propria are below.

According to this threshold, high calcium signals occurred more frequently in 2D2 T cells than in polyclonal T cells in the lamina propria (Fig. 3.2.3). A representative example of 2D2 T cells showing continuous calcium signaling in the lamina propria of ileum was illustrated (Fig. 3.2.3 A and B). In contrast, polyclonal T cells showed only short calcium signaling (Fig. 3.2.3 C) which lasted typically less than 1 min (Fig. 3.2.3 D).

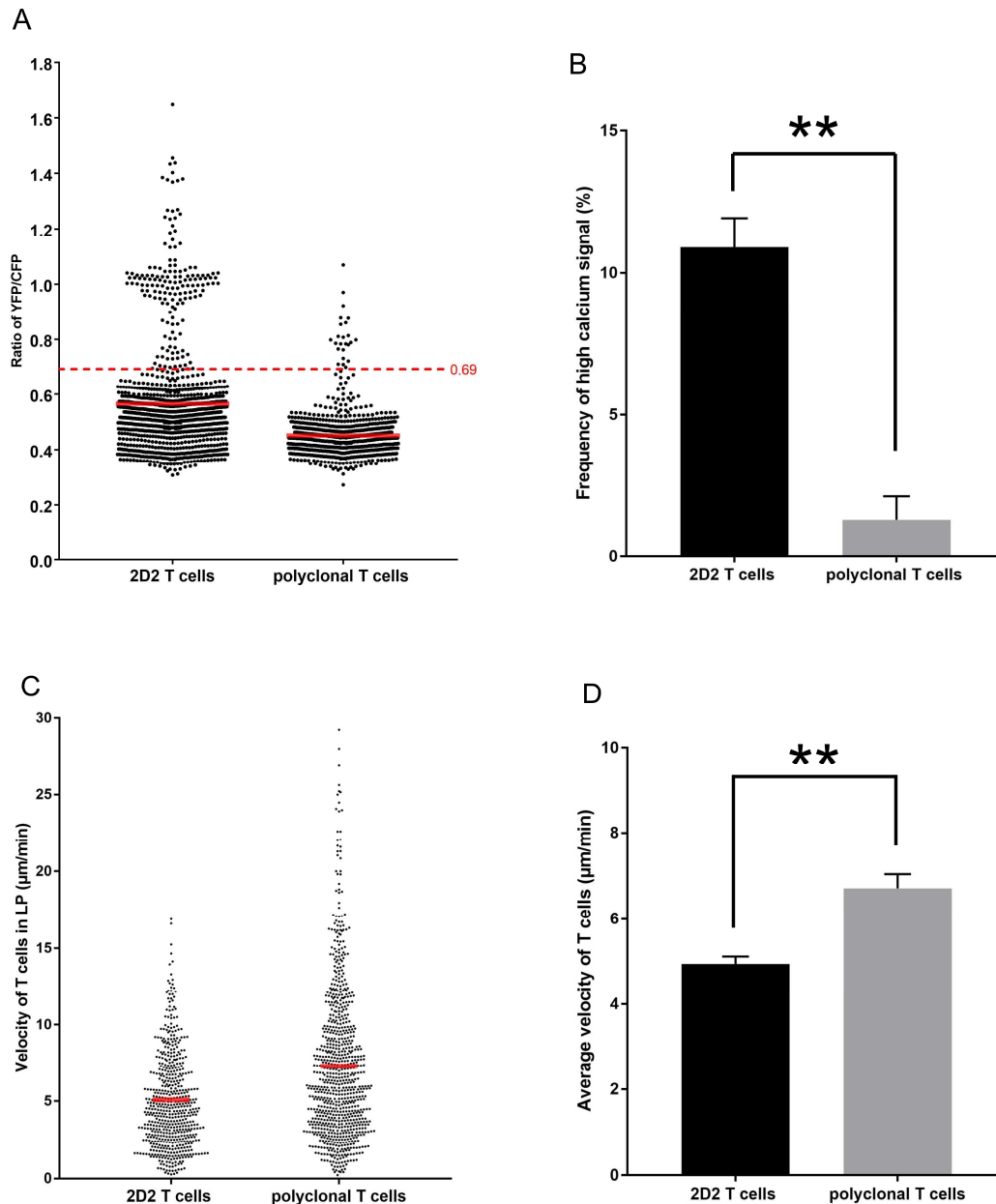


Figure 3.2.4 Analysis of calcium level and velocity of 2D2 T cells and polyclonal T cells in the lamina propria. **A.** A representative cumulative calcium levels (ratio of YFP/CFP) in 2D2 T cells and polyclonal T cells from 3 experiments are shown. **B.** Percentage of high calcium signal in 2D2 T cells and polyclonal T cells. **C.** A representative plot of velocity of 2D2 T cells and polyclonal T cells from 3 experiments is shown. **D.** Average velocity of 2D2 T cells and polyclonal T cells. In A and C, each dot represents the calcium level (A) or velocity (C) at a given time point and red lines indicate the mean. In B and D, means \pm SEM from three independent experiments are shown. Statistical differences were analysed by independent sample T-test.

All FRET and motility values from 2D2 and polyclonal T cells were plotted in Fig. 3.2.4. in the lamina propria, the ratio values of for YFP/CFP in 2D2 T cells were significantly higher than polyclonal T cells (Fig. 3.2.4 A). 2D2 T cells showed high calcium signals more frequently than polyclonal T cells (Fig. 3.2.4 B). High calcium signal occurred in 2D2 T cells was around 11%, which is 8 times more than in polyclonal T cells (Fig. 3.2.4 B). Additionally, motility of 2D2 T cells in lamina propria was slower than motility of the polyclonal T cells (Fig. 3.2.4 C and D).

The duration of high calcium signal persisting in 2D2 T cells and polyclonal T cells in lamina propria was also compared (Fig. 3.2.5). 2D2 T cells presented longer lasting high calcium signal in the lamina propria than polyclonal T cells. Several 2D2 T cells showed continuous calcium signaling, which suggested that T cells got stimulated in the lamina propria. In contrast, most of the calcium signaling shown by polyclonal T cells was shorter than 2 mins (Fig. 3.2.5 A).

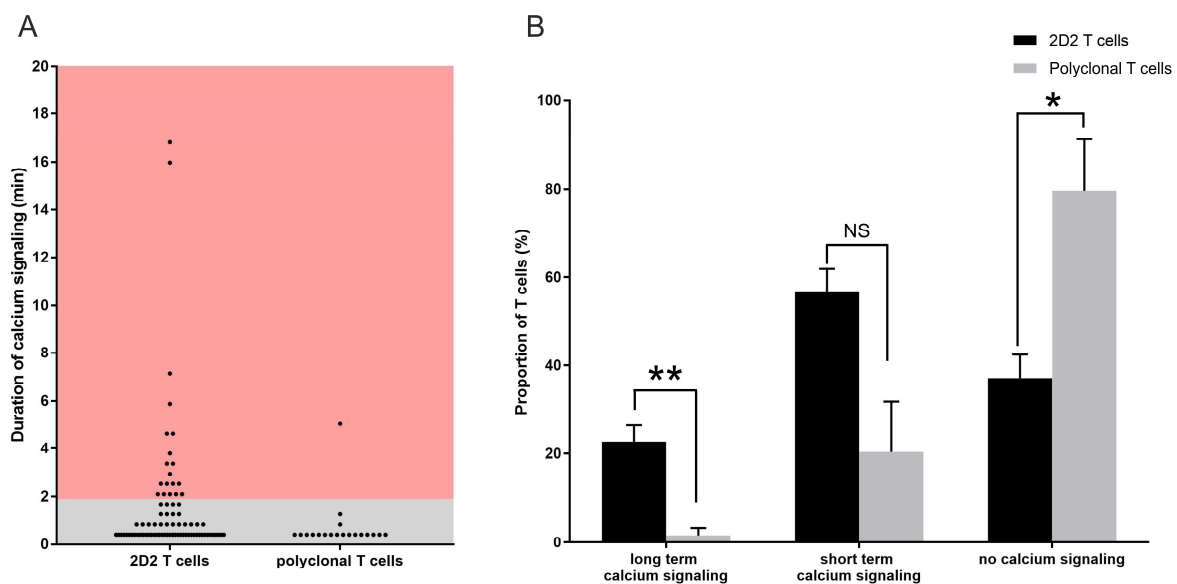


Figure 3.2.5 Duration of calcium signaling in 2D2 T cells and polyclonal T cells in the lamina propria. **A.** Each cumulative plot represents the duration of calcium signaling in 2D2 or polyclonal T cells. Each dot represents a single calcium signaling event. Sum of 3 experiments are shown. **B.** The proportion of calcium signaling duration in 2D2 vs. polyclonal T cells. Mean \pm SEM from 3 independent experiments are shown. Statistical differences were analysed by independent sample T-test.

In order to extract more details, the duration of calcium signaling was further analysed (Fig. 3.2.5 B). First, the percentage of T cells with long term high calcium signal (>2 min) was analysed. Out of 60 2D2 T cells and 56 polyclonal T cells in the lamina propria from 3

independent experiments, 19 2D2 T cells (20%) presented continuous calcium signaling whereas only one polyclonal T cell presented continuous calcium signaling (Fig. 3.2.5 B). Secondly, short calcium signaling (<2min) was analysed. There was no significant difference in short calcium signaling between 2D2 T cells and polyclonal T cells (Fig. 3.2.5 B). However, there is a significantly greater number of polyclonal T cells that show no calcium signaling (~80%) (Fig. 3.2.5 B).

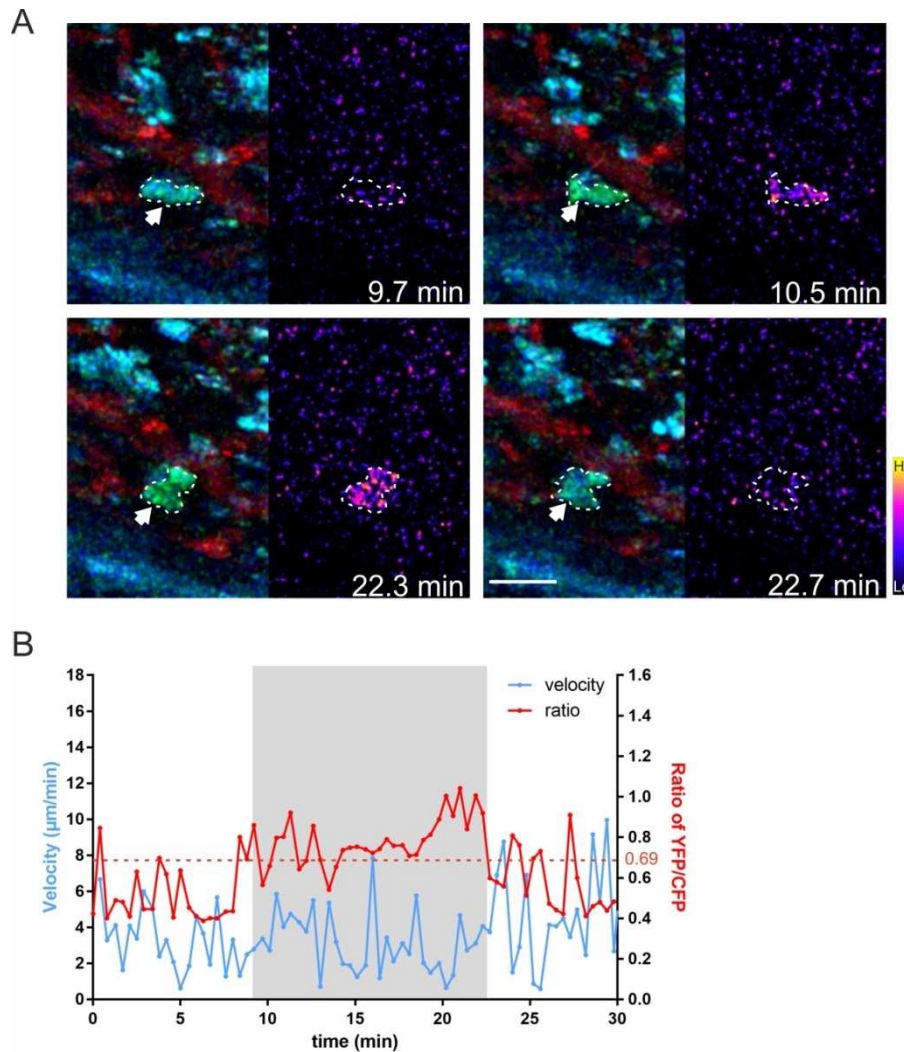


Figure 3.2.6 Calcium imaging of TCR1640 T cells in the lamina propria. **A.** Representative images of a TCR1640 T cell showing long calcium signaling that lasts around 12 min. Arrows in fluorescent overlay (left) and dotted outlines in pseudocolour ratio images (right) indicate a cell of interest. Blood vessels are labelled in red with Rhodamine; T cells are labelled in blue/green with Twitch2b; Scale bar, 10 μm . **B.** Time course tracking of a TCR1640 T cell. Intracellular calcium fluctuation (red line) and velocity (blue line). Gray shadow indicates the time window visualized in **A**.

In addition to imaging 2D2 T cells, TCR1640 T cells in the lamina propria were also investigated by two-photon microscopy. As described above, 2D2 T cells express a TCR that

recognizes MOG peptide 35-55, whereas TCR1640 T cells contain a TCR that recognizes MOG peptide 92-106. Therefore, probing TCR1640 T cells functionality in the lamina propria provides further insight into antigen specificity and T cell stimulation.

TCR1640 T cells were transduced with Twitch2b coding retrovirus by using the same method as 2D2 T cells, and then intravenously transferred to wildtype SJL/J mice. Intravital imaging was performed 3 days after the transfer. Similar to 2D2 T cells in C57BL/6 mice, TCR1640 T cells show calcium signaling in lamina propria more frequently than polyclonal T cells from SJL/J mice (Fig. 3.2.6 and Fig. 3.2.7).

Calcium signals from TCR1640 and polyclonal T cells were displayed in figure 3.2.7 A. Similar to 2D2 T cells, a greater number of TCR1640 T cells were above threshold than polyclonal T cells in the lamina propria of ileum (Fig. 3.2.7 A). Furthermore, TCR1640 T cells undergo High calcium signals more frequently than polyclonal T cells (Fig. 3.2.7 B). High calcium signal was observed in approximately 14% of TCR1640 T cells – a significantly greater percentage than polyclonal T cells (Fig. 3.2.7 B). Additionally, duration of continuous calcium signaling in TCR1640 T cells and polyclonal T cells in the lamina propria was analysed (Fig. 3.2.7 C and D). Compared with polyclonal T cells, TCR1640 T cells showed longer calcium signaling in the lamina propria, suggesting stimulation (Fig. 3.2.7 C). This duration of calcium signaling was analysed in further details (Fig. 3.2.7 D). In total, 59 TCR1640 T cells and 59 polyclonal T cells in the lamina propria from 3 independent experiments were analysed. Similar to the relationship between 2D2 T cells and polyclonal T cells, a statistically greater proportion (25%) of TCR1640 T cells show long term calcium signaling compared to polyclonal T cells (Fig. 3.2.7 D). Additionally, there was no significant difference between TCR1640 T cells and polyclonal T cells with short calcium signaling (<2min) and no calcium signaling (Fig. 3.2.7 D).

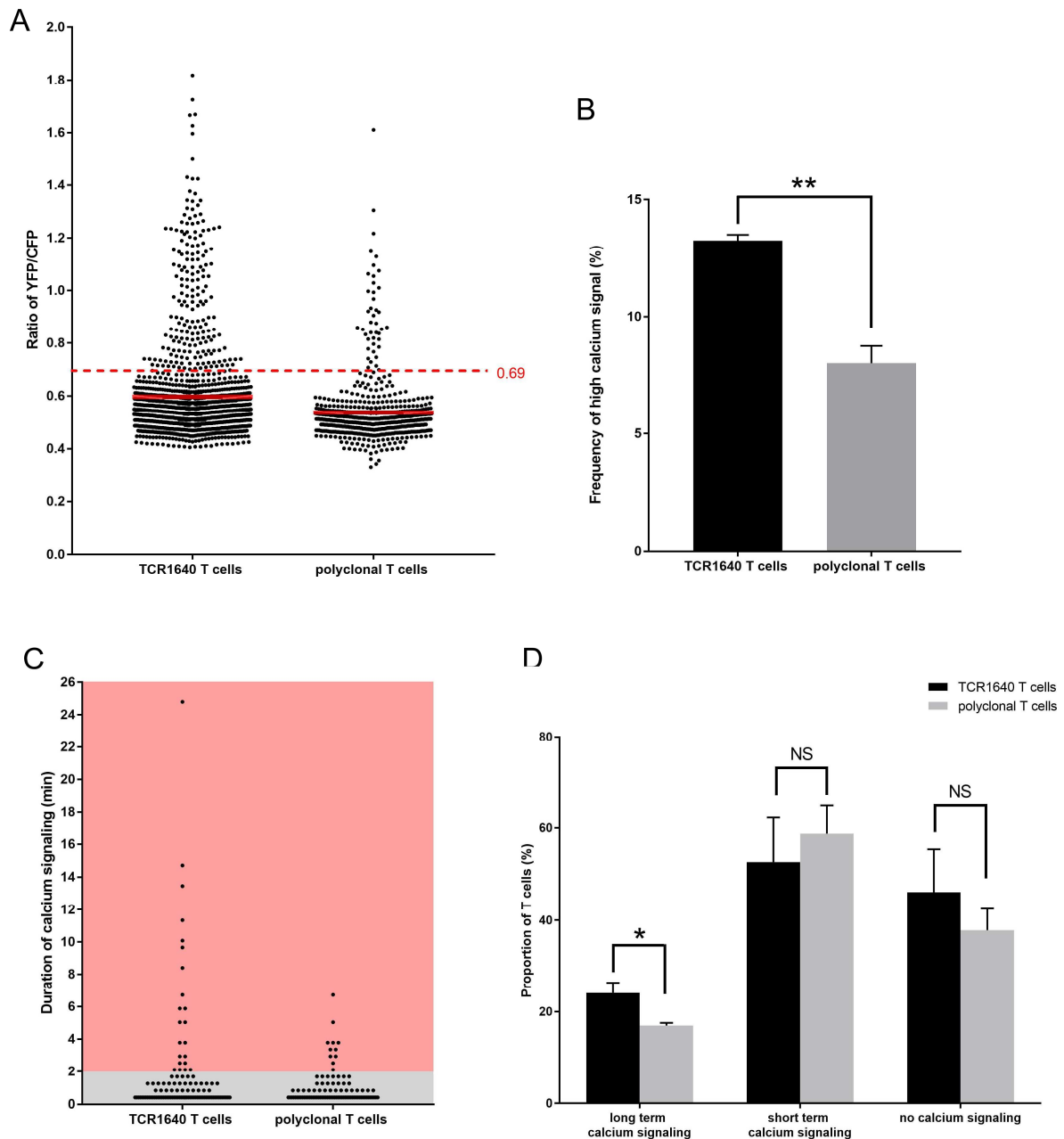
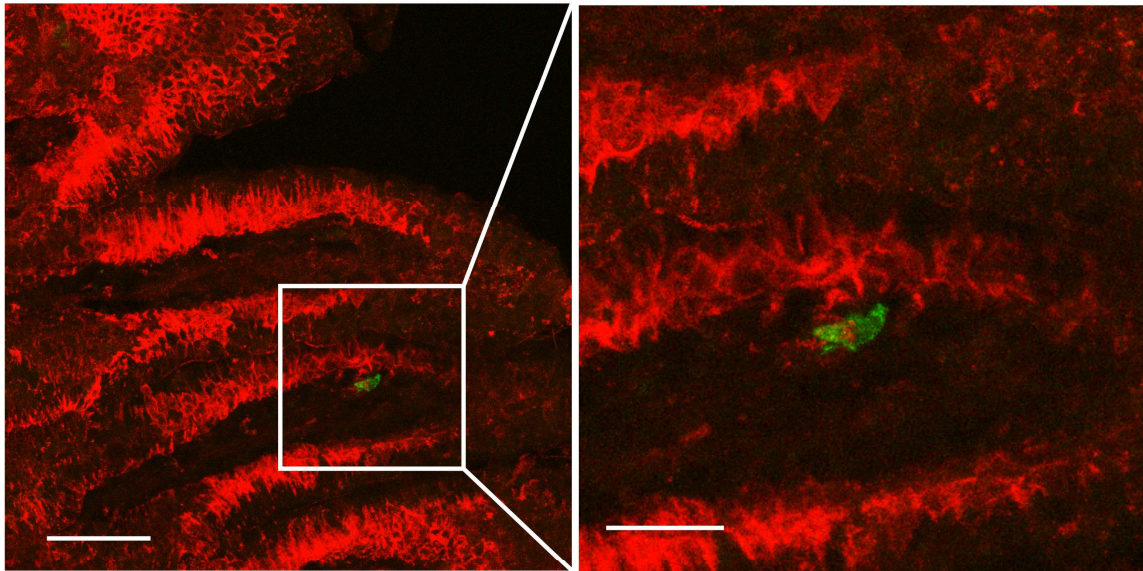


Figure 3.2.7 Analysis of calcium signaling in TCR1640 T cells and polyclonal T cells in the lamina propria. A. Representative cumulative calcium levels (ratio of YFP/CFP) in TCR1640 T cells and polyclonal T cells. Each dot represents a calcium level shown by a single cell in each time point. **B.** Percentage of high calcium signal in TCR1640 T cells and polyclonal T cells. **C.** Duration of calcium signaling in TCR1640 or polyclonal T cells. Each dot represents a duration of a calcium signaling event. **D.** Proportion of T cells with different calcium signaling duration in TCR1640 or polyclonal T cells. In A and C, cumulative results from 3 experiments are shown. In B and D, mean \pm SEM from 3 independent experiments are shown. Statistical differences were analysed by independent sample T-test.

Following the identification of continuous calcium signaling in MOG specific T cells in the lamina propria, the possibility that stimulation induces NFAT nuclear translocation was

investigated. Precise detection of the subcellular location of NFAT-GFP requires high resolution. Therefore, confocal imaging was performed instead of two-photon intravital imaging.

A



B

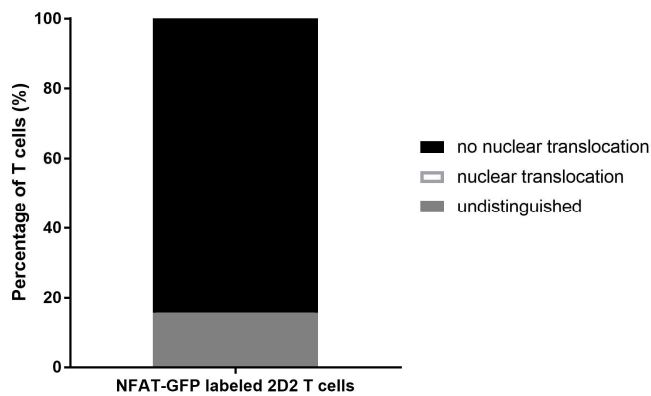


Figure 3.2.8 A. A representative image of NFAT-GFP labelled 2D2 T cells in the lamina propria of ileum. Image on the left shows an overview of villi within the lamina propria, scale bar, 50 μ m. Image on the right is a high magnification view of the villi, scale bar, 20 μ m. Epithelial cells are shown in red by anti-Ep-CAM antibody, T cells are shown in green by NFAT-GFP. **B.** Analysis of nuclear translocation of NFAT-GFP labelled 2D2 T cells in lamina propria of ileum. The graph contains 19 cells from 3 experiments

MOG specific 2D2 T cells were transduced with NFAT-GFP sensor coding retrovirus and transferred to C57BL/6 mice. 3 Days later, the ileum of the recipient was fixed by 4% PFA and 20 μ m cryosections were prepared. Epithelial cells were stained by anti-Ep-CAM

antibody in order to elucidate tissue structure and images were acquired by confocal microscopy. NFAT-GFP labelled MOG specific T cells in the lamina propria of the ileum did not show nuclear translocation (Fig. 3.2.8). In total, 19 NFAT-GFP labelled 2D2 T cells in the lamina propria of the ileum were imaged and analysed, of which none showed nuclear translocation in the lamina propria of ileum (Fig. 3.2.8 B).

3.2.3 MOG Specific T Cells in the Peyer's Patch of the Small Intestine

As introduced in the previous context, Peyer's patch is one of the most important immune organs in the small intestine. Therefore, calcium fluctuation of MOG specific T cells was also investigated there. Similarly to previous experiments in the lamina propria, Twitch2b labelled 2D2 T cells or polyclonal T cells from C57BL/6 mice were intravenously transferred to wildtype C57BL/6 mice. Intravital imaging of Peyer's patch was performed 3 days after the adoptive transfer.

The Peyer's patch demonstrates a different level of background calcium signals from lamina propria. Therefore, the threshold ratio of YFP/CFP was redefined as 0.73 in Peyer's patch-- which 95% of polyclonal T cells are below. No difference in calcium events was observed between 2D2 T cells and polyclonal T cells (Fig. 3.2.9). One Twitch2b labelled 2D2 T cell in the Peyer's patch was shown as a representative example (Fig.3.2.9 A). Continuous calcium signaling lasting around 2 mins was observed, but the signaling was much shorter than the events detected in the lamina propria. FRET values from 2D2 T cells and polyclonal T cells were further plotted and analysed. The ratio values of YFP/CFP and the frequency of high calcium signals in 2D2 T cells were similar to polyclonal T cells (Fig. 3.2.9 B and C). High calcium signal was observed in around 5% of total calcium datasets in both 2D2 T cells and polyclonal T cells (Fig.3.2.9 C). This is fewer than that observed in the lamina propria of the ileum (Fig. 3.2.4 B and Fig. 3.2.7 B). In addition, the duration of calcium signaling was analysed in more detail by using 55 2D2 T cells and 99 polyclonal T cells in Peyer's patch from 3 independent experiments (Fig.3.2.9 D). No significant difference was observed in the proportion of T cells across the tree categories of calcium signaling: long term, short term and no signaling (Fig. 3.2.9 D).

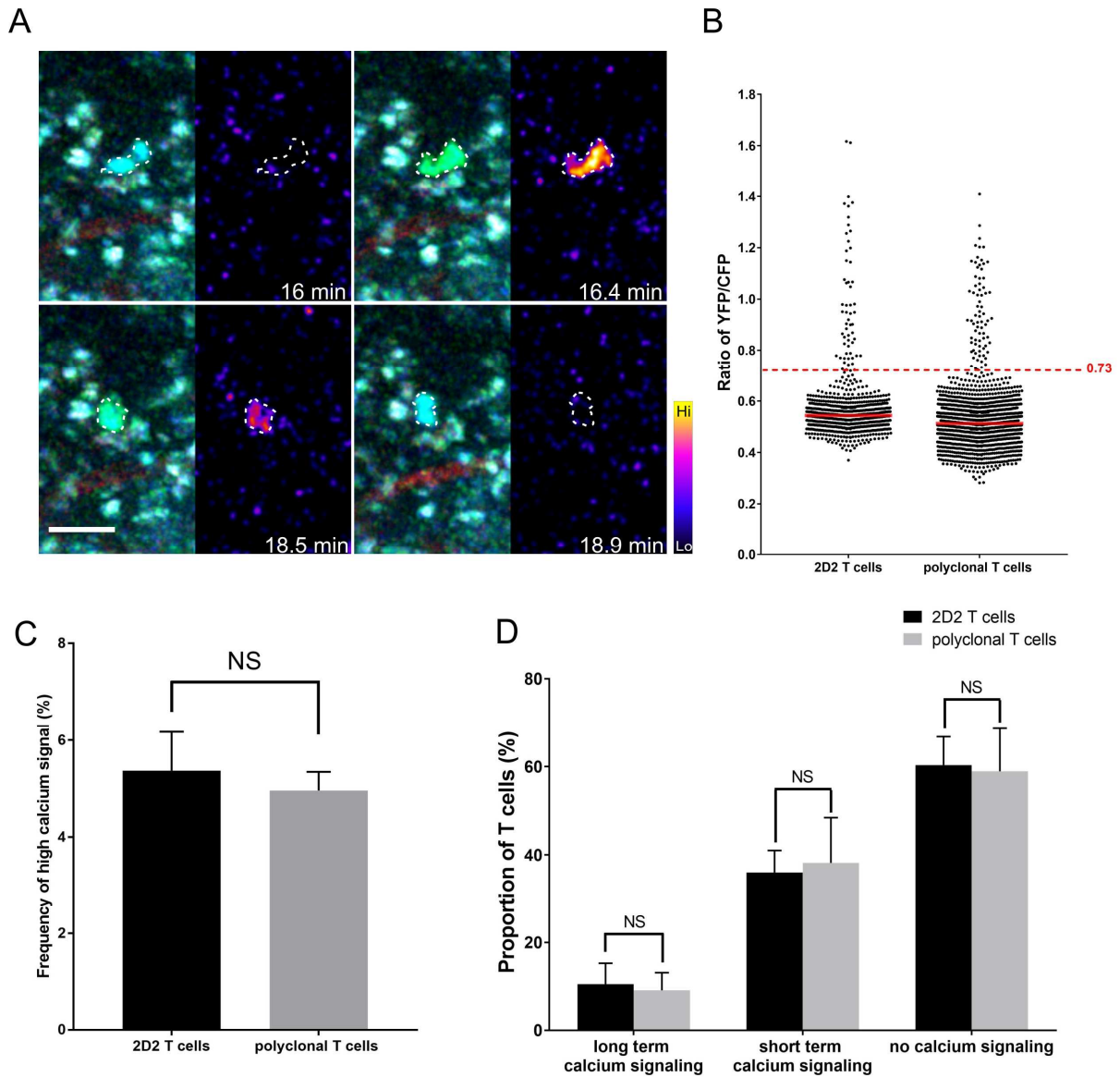


Figure 3.2.9 Calcium imaging and analysis of 2D2 T cells in the Peyer's patch. **A.** Representative images of a 2D2 T cell showing continuous calcium signaling lasting ~2 min. Dotted outlines in fluorescent overlay (left) and pseudocolour ratio images (right) indicate a cell of interest. Blood vessels are labelled in red with Rhodamine; T cells are labelled in blue/green with Twitch2b; Scale bar, 20 μ m. **B.** Representative calcium signals (ratio of YFP/CFP) in 2D2 T cells and polyclonal T cells in Peyer's patch from 3 experiments are shown by cumulative plot. **C.** Percentage of high calcium signal in 2D2 T cells and polyclonal T cells. **D.** Proportion of T cells with different calcium signaling duration in 2D2 or polyclonal T cells. In C and D, mean \pm SEM from 3 independent experiments are shown. Statistical differences were analysed by independent sample T-test.

2D2 T cells transduced with the NFAT-GFP sensor were also imaged in the Peyer's 3 days after cell transfer. Representative images of NFAT-GFP labelled 2D2 T cells in Peyer's patch were shown in figure 3.2.10 A. 52 2D2 T cells in total were analysed in Peyer's patch. However, no nuclear translocation of NFAT was observed (Fig. 3.2.10 B).

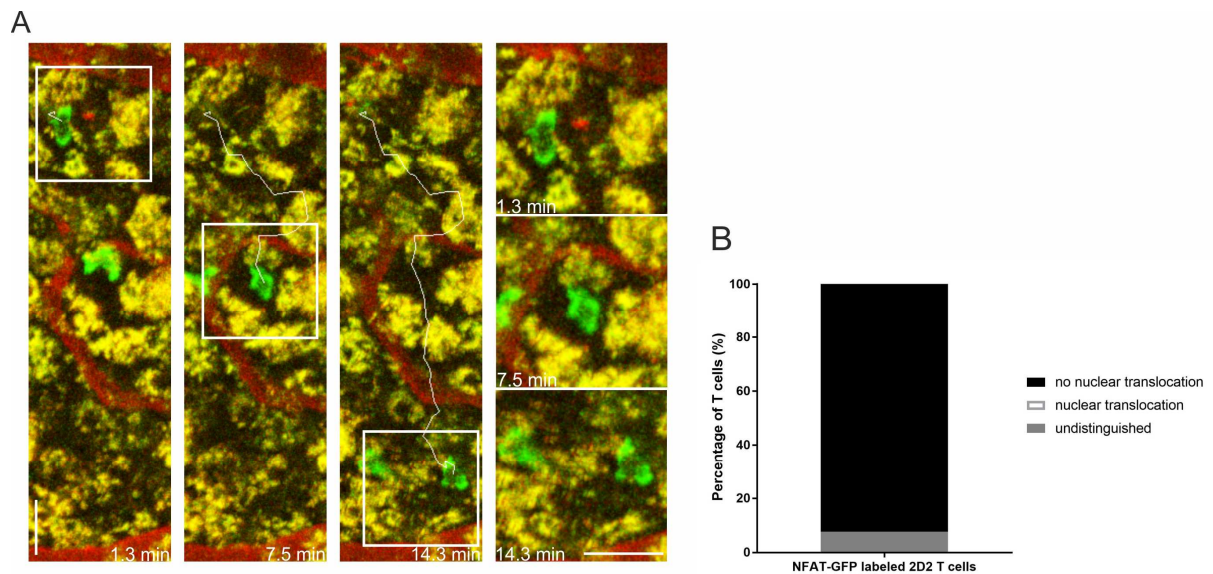


Figure 3.2.10 NFAT-GFP labeled 2D2 T cells in Peyer's patch. A. Representative time lapse tracking of NFAT-GFP labeled 2D2 T cells in the Peyer's patch. Blood vessels are labeled in red with Rhodamine; 2D2 T cells are labeled in green with NFAT-GFP; Yellow is due to autofluorescent signal from Peyer's patch. Scale bar: 15 μ m. B. Analysis of nuclear translocation of NFAT in 2D2 T cells in Peyer's patch. The graph contains 52 cells from 3 experiments

3.3 Phenotypes of Encephalitogenic T Cells from the Mesenteric Lymph

3.3.1 Th17 Cells Emigrated from the Mesenteric Lymph

The persistent calcium signaling seen in 2D2 T cells suggests lamina propria specific stimulation. Therefore, MOG specific T cells in the efferent lymphatic vessel from mesenteric lymph nodes were probed to examine phenotypic changes due to stimulation in the lamina propria. Lymphatic cannulation was performed to the efferent lymph vessel located upstream of the thoracic duct in order to obtain the T cells emigrating from intestine (Druzd, Matveeva et al. 2017). Cellular phenotype was assessed with emphasis on cellular markers known to influence CNS infiltration and inflammation. With the given antigen of interest, it is particularly intriguing to consider how GALT associated phenotypic changes in T cells may contribute to the pathogenesis of EAE.

Nowadays, Th17 cells have been considered the most important driver in autoimmune disease. Therefore, IL17A expression was analysed in CD4⁺ cells. The T cells from 2D2 mice

were compared with those from wildtype mice. 2D2 T cells were further gated for expression of V α 3.2 and V β 11, which is expressed on MOG specific transgenic T cells. In the lymph sample, 2D2 mice expressed a significantly higher percentage of Th17 cells compared with C57BL/6 mice (Fig. 3.3.1 A, B).

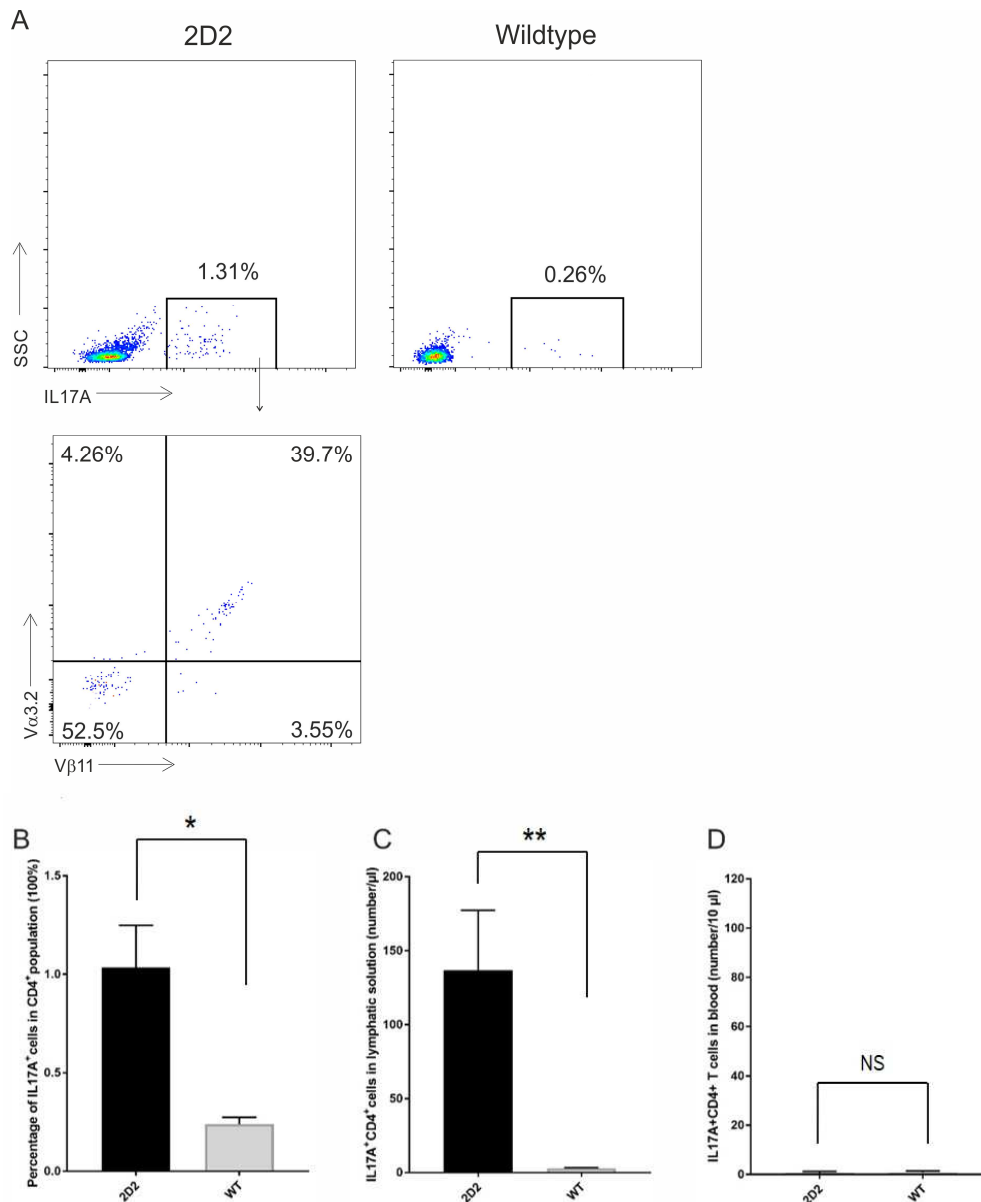


Figure 3.3.1 Expression of IL17A in T cells emigrating from the mesenteric lymph. **A**. CD4⁺ T cells from 2D2 mice and WT mice were evaluated by IL17A staining and analysed by flow cytometry. Representative flow cytometry plots from 3 experiments are shown. **BC**. Percentage (**B**) and concentration (**C**) of IL17A⁺CD4⁺ T cells from efferent mesenteric lymph of 2D2 and wildtype mice. **D**. Concentration of IL17A⁺CD4⁺ T cells in the blood of 2D2 and wildtype mice serves as a control for the cells obtained from the lymph vessel. 2D2 lymph sample: n=5; wildtype lymph sample: n=6; 2D2 blood sample: n=4; wildtype blood sample: n=6; Dataset was analysed by independent sample T-test. Values represent means \pm SEM.

The concentration of IL17 producing T cells (Th17 cells) in the lymph sample was also analysed. By adding defined number of FITC-conjugated beads, the cell number in each sample can be quantified by flow cytometry. By considering the mixture as homogeneous, the actual number of cells in the defined volume of lymph sample could be quantified from the number of beads detected by flow cytometry. The concentration of Th17 cells in the lymph of 2D2 mice was 20 times higher than that found in the lymph of C57BL/6 mice (Fig. 3.3.1 C). As a control, the concentration of Th17 cells in peripheral blood was analysed. There were very few Th17 cells in the blood and no significant difference between 2D2 mice and C57BL/6 mice (Fig. 3.3.1 D).

3.3.2 Th1 Cells Efferent from the Mesenteric Lymph

IFN γ -producing CD4⁺ T cells (Th1 cells) have been well characterized as another instigator of EAE (Pierson, Simmons et al. 2012). Adoptive transfer of *in vitro* differentiated Th1 cells is capable of inducing EAE (Baron, Madri et al. 1993). In addition, loss of T-bet, a transcription factor that controls the expression of IFN γ , has been found to contribute the resistance to EAE in mice (Bettelli, Sullivan et al. 2004). Therefore, Th1 cells were also quantified in the lymph of 2D2 mice and C57BL/6 mice.

The concentration of Th1 cells in the lymph sample was determined as described previously for Th17 cells. Although no difference in the percentage was seen, the concentration of Th1 cells in the lymph of 2D2 mice was 4 times higher than that of C57BL/6 mice (Fig. 3.3.2 A, B and C). In contrast, the concentration of Th1 cells in the blood was comparable between 2D2 mice and C57BL/6 mice (Fig. 3.3.2 D).

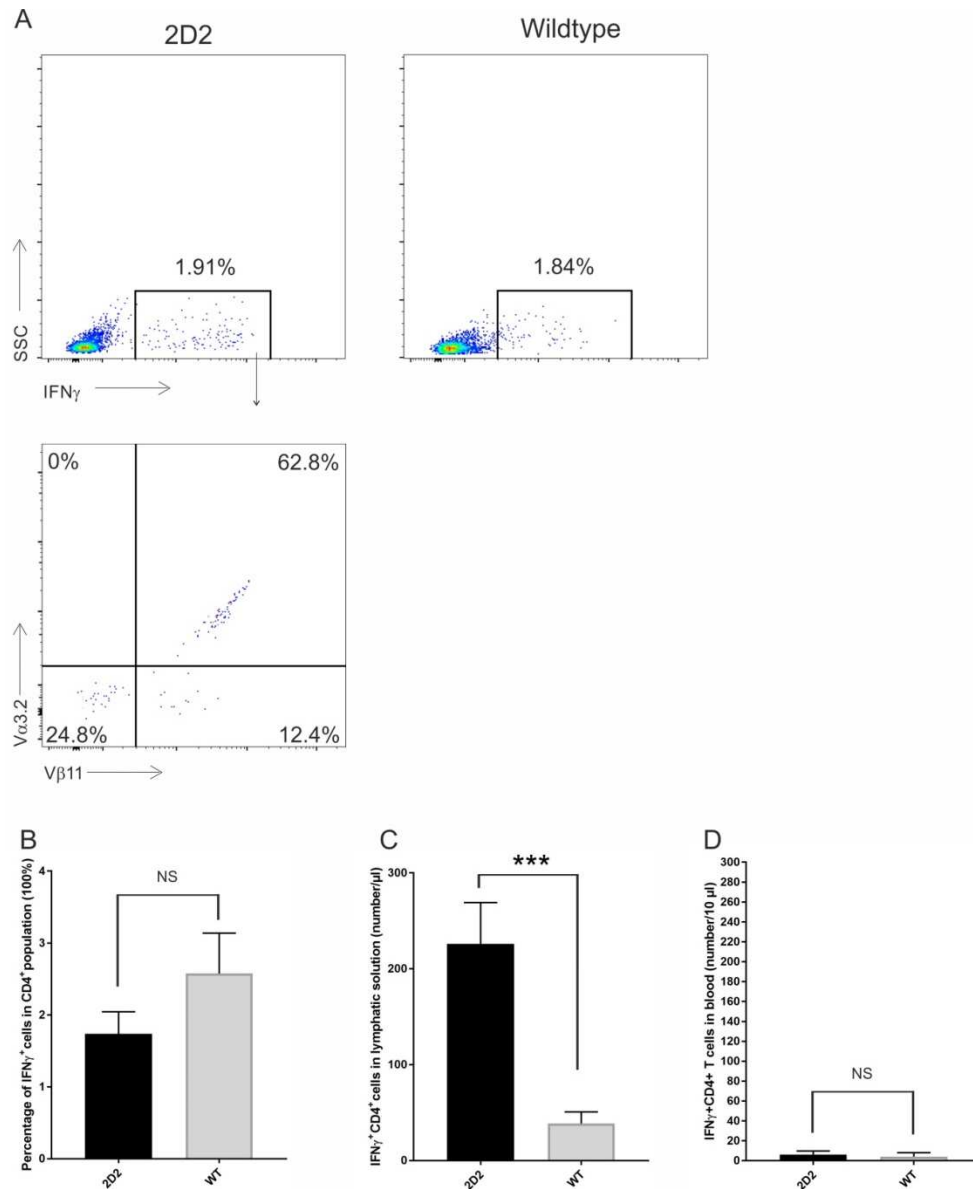


Figure 3.3.2 IFN γ expressing in T cells emigrating from mesenteric lymph. **A.** CD4⁺ T cells from 2D2 T cells and polyclonal T cells were evaluated by IFN γ staining and analysed by flow cytometry. Representative flow cytometry plots from 3 experiments were shown. **BC.** Percentage (**B**) and concentration (**C**) of IFN γ ⁺CD4⁺ T cells from efferent mesenteric lymph of 2D2 and C57BL/6 mice. **D.** Concentration of IFN γ ⁺CD4⁺ T cells in the blood of 2D2 and wildtype mice serves as a control. 2D2 lymph sample: n=5; wildtype lymph sample: n=6; 2D2 blood sample: n=4; wildtype blood sample: n=6; Dataset was analysed by independent sample T-test. Values represent means \pm SEM.

3.3.3 CD44⁺CD4⁺ T cells Efferent from the Mesenteric Lymph

CD44 is a membrane receptor that recognizes osteopontin and hyaluronan (Aruffo, Stamenkovic et al. 1990, Ghazi-Visser, Laman et al. 2013). It has been found that CD44 is chronically elevated in the demyelinating lesions of MS patients (Soilu-Hanninen, Laaksonen

et al. 2005). Increased expression of CD44 in the T cells from peripheral blood was reported during the relapse phase of MS (Soilu-Hanninen, Laaksonen et al. 2005). EAE studies have provided further evidence supporting the role of CD44. Deletion of CD44 results in a reduction in severity of EAE (Guan, Nagarkatti et al. 2011). Application of anti-CD44 blocking antibody prevented the development of EAE induced by adoptive transfer of MBP specific T cells (Brocke, Piercy et al. 1999). The mechanism by which CD44 influences EAE pathogenesis may act through T helper cell survival, differentiation and/or adhesion (Guan, Nagarkatti et al. 2011). Therefore, in addition to analysing the number of Th1 and Th17 cells, CD44⁺CD4⁺ T cells were also investigated.

Compared with wildtype mice, the lymph sample from 2D2 mice contained a similar frequency of CD44 expressing CD4⁺ T cells (Fig. 3.3.4 A and B). The proportion of CD44⁺ cells in the CD4⁺ T cell population reached 4% in both 2D2 mice and C57BL/6 mice (Fig. 3.3.3 B). However, the concentration of CD44⁺CD4⁺ T cells in the lymph sample from 2D2 mice and wildtype mice was different to the frequency pattern. The concentration of CD44⁺CD4⁺ T cells was quantified similarly to IL17A and IFN γ expression. The lymph sample from 2D2 mice contained a three times greater number of CD4⁺CD44⁺ T cells than C57BL/6 mice (Fig. 3.3.3 C). Again, blood was used as a control. Very few CD44⁺CD4⁺ T cells were detected in the blood of both 2D2 mice and wildtype mice and no significant difference was observed (Fig. 3.3.3 D).

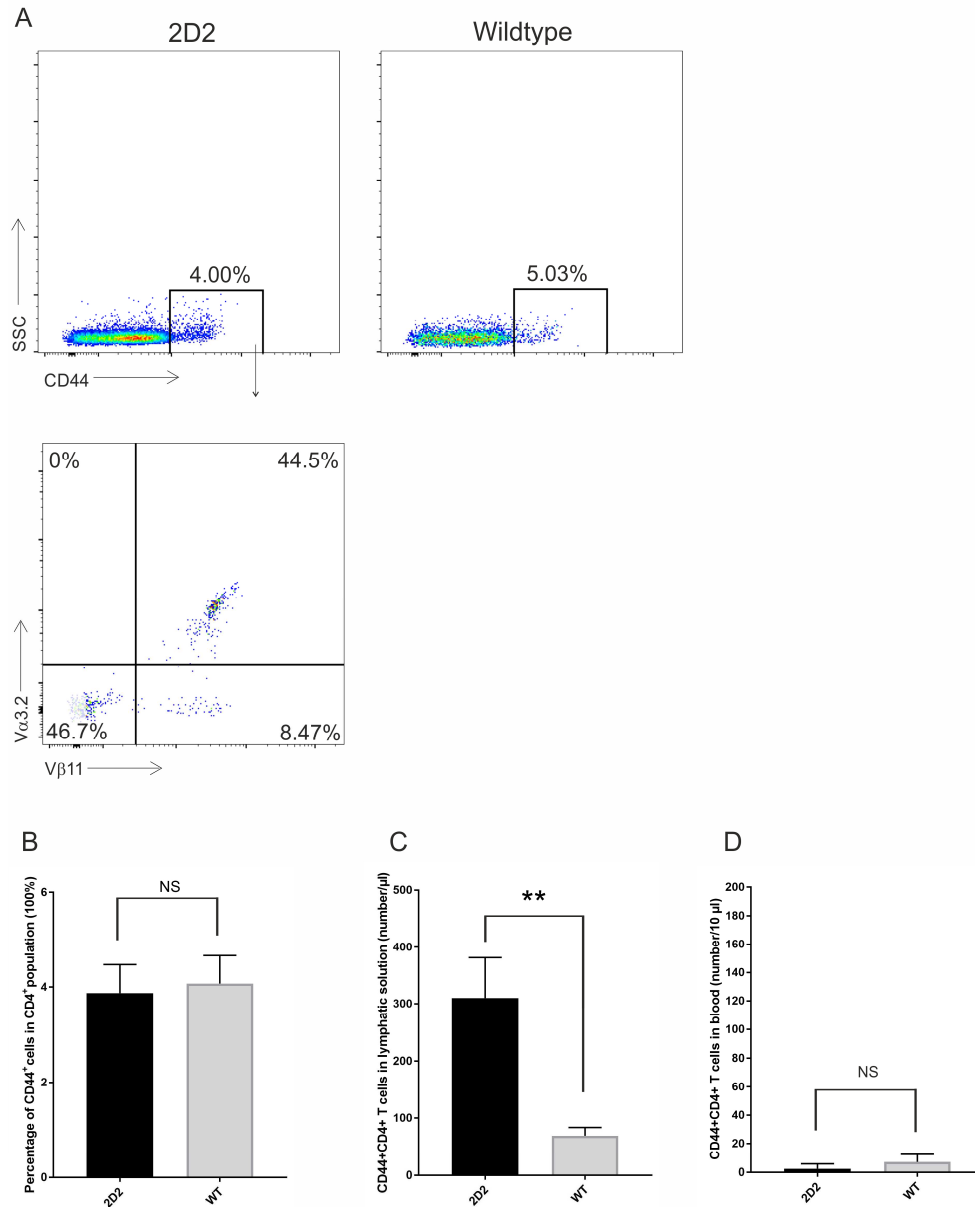
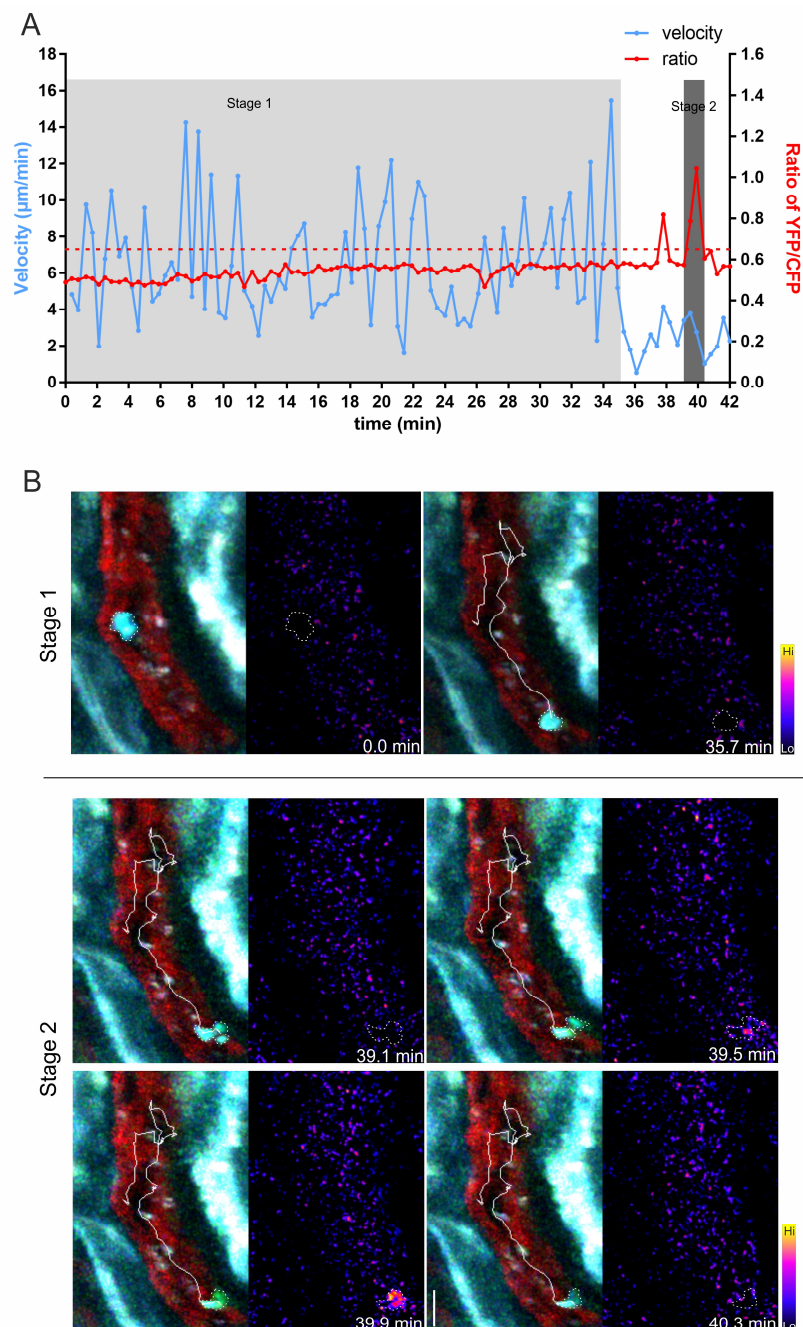


Figure 3.3.3 Expression of CD44 in T cells emigrating from mesenteric lymph. **A**. CD4⁺ T cells from 2D2 T cells and polyclonal T cells were evaluated by CD44 staining and analysed by flow cytometry. Representative flow cytometry plots from 3 experiments are shown. **B**, **C**. Percentage (**B**) and concentration (**C**) of CD44⁺ T cells from efferent mesenteric lymph of 2D2 and wildtype mice. **D**. Concentration of CD44⁺ T cells in the blood of 2D2 and wildtype mice serves as a control. 2D2 lymph sample: n=5; wildtype lymph sample: n=6; 2D2 blood sample: n=4; wildtype blood sample: n=6; Dataset was analysed by independent sample T-test. Values represent means \pm SEM.

3.4 The Influence of Microbiota on Encephalitogenic T Cells

After confirming the stimulation of MOG specific T cells, but not polyclonal T cells, in the lamina propria, naturally the next question was: what factors are responsible for this

stimulation? Previous studies have demonstrated that the intestinal microbiota exerts significant influence on T cell proliferation and differentiation in the GALT (Berer, Mues et al. 2011). Through the use of germ free recipients, calcium fluctuations of MOG specific T cells were further investigated in the lamina propria. The germ free recipients in this experiment were C57BL/6 mice born and cultivated in germ free condition. 3 days before intravital imaging, recipients were imported to conventional condition and received an i.v. injection of Twitch 2b labelled 2D2 T cells. This protocol minimizes colonization of microbiota.



*Figure legend see next page

Figure 3.4.1 Calcium imaging of 2D2 T cells in the lamina propria of germ free C57BL/6 mouse. A. A representative track of a 2D2 T cell in the lamina propria of germ free wildtype C57BL/6 mouse. Intracellular calcium fluctuation (red line) and velocity (blue line) of the cell is shown. The light grey shadow highlights the imaging frames where the T cell moves continuously without calcium signaling (stage 1). The dark grey shadow highlights the imaging frames where the T cell shows both a decrease in velocity and calcium signaling (stage 2). B. Images from intravital calcium imaging of the tracked 2D2 T cell from stage1 and stage2 as indicated in A. Fluorescent overlay (left) and pseudocolour ratio images (right) of the indicated cell are depicted. The white line shows the trajectory of the T cell. Blood vessels are labelled in red with Rhodamine; T cells are labelled in blue/green with Twitch2b; collagen fibers are in blue due to autofluorescent signal. Scale bar, 25 μ m.

A representative tracking of a 2D2 T cell in the lamina propria of a germ free mouse is shown in figure 3.4.1 A. In most of the recorded time (~35 min, indicated as stage 1), no calcium signaling was observed and the T cell continuously moved with a high velocity (Fig. 3.4.1). Short calcium signaling (<1 min) only occurred in the cell concurrently with decreased velocity (Stage 2 in Fig. 3.4.1).

Calcium levels in 2D2 T cells at each time point were recorded and compared between conventional and germ free recipients (Fig. 3.4.2 A). In the lamina propria of germ free recipients, the frequency of the high ratio values of YFP/CFP (>0.69) in 2D2 T cells is 1.1%, which was significantly lower than the frequency observed in conventional recipients (Fig. 3.4.2 C). Additionally, motility of 2D2 T cells in lamina propria of germ free recipients was greater as shown by an increase in velocity (Fig. 3.4.2 B and D). Furthermore, compared with recipients in conventional conditions, 2D2 T cells in germ free recipients show less long term calcium signaling in the lamina propria (Fig. 3.4.3 B). Collectively, these results demonstrate the influence of commensal microbiota on the calcium based stimulation of MOG specific T cells in the lamina propria.

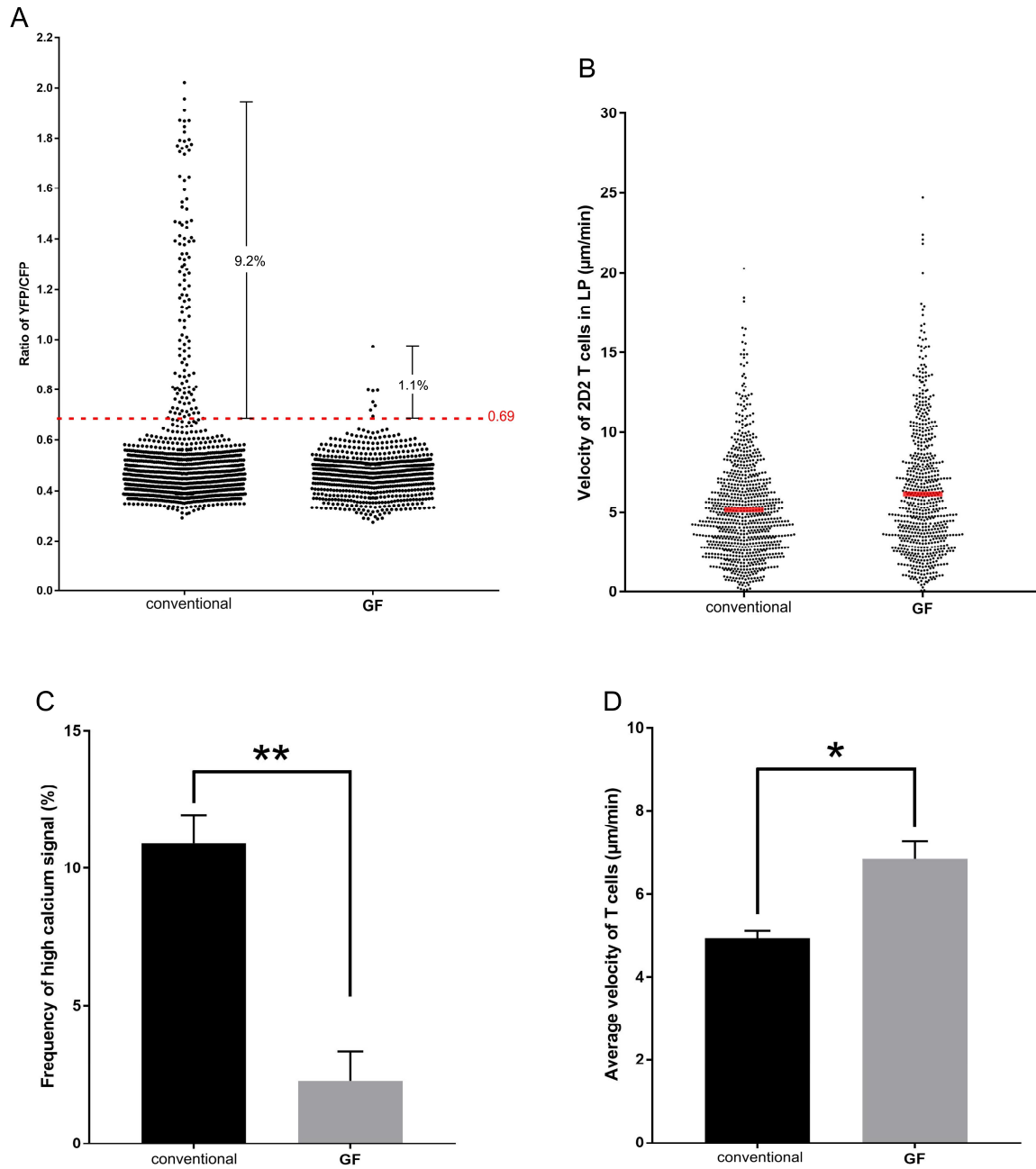


Figure 3.4.2 Calcium level and velocity of 2D2 T cells in the lamina propria of conventional and germ free recipients. **A.** Representative calcium levels (ratio of YFP/CFP) in 2D2 T cells of different groups from 3 experiments were shown by cumulative plots. Each dot represented a calcium level shown by a single cell in each time point. The percentage of the ratio higher than 0.69 are indicated in the figure. **B.** Representative velocity of 2D2 T cells in conventional and germ free recipients from 3 experiments were shown by cumulative plots. The red bar represents the mean. Datasets of conventional group were from previous experiment (Fig. 3.2.4).

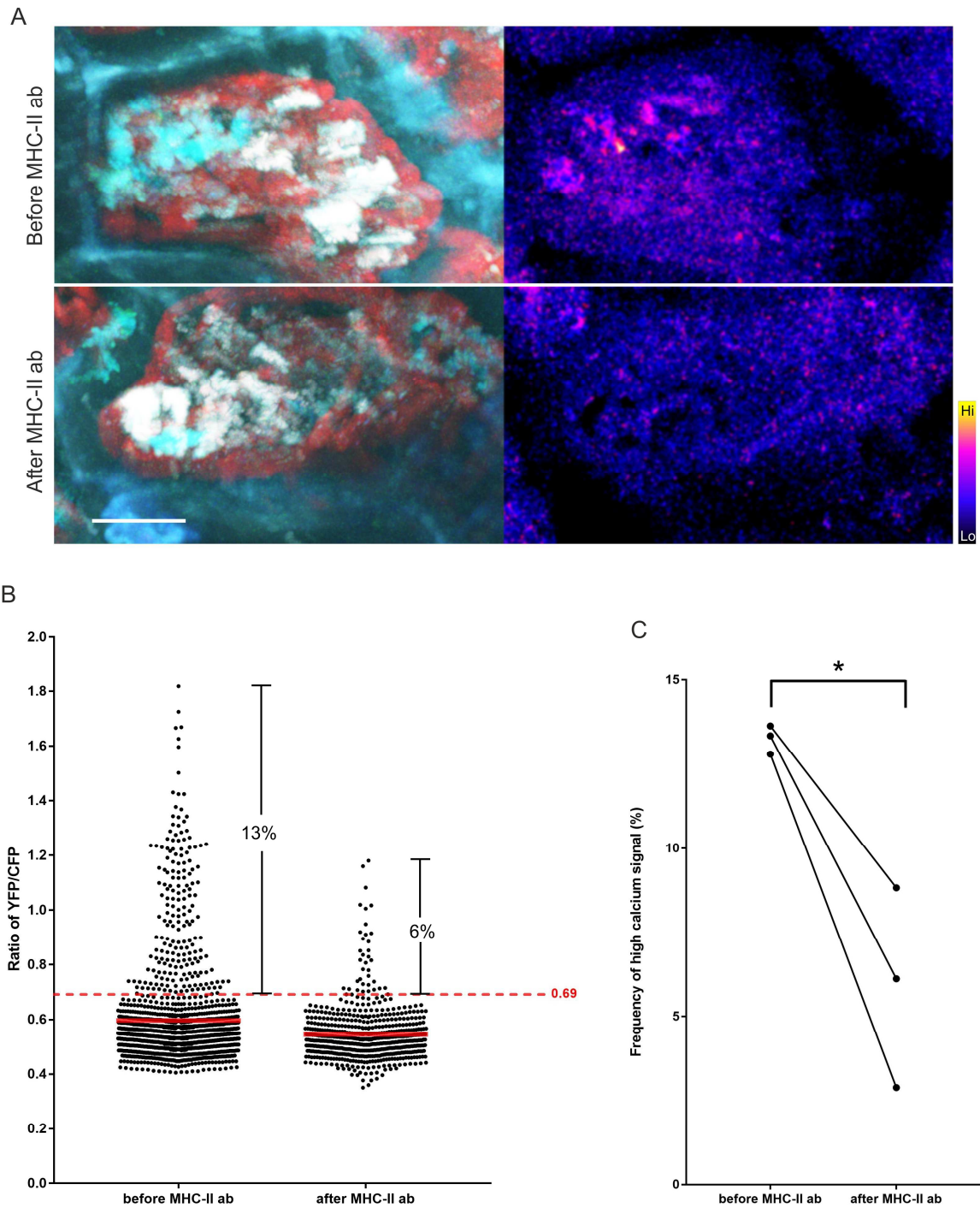


Figure 3.5.1 Calcium signaling in TCR1640 T cells in the lamina propria before and after the application of anti-MHC class II blocking antibody. A. Representative time projection pictures of TCR1640 T cells in the lamina propria before and after the application of anti-MHC class II blocking antibody. Fluorescent overlay (left) and pseudocolour ratio images (right) are depicted. Blood vessels are labelled in red with Rhodamine; T cells are labelled in blue/green with Twitch2b; collagen fibers are labelled in blue due to autofluorescent signal. Scale bar, 20 μ m. **B.** Representative cumulative plots show calcium levels (ratio of YFP/CFP) in TCR1640 T cells before and after the injection of anti-MHC class II antibody. Each dot represents a calcium level shown by a single cell in each time point. **C.** Frequency changes of calcium signaling by the administration of anti-MHC class II antibody. Data obtained from same animal (before and after injection) is paired. Results from 3 independent experiments are shown. Datasets of TCR1640 T cells without administration of anti-MHC class II blocking antibody were from previous experiment (Fig. 3.2.7)

The influence of anti-MHC class II blocking antibody on the duration of calcium signaling in TCR1640 T cells in the lamina propria was further analysed (Fig.3.5.2). Before injection of the blocking antibody, several TCR1640 T cells in the lamina propria showed continuous calcium signaling, some lasting more than 10 min (Fig.3.5.2 A). However, after injection of the anti-MHC class II blocking antibody, less continuous calcium signaling was observed in TCR1640 T cells and the length of calcium signaling was reduced (Fig.3.5.2 A).

The proportion of TCR1640 T cells with long term calcium signaling (> 2 min) in the lamina propria reached to 27%, and was then significantly reduced by the administration of anti-MHC class II blocking (Fig.3.5.2 B). However, anti-MHC class II blocking antibody did not exert any influence on the proportion of TCR1640 T cells with short calcium signaling or those that lacked calcium signaling (Fig.3.5.2 C).

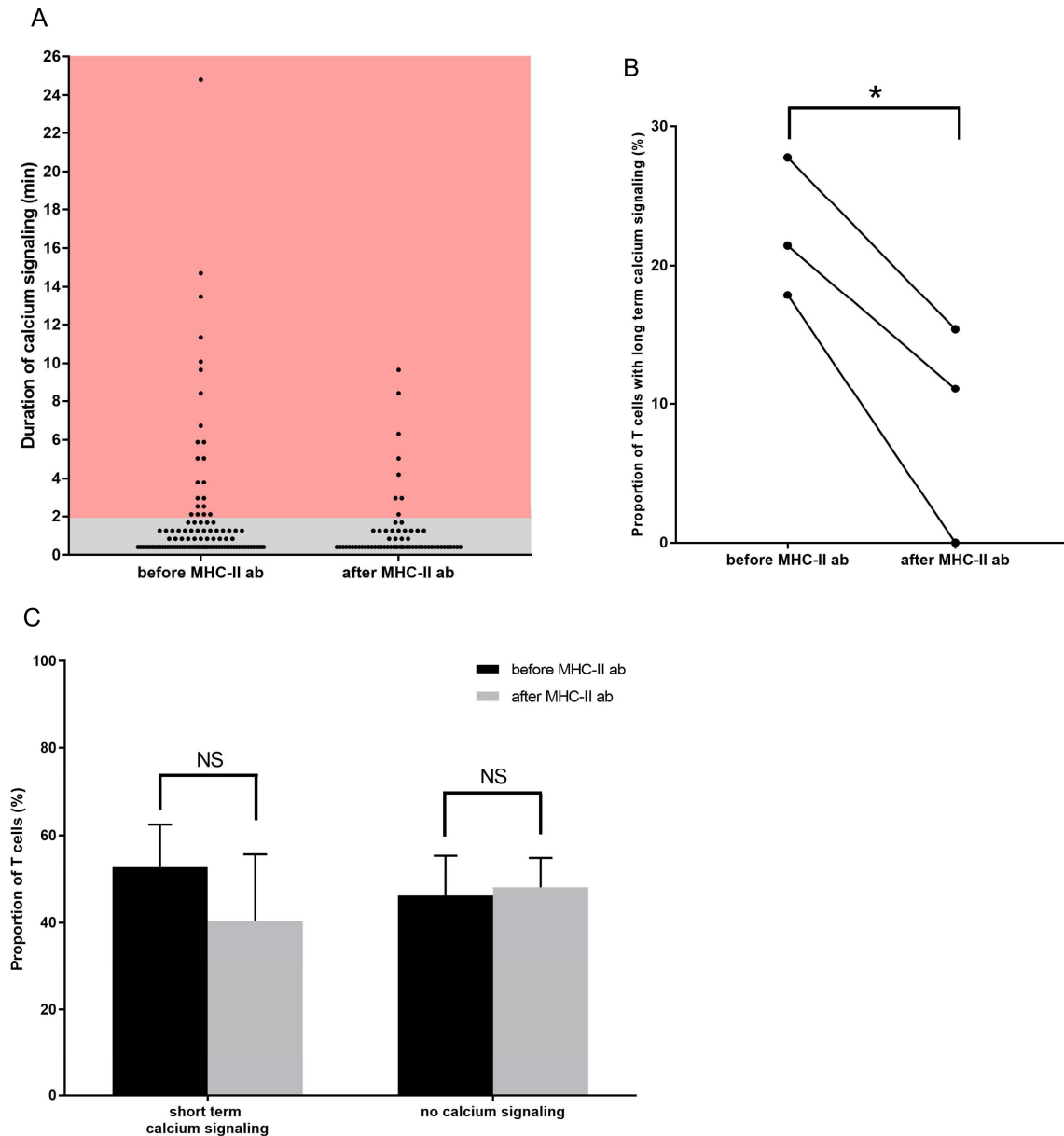


Figure 3.5.2 A. Duration of calcium signaling in TCR1640 T cells in the lamina propria before and after the administration of anti-MHC class II antibody. Each cumulative plot represents the duration of each continuous calcium signaling. Each dot represents a duration of a calcium signaling event. **B.** The effect of anti-MHC class II blocking antibody on the T cells with long calcium signaling. Results from a mouse are paired. **C.** The influence of anti-MHC class II blocking antibody on the T cells with short calcium signaling and without calcium signaling. When a T cell shows calcium signaling multiple times during the recoding, each calcium signaling is counted. Proportion of T cells is calculated as: number of T cells with calcium events/total number of T cells. Dataset were analysed by paired T-test. Mean \pm SEM from at least 3 animals per group are shown. Datasets of TCR1640 T cells without administration of anti-MHC class II blocking antibody were from previous experiment (Fig. 3.2.7)

3.6 Intravital Imaging of T cells in the Lamina Propria of the Colon

In addition to the small intestine, intravital imaging of T cells was also performed in the lamina propria of the colon. The colon hosts a larger number of microbiota than the small intestine (Mowat and Agace 2014) and exerts a major influence on shaping immune homeostasis (Sarrabayrouse, Bossard et al. 2014). Therefore, it is another important environment to investigate the behaviour of MOG specific T cells. Intravital imaging of T cells was established in the lamina propria of the colon.

Representative images of Twitch2b labelled polyclonal T cells in the lamina propria of the colon were shown in figure 3.6.1. Using the same imaging setup established with the small intestine, T cells in the colon can be filmed with a stable viewing frame. The tracking analysis of the indicated T cell in the image showed no calcium signaling and high velocity.

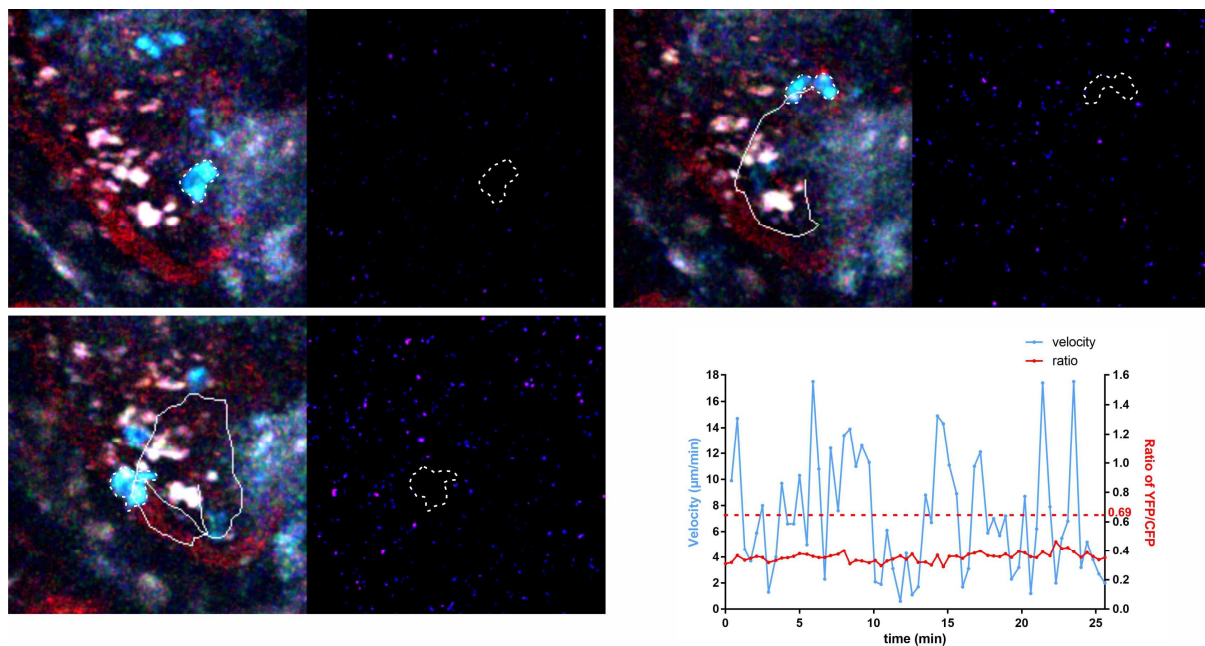


Figure 3.6.1 Calcium imaging of polyclonal T cells in the lamina propria of colon. Fluorescent overlay (left) and pseudocolour ratio images (right) of the polyclonal T cell were depicted. White line shows the trajectory of the indicated T cell. Blood vessels are labelled in red with Rhodamine; T cells are labelled in blue/green with Twitch2b; collagen fibers are labelled in blue due to autofluorescent signal. Scale bar, 25 μm . The tracking curves of the T cell displayed the velocity (blue line) and the intracellular calcium signaling (red line).

3.7 Transduction of Cultured B Cells with Activation Sensor

3.7.1 *In vitro* Expansion of B cells

B cells can act as antigen presenting cells to stimulate T cells and T cells can support B cell maturation. Although very little is known about B cells in the intestine, B cells may play an important immunogenic role in the GALT. Therefore, it is important to integrate B cells in the study of stimulation of T cells in the GALT as trigger of EAE. To explore the behaviour of B cells in the GALT by two-photon microscopy, B cells were cultured *in vitro* with feeder cells that express CD40L on their surface and secrete BAFF (Nojima, Haniuda et al. 2011). IL4 was added for first 3 days, followed by IL21 to induce B cell maturation. 4 days after starting the culture, these *in-vitro*-induced germinal centre B cells (iGBs) were harvested and phenotypically analysed by flow cytometry. Almost all of the cultured B cells expressed CD19 (Fig. 3.6.1). The proportion of IgG1 and Fas expressing B cells surpassed 95% whereas the proportion of IgM expressing B cells was only around 10% (Fig. 3.6.1). There are around 7% cultured B cells expressing CD138 which indicates a small amount of Ig⁺ plasma cells (Fig. 3.6.1).

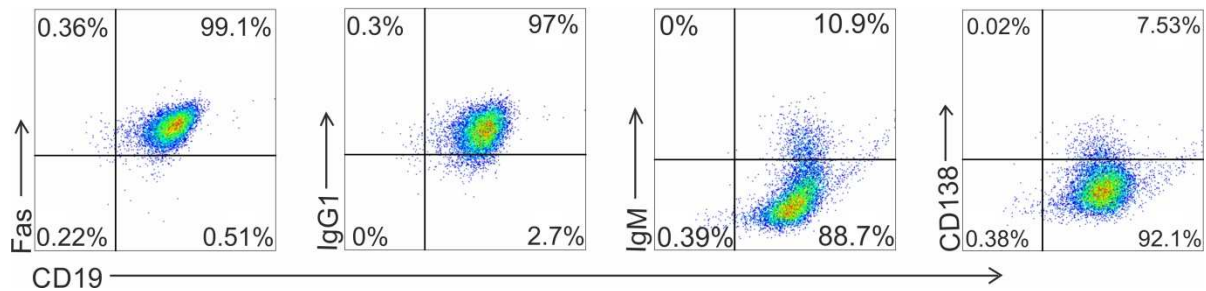


Figure 3.6.1 Representative flow cytometry analysis of B cell phenotypes 4 days after culture.

3.6.2 Retroviral Transduction of B cells

After culturing for 4 days, B cells proliferate nicely and can be efficiently transduced. The spin-down transduction with NFAT-GFP and Twitch2b sensor is performed. Transduction

efficiency was analysed by flow cytometry 24 hrs after the transduction. Cultured B cells could be successfully labelled by both Twitch2b and NFAT-GFP (Fig.3.6.2).

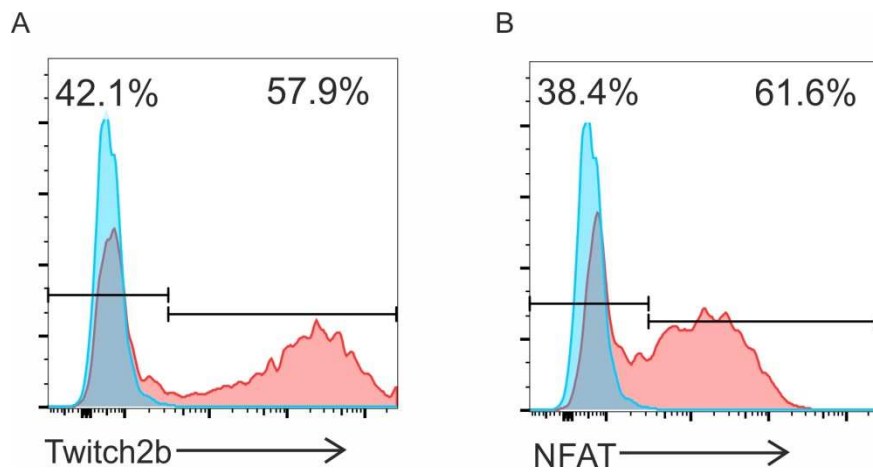


Figure 3.6.2 Representative flow cytometry histograms confirming the retroviral transduction efficiency of Twitch2b and NFAT-GFP in T cells.

DISCUSSION

4.1 Calcium Signaling of MOG Specific T Cells in LP

In this study, two lineages of MOG specific T cells are examined as paradigms to study the stimulation of encephalitogenic T cells in the GALT as a possibly relevant scenario before onset of clinical EAE. Encephalitogenic T cells obtained from 2D2 are specific for MOG peptide 35-55 whereas encephalitogenic T cells obtained from TCR1640 mice present specificity for MOG peptide 92-106. Both 2D2 mice and TCR1640 mice develop spontaneous EAE, with an incidence rate of 4% in 2D2 mice and 80% in TCR1640 mice (Bettelli, Pagany et al. 2003, Pollinger, Krishnamoorthy et al. 2009). The current study focuses on the stimulation of encephalitogenic T cells in the GALT before the onset of EAE. To achieve this, 2D2 and TCR1640 mice without appreciable EAE symptoms are used as donors of MOG specific T cells. MOG specific T cells are stimulated *in vitro* with anti-CD3/CD28 Abs to induce potent proliferation that allows for the efficient uptake of retrovirally delivered activation sensors. Antibody stimulation was used since it provides similar stimulation to both MOG specific T cells and polyclonal T cells. Labelled T cells were then adoptively transferred to recipients 4 days after stimulation and were subsequently imaged *in vivo* 3 days later. Importantly, at the time point of adoptive transfer, T cells did not show calcium activity. Therefore, the activation resulted from CD3/CD28 induced activation of T cells *in vitro* does not serve as a confounding variable for the intravital analysis of T cell behaviour in the GALT.

The small intestine can be segmented into three regions, namely duodenum, jejunum and ileum. The duodenum and jejunum play a vital role in digestion. They contain relatively less and more simple microbial species, mainly Lactobacilli and Streptococci (Mowat and Agace 2014). Although there are a large number of Th17 cells in the duodenum and jejunum, there is no evidence to suggest that these parts of the small intestine are involved in the pathogenesis of EAE/MS. Compared with the duodenum and jejunum, a large variety of immunological events related to autoimmune diseases have been reported in the ileum. Furthermore, the ileum is the region that contains highest density and diversity of luminal microbial cells in the small intestine (Sommer and Backhed 2013). During the establishment of T cell mediated experimental arthritis, the elimination of intestinal microbiota reduces the number of Th17 cells in the ileum. This effect has been shown to be due to the impaired

production of serum amyloid A (SAA) from epithelial cells, resulting in ameliorated disease (Rogier, Evans-Marin et al. 2017). SAA production requires ILC3s to secrete IL22, which depends on the expression of IL23R on the ILC3s (Sano, Huang et al. 2015). In addition, SFB, which induces robust IL17A production in ROR γ t⁺ T cells, is restricted to the terminal ileum (Sano, Huang et al. 2015). Taken together, these findings highlight the lamina propria of the ileum as a promising region to investigate the stimulation of MOG specific T cells by two-photon microscopy.

Compared with polyclonal T cells, both 2D2 and TCR1640 MOG specific T cells showed higher frequency and longer lasting calcium signaling in the lamina propria of the ileum (Fig. 3.2.4 A and B, Fig. 3.2.5. Fig. 3.2.7). Continuous calcium signaling, which lasted longer than 2 min, was observed in 20% of recorded MOG specific T cells, whereas it is barely detected in polyclonal T cells (Fig. 3.2.5). As shown in our previous publication, such continuous calcium signaling is induced in an antigen dependent manner (Kyratsous, Bauer et al. 2017). Therefore, the datasets created through intravital imaging in this study prompt the possibility that MOG specific T cells are stimulated in an antigen dependent manner in the lamina propria of the ileum. Indeed, administration of anti-MHC class II antibody diminished continuous calcium signaling (Fig. 3.5.2). In contrast, Twitch2b expressing MOG specific T cells in the Peyer's patch rarely displayed continuous calcium signaling (Fig. 3.2.9). The reason for such regional differences in calcium signaling needs to be further investigated. As the stimulatory potential of APCs can be variable in different anatomical location, it is reasonable to apply transcriptome analysis to distinguish relevant APCs in Peyer's patch and the lamina propria.

In contrast to the long term calcium signaling which was seen mostly in MOG specific T cells, short lasting calcium signaling took place in both MOG specific and polyclonal T cells. The short lasting calcium spikes in Twitch sensor labelled T cells has already been reported in the spleen and spinal cord (Kyratsous, Bauer et al. 2017). This short lived calcium signaling exists under non-inflammatory conditions and is not strong enough to induce the NFAT translocation (Kyratsous, Bauer et al. 2017). This study further demonstrates that short lasting calcium signaling can be blocked, at least partially, by chemokine receptor antagonists. In addition, it is speculated that short lasting calcium signaling induces a migratory phenotype. Taking these results into consideration, it is tempting to believe that

short lasting calcium signaling seen in MOG specific T cells in the GALT are antigen independent. Indeed, the short calcium signaling is not effected by anti-MHC class II blocking antibody as shown in this study as well as Kyratsous et al. (Kyratsous, Bauer et al. 2017).

As observed in this study, sustained calcium signaling could persist from 2 mins to 24 mins in MOG specific T cells, which was much shorter than the sustained calcium signaling caused by immunization in other studies (Wei, Safrina et al. 2007). The difference can be explained by the quality and quantity of antigen presentation. In the lymph node, there are many professional APCs that are loaded with an excess amount of exogenous antigen provided by immunization. In the small intestine, APCs, including macrophages and DCs disseminate throughout the intestine but maintain distinct phenotypes and functions in various anatomical sites (Faria, Reis et al. 2017). Among them, macrophages expressing the fractalkine receptor (CX3CR1) constitute the majority of intestinal APCs whereas lymph node macrophages contain different subsets, such as CD169⁺CX3CR1⁺F4/80⁻ subcapsular sinus macrophage, CD169⁻CX3CR1⁻F4/80⁺ medullary cord macrophage and etc.. Intestinal DCs comprise less than 10% of intestinal APCs and are characterized by high expression of CD11c and MHC class II, but lack of a high affinity IgG receptor FC γ R1 (CD64). Intestinal DCs can further be divided into three subsets: CD103⁺CD11b⁺, CD103⁺CD11b⁻ and CD103⁻CD11b⁺ (Bekiaris, Persson et al. 2014). Each subset contributes to intestinal immunological reactions in different ways. For instance, intestinal macrophages most efficiently sample soluble luminal proteins, but lamina propria DCs are not capable of this process (Schulz et al., 2009; Farache et al., 2013). The regulatory effects of intestinal DCs are associated with the metabolites of luminal bacteria. For example, capsular polysaccharides from bacteroides fragilis can interact directly with plasmacytoid DC, resulting in the expression of molecules against colitis via TLR-2 and stimulation of CD4⁺ T cells to release IL10 (Dasgupta, Erturk-Hasdemir et al. 2014). Therefore, the miscellaneous APCs subsets and the multifarious luminal antigens lower the occurrence of antigen saturation, which may shorten the duration of calcium signaling in intestinal MOG specific T cells (Celli, Lemaitre et al. 2007, Kyratsous, Bauer et al. 2017).

Continuous calcium signaling is associated with the proliferation and differentiation of T cell. Calcium influx can activate several intracellular signaling pathways, including the

serine/threonine phosphatase calcineurin and its target transcription factor NFAT, CaMK (calmodulin kinase) and its target CREB (cyclic AMP-responsive element-binding protein), MEF2 (myocyte enhancer factor 2) which is regulated by both of calcineurin and CaMK pathways, and NF- κ B (Oh-hora 2009). Among them, the calcineurin-NFAT pathway has been best unravelled in terms of its downstream contributions to transcriptional effects. NFAT is composed of five transcription factors: NFAT1 (also known as NFATc2), NFAT2, NFAT3, NFAT4 and NFAT5 (Oh-hora 2009). The TCR dependent calcium influx can activate NFAT1, which is prominent in peripheral T cells and has been well known to play a crucial role during the differentiation of Th17 cell. The defect in NFAT1 nuclear translocation affects the activation of IL17A promoter, resulting in the diminished production of IL17A (Gomez-Rodriguez, Sahu et al. 2009). Another study shows that the inhibition of calcineurin in naïve T cells during the Th17-polarized culturing causes a severe reduction of the IL17A⁺ population (Kim, Srikanth et al. 2014). Orai1-deficient T cells, which lack the CRAC channel, have impaired calcium signaling and can not differentiate into Th17 cells. However, transducing Orai1-deficient T cells with constitutively active mutant of NFAT can rescue the impairment of Th17 differentiation (Kim, Srikanth et al. 2014). Consistently with the *in vitro* data, inhibition of CRAC channel *in vivo* ameliorates active EAE by significantly reducing the IL17A⁺ T cell population (Schuhmann, Stegner et al. 2010, Kim, Srikanth et al. 2014). Taken together, both long lasting calcium signaling and NFAT nuclear translocation are critical steps in Th17 cell induction. Although continuous calcium signaling is capable of inducing NFAT nuclear translocation, this was not observed in MOG specific T cells in the lamina propria or Peyer's patch (Fig. 3.2.8 and Fig. 3.2.10) (Kyratsous, Bauer et al. 2017). However, it can be speculated that long lasting calcium signaling observed in the T cells in the lamina propria of the ileum still influences their migratory phenotype. Indeed, the number of trafficking of MOG specific T cells in GALT efferent lymphatics was greater than that of polyclonal T cells (Fig. 3.3.1, Fig. 3.3.2 and Fig. 3.3.3).

To identify if the stimulation of MOG specific T cells was antigen-dependent, anti-MHC class II blocking antibody was administrated intravenously to the recipients of MOG specific T cells during intravital imaging. This allows for the comparison of T cell calcium signaling before and after infusion of antibody in the same animal. Both frequency and duration of the calcium signaling were significantly decreased after the antibody administration,

although there was still a small proportion of MOG specific T cells that showed the brief and continuous calcium signaling (Fig.3.5.1 and Fig.3.5.2). This reduction suggests that the calcium signaling detected in MOG specific T cells in the lamina propria relies on TCR-antigen/MHC interaction. As speculated, anti-MHC class II blocking antibody did not influence brief calcium signaling since these calcium events are considered to be antigen independent.

Result similar to these has been observed in the previous study investigating Twitch sensor labelled encephalitogenic T cells in the spinal cord leptomeninges. The long term calcium signaling is reduced by the administration of MHC class II blocking antibody, whereas short lasting calcium signaling is unaffected. Thereby, the calcium signaling retained in this study after the administration of MHC class II blocking antibody can be due to the antigen independent mechanism shown in the previous study (Kyratsous, Bauer et al. 2017). In addition, it has been shown that short-lived interaction between T cells and DCs, which do not require MHC molecules-antigen complex, induce short lasting calcium signaling *in vitro* (Revy, Sospedra et al. 2001). As opposed to clinging to DCs, T cells continuously crawl across the DC surface, leading to infrequent and transient calcium oscillations that are shorter than those produced by antigen recognition (Montes, McIlroy et al. 1999, Gunzer, Schafer et al. 2000). Notably, integrins and selectins can cause intracellular calcium signaling in lymphocytes. However, these signals may be too weak to be detected by the Twitch2b sensor (Weismann, Guse et al. 1997, Thestrup, Litzlbauer et al. 2014).

In addition to investigating T cells in the ileum, this study also performs intravital imaging of T cells in the colon. The colon is the main region for the trillions of commensal bacteria that inhabit the gut (Mowat and Agace 2014). Compare with the ileum, Tregs are the dominant population of CD4⁺ T cells in the lamina propria of the colon (Maynard, Harrington et al. 2007). Therefore, it is possible that MOG specific T cells are stimulated in the colon but then subsequently suppressed by colonic Tregs. They are probably not as well stimulated as in the small intestine. Further experiments need to be performed to conclude the stimulation of MOG specific T cells in the colon.

4.2 Influence of Microbiota on T cell Activation and EAE Incidence

It has been shown that the transfer of human microbiota from MS patients increase the incidence of spontaneous EAE through reducing IL10 production in the peripheral blood of recipient mice (Berer, Gerdes et al. 2017). In another spontaneous EAE mouse model which harbours MBP specific T cells, oral treatment of antibiotics dramatically decreases the incidence of EAE. Furthermore, gut dysbiosis during the young adulthood of transgenic mice with MBP specific T cells triggers CNS inflammation by impairing the development of Foxp3⁺CD4⁺ T cells and expression of E3 ubiquitin ligase genes (Yadav, Boppana et al. 2017). Taken together, modification of microbiota influences EAE pathogenesis. However, the cellular mechanisms of these processes have not been well studied. This study was generated by the hypothesis that commensal microbiota stimulate encephalitogenic T cells in the GALT. Indeed, through performing intravital imaging, it was shown that encephalitogenic T cells were stimulated in the lamina propria (Fig. 3.2.5 and Fig. 3.2.7). Since MHC class II serves a crucial role during the stimulation of GALT T cells (Fig. 3.5.1 and Fig. 3.5.2), it is reasonable to believe that intestinal APCs capture antigens, such as endogenous MOG or metabolites that can mimic MOG peptides and introduce them to T cells. To evaluate the influence of endogenous MOG, intravital imaging of Twitch2b expressing MOG specific T cells in MOG deficient mice will be performed. If MOG specific T cells are still stimulated in the GALT of MOG deficient mice, this stimulation should be induced by MOG-like peptides. However, even if this is the case, it will be very difficult to identify the peptide since there are a huge amount of metabolites from microbiota in small intestine.

Previously, studies have shown that the commensal microbiota can promote inflammatory T helper responses during EAE development (Ochoa-Reparaz, Mielcarz et al. 2009, Berer, Mues et al. 2011). To further study the functional role of microbiota in EAE incidence, microbiota from monozygotic twin pairs who are discordant for MS were transplanted into germ free TCR1640 mice. The mice colonized with microbiota from MS-affected siblings develop higher rate of EAE than those colonized with microbiota from the healthy control-derived counterparts (Berer, Gerdes et al. 2017). Therefore, it is reasonable to hypothesize that gut microbiota aggravate the stimulation of encephalitogenic T cells in the GALT. In this

study, calcium signaling of MOG specific T cells (as an indication of T cell stimulation) was investigated in the lamina propria of animals imported from a germ free environment. Limited by experimental parameters, the germ free recipients were housed in conventional conditions for 3 days before intravital imaging – minimizing the colonization of microbiota compared with other conventional recipients. Consequently, the frequency of calcium signaling was diminished in MOG specific T cells in the lamina propria of these germ free recipients (Fig. 3.4.2 and Fig. 3.4.3). This study visualizes the influential role of the gut microbiome in the stimulation of encephalitogenic T cells.

Although some commensal microbes may stimulate encephalitogenic T cells and induce clinical EAE, there are some bacteria strains that could ameliorate EAE through increasing the number of intestinal Tregs (Calvo-Barreiro, Eixarch et al. 2017). The incidence of PLP 91-110 induced EAE is reduced in mice gavaged with human gut derived *Prevotella histicola* (*P. histicola*) (Mangalam, Shahi et al. 2017). Colonization with *P. histicola* increases Tregs and activates CD103⁺ DCs in the mesenteric lymph nodes, resulting in reduced CNS inflammation (Mangalam, Shahi et al. 2017). Oral administration of a Gram-negative microorganism named *Escherichia coli* strain Nissle 1917 can also reduce the severity of EAE. During the treatment, autoreactive T cells produce higher levels of IL10 and exhibit less infiltration into the CNS following EAE induction. In treated mice, the intestinal barrier is protected from the dysfunction correlated with EAE development (Secher, Kassem et al. 2017). It is possible that these microbial treatments induce immune tolerance by regulating the host-microbiota homeostasis and ameliorate CNS inflammation. Although the treatments discussed above may highlight the beginnings of promising therapeutic routes for MS, clinical trials still need to be performed.

4.3 Phenotypes of T cells Emigrating from the GALT

In this study, MOG specific T cells stimulation in the GALT may influence the differentiation/maturation of T cells. In order to investigate the effect of this stimulation, surface molecules and intracellular cytokines of the MOG specific T cell emigrating from mesenteric lymph nodes were determined.

Th17 cells, detected by expression of IL17A, were found in the efferent mesenteric lymph emigrating from GALT. Compared with wildtype mice, both the proportion and absolute number of Th17 cells were increased significantly in 2D2 mice that did not show any clinical sign of EAE (Fig.3.3.1 A, B and C). In a previous study, the dynamics of intestinal Th17 cell frequency have been found to increase before the onset of EAE but gradually reduced after onset (Haghikia, Jorg et al. 2015). These results suggest that intestinal Th17 cells migrate into the CNS via GALT efferent lymphatic vessel during the development of EAE but not after onset. In line with this, our results suggest that the migration of GALT stimulated T cells increases before EAE onset.

Intestinal Th17 cells can be induced by different subsets of mononuclear phagocytes in the lamina propria in response to different situations (Stockinger and Omenetti 2017). For example, the induction of SFB-specific Th17 cells is mediated by CX3CR1 positive macrophages, but not conventional CD103⁺ DC (Panea, Farkas et al. 2015). However, in the mice which develop spontaneous small intestine inflammation, both CD103⁺ and CD103⁻ DCs instruct pathologic Th17 cells (Liang, Huang et al. 2016). It is still not clear whether there is a certain DC subset that activates MOG specific T cells to mediate this differentiation. In the future, transgenic mouse lineages with fluorescent labels for different APCs, such as CCR2-RFP, CD11c-YFP and CX1CR3-GFP, can be applied to intravital imaging to identify the partnership of MOG specific T cells in the small intestine.

Furthermore, expression of IFN γ is analysed in the T cells migrating out of mesenteric lymph, since IFN γ producing Th1 cells can induce EAE. Although there was no difference in the frequency, the absolute number of IFN γ ⁺CD4⁺ T cells was elevated in the efferent mesenteric lymph of 2D2 mice (Fig. 3.3.2 B and C). This was due to the increased number of CD4⁺ T cells in the efferent mesenteric lymph of 2D2 mice (data not shown), which suggested traffic of the lymphocytes in the small intestine was enhanced.

In the GALT, production of IFN γ is instructed in by CD103⁻CD11⁺ and CD103⁺CD11^{b-} DCs, but not CD103⁺CD11^{b+} DCs (Liang, Huang et al. 2016).

Although proximal signals required for Th1 differentiation clearly differ from signals governing Th17 development, some CD4⁺ T cells in the MS lesion have an intermediate phenotype, expressing IFN γ and IL17A simultaneously (Dendrou, Fugger et al. 2015). In

addition, Th17 can switch to Th1 under inflammatory conditions in the presence of certain cytokines like IL23 (Bhaumik and Basu 2017). Therefore, besides the classical induction of Th1 cells, the possibility that intestinal Th17 cells convert to Th1 cells in the GALT is possible. A previous study has found that both Th17 and Th1 cells are enhanced in the lamina propria during the preclinical phase of EAE (Haghikia, Jorg et al. 2015).

Additionally, the expression of CD44 on the T cells from the efferent mesenteric lymph of 2D2 and wildtype mice was also investigated. The absolute number of CD44⁺CD4⁺ T cells was increased in the 2D2 mice (Fig.3.3.3 C). CD44 serves as a marker of antigen-experienced, activated T cells (Firan, Dhillon et al. 2006, Alvarez-Sanchez, Cruz-Chamorro et al. 2015). Therefore, increased CD44⁺CD4⁺ T cells in the mesenteric lymph of 2D2 mice reflect upregulated migration of activated antigen-dependent T cells from the GALT. Moreover, CD44 is also involved in T cell polarization during EAE. Deletion of CD44 in encephalitogenic T cells inhibits the Th1/Th17 polarization in an *in vitro* cell culture (Guan, Nagarkatti et al. 2011). In addition, genetic depletion of CD44 impairs the Th1/Th17 polarization through altering the gut microbiome and ameliorates EAE (Chitrala, Guan et al. 2017). Furthermore, CD44 has an important role for adhesion and cell migration as described in section 1.3.4 and 3.3.3 (DeGrendele, Estess et al. 1996, Guan, Nagarkatti et al. 2011). Therefore, increased CD44⁺CD4⁺ T cells might also be associated with the increase of Th1/Th17 cells that emigrate from the GALT. Taking into consideration the elevated number of Th17 cells, Th1 cells and CD44⁺CD4⁺ cells in GALT efferent lymph, MOG specific T cells have already experienced differentiation or expansion in the GALT. Restricted to the existing techniques, it is difficult to monitor the fate of a stimulated T cell *in vivo*. That is, following stimulation it is challenging to track where an individual T cell goes and how it phenotypically changes. Although relating intestinal MOG specific T cells to the demyelination in CNS is still quite challenging, enhanced Th17 cells differentiation in the efferent mesenteric lymph implies the pathogenic risk of EAE exerted by T cell stimulation in the GALT.

organ	T cells	Administration	Frequency of high Calcium signal (Mean \pm SEM) (%)	Proportion of T cells with long calcium signaling (Mean \pm SEM) (%)
Lamina propria	2D2	-	10.9 \pm 1.0	22.7 \pm 3.8
	C57BL/6	-	1.3 \pm 0.8	1.7 \pm 1.7
	TCR1640	-	13.3 \pm 0.3	24.0 \pm 2.3
	TCR1640	Blocking MHC class II	5.9 \pm 1.7	7.6 \pm 3.8
	SJL/J	-	8.0 \pm 0.7	16.9 \pm 0.6
	2D2	Germ free recipients		
Peyer's patch	2D2	-	5.4 \pm 0.8	10.5 \pm 4.9
	C57BL/6	-	5.0 \pm 0.4	9.1 \pm 4.0

Table 4.3.1 Summary of calcium signaling shown by MOG specific T cells and polyclonal T cells in the ileum.

Overall, by combining activation sensors and intravital imaging, this study visualizes the calcium signaling of MOG specific T cells in the ileum (Table 4.3.1). The stimulation of MOG specific T cells has been localized mainly to the lamina propria, not the Peyer's patch. In addition to location specificity, this study illustrates that the stimulation of encephalitogenic T cells in the GALT depended on MHC class II mediated antigen presentation. Emigrating MOG specific T cells are phenotypically altered by stimulation in the GALT, and appear to show a pathogenic tendency towards autoimmune disease. Overall, these findings suggest the essential role of gut microbiota in the stimulation of encephalitogenic T cells, implicating the gut origin of experimental CNS autoimmunity. This study was focusing on the ileum, but also established intravital imaging in the colon. It would be interesting to further explore the behaviour of encephalitogenic T cells in the colon. Last but not least, the possibility that GALT stimulated encephalitogenic T cells subsequently migrate to the CNS needs to be carefully examined in order to extend our understanding of the induction and development of CNS autoimmunity.

REFERENCES

- Alvarez-Sanchez, N., I. Cruz-Chamorro, A. Lopez-Gonzalez, J. C. Utrilla, J. M. Fernandez-Santos, A. Martinez-Lopez, P. J. Lardone, J. M. Guerrero and A. Carrillo-Vico (2015). "Melatonin controls experimental autoimmune encephalomyelitis by altering the T effector/regulatory balance." Brain Behav Immun **50**: 101-114.
- Andersen, O., I. Elovaara, M. Farkkila, H. J. Hansen, S. I. Mellgren, K. M. Myhr, M. Sandberg-Wollheim and P. Soelberg Sorensen (2004). "Multicentre, randomised, double blind, placebo controlled, phase III study of weekly, low dose, subcutaneous interferon beta-1a in secondary progressive multiple sclerosis." J Neurol Neurosurg Psychiatry **75**(5): 706-710.
- Andersson, M., M. Yu, M. Soderstrom, S. Weerth, S. Baig, G. Solders and H. Link (2002). "Multiple MAG peptides are recognized by circulating T and B lymphocytes in polyneuropathy and multiple sclerosis." Eur J Neurol **9**(3): 243-251.
- Ando, D. G., J. Clayton, D. Kono, J. L. Urban and E. E. Sercarz (1989). "Encephalitogenic T cells in the B10.PL model of experimental allergic encephalomyelitis (EAE) are of the Th-1 lymphokine subtype." Cell Immunol **124**(1): 132-143.
- Aruffo, A., I. Stamenkovic, M. Melnick, C. B. Underhill and B. Seed (1990). "CD44 is the principal cell surface receptor for hyaluronate." Cell **61**(7): 1303-1313.
- Atarashi, K., T. Tanoue, M. Ando, N. Kamada, Y. Nagano, S. Narushima, W. Suda, A. Imaoka, H. Setoyama, T. Nagamori, E. Ishikawa, T. Shima, T. Hara, S. Kado, T. Jinnohara, H. Ohno, T. Kondo, K. Toyooka, E. Watanabe, S. Yokoyama, S. Tokoro, H. Mori, Y. Noguchi, H. Morita, Ivanov, I., T. Sugiyama, G. Nunez, J. G. Camp, M. Hattori, Y. Umesaki and K. Honda (2015). "Th17 Cell Induction by Adhesion of Microbes to Intestinal Epithelial Cells." Cell **163**(2): 367-380.
- Baron, J. L., J. A. Madri, N. H. Ruddle, G. Hashim and C. A. Janeway, Jr. (1993). "Surface expression of alpha 4 integrin by CD4 T cells is required for their entry into brain parenchyma." J Exp Med **177**(1): 57-68.
- Bartholomaeus, I., N. Kawakami, F. Odoardi, C. Schlager, D. Miljkovic, J. W. Ellwart, W. E. Klinkert, C. Flugel-Koch, T. B. Issekutz, H. Wekerle and A. Flugel (2009). "Effector T cell interactions with meningeal vascular structures in nascent autoimmune CNS lesions." Nature **462**(7269): 94-98.
- Bashir, M., B. Prietl, M. Tauschmann, S. I. Mautner, P. K. Kump, G. Treiber, P. Wurm, G. Gorkiewicz, C. Hogenauer and T. R. Pieber (2016). "Effects of high doses of vitamin D3 on mucosa-associated gut microbiome vary between regions of the human gastrointestinal tract." Eur J Nutr **55**(4): 1479-1489.
- Bekiaris, V., E. K. Persson and W. W. Agace (2014). "Intestinal dendritic cells in the regulation of mucosal immunity." Immunol Rev **260**(1): 86-101.
- Ben-Nun, A., H. Wekerle and I. R. Cohen (1981). "The rapid isolation of clonable antigen-specific T lymphocyte lines capable of mediating autoimmune encephalomyelitis." Eur J Immunol **11**(3): 195-199.
- Berer, K., L. A. Gerdes, E. Cekanaviciute, X. Jia, L. Xiao, Z. Xia, C. Liu, L. Klotz, U. Stauffer, S. E. Baranzini, T. Kumpfel, R. Hohlfeld, G. Krishnamoorthy and H. Wekerle (2017). "Gut microbiota from multiple sclerosis patients enables spontaneous autoimmune encephalomyelitis in mice." Proc Natl Acad Sci U S A **114**(40): 10719-10724.
- Berer, K., M. Mues, M. Koutrolos, Z. A. Rasbi, M. Boziki, C. Johner, H. Wekerle and G. Krishnamoorthy (2011). "Commensal microbiota and myelin autoantigen cooperate to trigger autoimmune demyelination." Nature **479**(7374): 538-541.
- Bettelli, E., D. Baeten, A. Jager, R. A. Sobel and V. K. Kuchroo (2006). "Myelin oligodendrocyte glycoprotein-specific T and B cells cooperate to induce a Devic-like disease in mice." J Clin Invest **116**(9): 2393-2402.

- Bettelli, E., M. Pagany, H. L. Weiner, C. Lington, R. A. Sobel and V. K. Kuchroo (2003). "Myelin oligodendrocyte glycoprotein-specific T cell receptor transgenic mice develop spontaneous autoimmune optic neuritis." *J Exp Med* **197**(9): 1073-1081.
- Bettelli, E., B. Sullivan, S. J. Szabo, R. A. Sobel, L. H. Glimcher and V. K. Kuchroo (2004). "Loss of T-bet, but not STAT1, prevents the development of experimental autoimmune encephalomyelitis." *J Exp Med* **200**(1): 79-87.
- Bhaumik, S. and R. Basu (2017). "Cellular and Molecular Dynamics of Th17 Differentiation and its Developmental Plasticity in the Intestinal Immune Response." *Front Immunol* **8**: 254.
- Biedermann, L., J. Zeitz, J. Mwinji, E. Sutter-Minder, A. Rehman, S. J. Ott, C. Steurer-Stey, A. Frei, P. Frei, M. Scharl, M. J. Loessner, S. R. Vavricka, M. Fried, S. Schreiber, M. Schuppler and G. Rogler (2013). "Smoking cessation induces profound changes in the composition of the intestinal microbiota in humans." *PLoS One* **8**(3): e59260.
- Bilate, A. M. and J. J. Lafaille (2012). "Induced CD4+Foxp3+ regulatory T cells in immune tolerance." *Annu Rev Immunol* **30**: 733-758.
- Blum, J. S., P. A. Wearsch and P. Cresswell (2013). "Pathways of antigen processing." *Annu Rev Immunol* **31**: 443-473.
- Bo, L., C. A. Vedeler, H. I. Nyland, B. D. Trapp and S. J. Mork (2003). "Subpial demyelination in the cerebral cortex of multiple sclerosis patients." *J Neuropathol Exp Neurol* **62**(7): 723-732.
- Bouskra, D., C. Brezillon, M. Berard, C. Werts, R. Varona, I. G. Boneca and G. Eberl (2008). "Lymphoid tissue genesis induced by commensals through NOD1 regulates intestinal homeostasis." *Nature* **456**(7221): 507-510.
- Brocke, S., C. Piercy, L. Steinman, I. L. Weissman and T. Veromaa (1999). "Antibodies to CD44 and integrin alpha4, but not L-selectin, prevent central nervous system inflammation and experimental encephalomyelitis by blocking secondary leukocyte recruitment." *Proc Natl Acad Sci U S A* **96**(12): 6896-6901.
- Cadavid, D., L. Balcer, S. Galetta, O. Aktas, T. Ziemssen, L. Vanopdenbosch, J. Frederiksen, M. Skeen, G. J. Jaffe, H. Butzkueven, F. Ziemssen, L. Massacesi, Y. Chai, L. Xu, S. Freeman and R. S. Investigators (2017). "Safety and efficacy of opicinumab in acute optic neuritis (RENEW): a randomised, placebo-controlled, phase 2 trial." *Lancet Neurol* **16**(3): 189-199.
- Calvo-Barreiro, L., H. Eixarch, X. Montalban and C. Espejo (2017). "Combined therapies to treat complex diseases: The role of the gut microbiota in multiple sclerosis." *Autoimmun Rev*.
- Camp, R. L., A. Scheynius, C. Johansson and E. Pure (1993). "CD44 is necessary for optimal contact allergic responses but is not required for normal leukocyte extravasation." *J Exp Med* **178**(2): 497-507.
- Celli, S., F. Lemaitre and P. Bousso (2007). "Real-time manipulation of T cell-dendritic cell interactions in vivo reveals the importance of prolonged contacts for CD4+ T cell activation." *Immunity* **27**(4): 625-634.
- Chen, J., N. Chia, K. R. Kalari, J. Z. Yao, M. Novotna, M. M. Soldan, D. H. Luckey, E. V. Marietta, P. R. Jeraldo, X. Chen, B. G. Weinshenker, M. Rodriguez, O. H. Kantarci, H. Nelson, J. A. Murray and A. K. Mangalam (2016). "Multiple sclerosis patients have a distinct gut microbiota compared to healthy controls." *Sci Rep* **6**: 28484.
- Cheng, Q., L. Miao, J. Zhang, S. J. Ding, Z. G. Liu, X. Wang, X. J. Sun, Z. X. Zhao, Y. J. Song, X. Y. Ding, Z. L. Guo, Y. Yang, S. D. Chen, G. X. Jiang and S. Fredrikson (2007). "A population-based survey of multiple sclerosis in Shanghai, China." *Neurology* **68**(18): 1495-1500.
- Cheroutre, H., F. Lambomez and D. Mucida (2011). "The light and dark sides of intestinal intraepithelial lymphocytes." *Nat Rev Immunol* **11**(7): 445-456.
- Chitrala, K. N., H. Guan, N. P. Singh, B. Busbee, A. Gandy, P. Mehrpouya-Bahrami, M. S. Ganewatta, C. Tang, S. Chatterjee, P. Nagarkatti and M. Nagarkatti (2017). "CD44 deletion leading to attenuation of experimental autoimmune encephalomyelitis results from alterations in gut microbiome in mice." *Eur J Immunol* **47**(7): 1188-1199.

- Cho, J. H., C. J. Swanson, J. Chen, A. Li, L. G. Lippert, S. E. Boye, K. Rose, S. Sivaramakrishnan, C. M. Chuong and R. H. Chow (2017). "The GCaMP-R Family of Genetically Encoded Ratiometric Calcium Indicators." *ACS Chem Biol* **12**(4): 1066-1074.
- Cifelli, A., M. Arridge, P. Jezard, M. M. Esiri, J. Palace and P. M. Matthews (2002). "Thalamic neurodegeneration in multiple sclerosis." *Ann Neurol* **52**(5): 650-653.
- Cohen, J. A. (2013). "Mesenchymal stem cell transplantation in multiple sclerosis." *J Neurol Sci* **333**(1-2): 43-49.
- Cohen, J. A., G. R. Cutter, J. S. Fischer, A. D. Goodman, F. R. Heidenreich, M. F. Kooijmans, A. W. Sandroock, R. A. Rudick, J. H. Simon, N. A. Simonian, E. C. Tsao, J. N. Whitaker and I. Investigators (2002). "Benefit of interferon beta-1a on MSFC progression in secondary progressive MS." *Neurology* **59**(5): 679-687.
- Constantinescu, C. S., N. Farooqi, K. O'Brien and B. Gran (2011). "Experimental autoimmune encephalomyelitis (EAE) as a model for multiple sclerosis (MS)." *Br J Pharmacol* **164**(4): 1079-1106.
- Cornes, J. S. (1965). "Number, size, and distribution of Peyer's patches in the human small intestine: Part I The development of Peyer's patches." *Gut* **6**(3): 225-229.
- Correale, J., M. I. Gaitan, M. C. Ysraelit and M. P. Fiol (2017). "Progressive multiple sclerosis: from pathogenic mechanisms to treatment." *Brain* **140**(3): 527-546.
- Dasgupta, S., D. Erturk-Hasdemir, J. Ochoa-Reparaz, H. C. Reinecker and D. L. Kasper (2014). "Plasmacytoid dendritic cells mediate anti-inflammatory responses to a gut commensal molecule via both innate and adaptive mechanisms." *Cell Host Microbe* **15**(4): 413-423.
- DeGrendele, H. C., P. Estess, L. J. Picker and M. H. Siegelman (1996). "CD44 and its ligand hyaluronate mediate rolling under physiologic flow: a novel lymphocyte-endothelial cell primary adhesion pathway." *J Exp Med* **183**(3): 1119-1130.
- DeGrendele, H. C., P. Estess and M. H. Siegelman (1997). "Requirement for CD44 in activated T cell extravasation into an inflammatory site." *Science* **278**(5338): 672-675.
- Dendrou, C. A., L. Fugger and M. A. Friese (2015). "Immunopathology of multiple sclerosis." *Nat Rev Immunol* **15**(9): 545-558.
- Denning, T. L., B. A. Norris, O. Medina-Contreras, S. Manicassamy, D. Geem, R. Madan, C. L. Karp and B. Pulendran (2011). "Functional specializations of intestinal dendritic cell and macrophage subsets that control Th17 and regulatory T cell responses are dependent on the T cell/APC ratio, source of mouse strain, and regional localization." *J Immunol* **187**(2): 733-747.
- Druzd, D., O. Matveeva, L. Ince, U. Harrison, W. He, C. Schmal, H. Herzel, A. H. Tsang, N. Kawakami, A. Leliavski, O. Uhl, L. Yao, L. E. Sander, C. S. Chen, K. Kraus, A. de Juan, S. M. Hergenhan, M. Ehlers, B. Koletzko, R. Haas, W. Solbach, H. Oster and C. Scheiermann (2017). "Lymphocyte Circadian Clocks Control Lymph Node Trafficking and Adaptive Immune Responses." *Immunity* **46**(1): 120-132.
- El-Behi, M., B. Ciric, H. Dai, Y. Yan, M. Cullimore, F. Safavi, G. X. Zhang, B. N. Dittel and A. Rostami (2011). "The encephalitogenicity of T(H)17 cells is dependent on IL-1- and IL-23-induced production of the cytokine GM-CSF." *Nat Immunol* **12**(6): 568-575.
- Ellmerich, S., M. Mycko, K. Takacs, H. Waldner, F. N. Wahid, R. J. Boyton, R. H. King, P. A. Smith, S. Amor, A. H. Herlihy, R. E. Hewitt, M. Jutton, D. A. Price, D. A. Hafler, V. K. Kuchroo and D. M. Altmann (2005). "High incidence of spontaneous disease in an HLA-DR15 and TCR transgenic multiple sclerosis model." *J Immunol* **174**(4): 1938-1946.
- Eskandarieh, S., P. Heydarpour, A. Minagar, S. Pourmand and M. A. Sahraian (2016). "Multiple Sclerosis Epidemiology in East Asia, South East Asia and South Asia: A Systematic Review." *Neuroepidemiology* **46**(3): 209-221.
- Faria, A. M. C., B. S. Reis and D. Mucida (2017). "Tissue adaptation: Implications for gut immunity and tolerance." *J Exp Med* **214**(5): 1211-1226.
- Feske, S. (2007). "Calcium signalling in lymphocyte activation and disease." *Nat Rev Immunol* **7**(9): 690-702.

- Feske, S., J. Giltman, R. Dolmetsch, L. M. Staudt and A. Rao (2001). "Gene regulation mediated by calcium signals in T lymphocytes." *Nat Immunol* **2**(4): 316-324.
- Firan, M., S. Dhillon, P. Estess and M. H. Siegelman (2006). "Suppressor activity and potency among regulatory T cells is discriminated by functionally active CD44." *Blood* **107**(2): 619-627.
- Flachenecker, P. and K. Stuke (2008). "National MS registries." *J Neurol* **255 Suppl 6**: 102-108.
- Fracchia, K. M., C. Y. Pai and C. M. Walsh (2013). "Modulation of T Cell Metabolism and Function through Calcium Signaling." *Front Immunol* **4**: 324.
- Ghazi-Visser, L., J. D. Laman, S. Nagel, M. van Meurs, D. van Riel, A. Tzankov, S. Frank, H. Adams, K. Wolk, L. Terracciano, M. J. Melief, R. Sabat and U. Gunthert (2013). "CD44 variant isoforms control experimental autoimmune encephalomyelitis by affecting the lifespan of the pathogenic T cells." *FASEB J* **27**(9): 3683-3701.
- Gold, R., C. Lington and H. Lassmann (2006). "Understanding pathogenesis and therapy of multiple sclerosis via animal models: 70 years of merits and culprits in experimental autoimmune encephalomyelitis research." *Brain* **129**(Pt 8): 1953-1971.
- Gomez-Rodriguez, J., N. Sahu, R. Handon, T. S. Davidson, S. M. Anderson, M. R. Kirby, A. August and P. L. Schwartzberg (2009). "Differential expression of interleukin-17A and -17F is coupled to T cell receptor signaling via inducible T cell kinase." *Immunity* **31**(4): 587-597.
- Goverman, J., A. Woods, L. Larson, L. P. Weiner, L. Hood and D. M. Zaller (1993). "Transgenic mice that express a myelin basic protein-specific T cell receptor develop spontaneous autoimmunity." *Cell* **72**(4): 551-560.
- Guan, H., P. S. Nagarkatti and M. Nagarkatti (2011). "CD44 Reciprocally regulates the differentiation of encephalitogenic Th1/Th17 and Th2/regulatory T cells through epigenetic modulation involving DNA methylation of cytokine gene promoters, thereby controlling the development of experimental autoimmune encephalomyelitis." *J Immunol* **186**(12): 6955-6964.
- Gunzer, M., A. Schafer, S. Borgmann, S. Grabbe, K. S. Zanker, E. B. Brocker, E. Kampgen and P. Friedl (2000). "Antigen presentation in extracellular matrix: interactions of T cells with dendritic cells are dynamic, short lived, and sequential." *Immunity* **13**(3): 323-332.
- Haghikia, A., S. Jorg, A. Duscha, J. Berg, A. Manzel, A. Waschbisch, A. Hammer, D. H. Lee, C. May, N. Wilck, A. Balogh, A. I. Ostermann, N. H. Schebb, D. A. Akkad, D. A. Grohme, M. Kleinewietfeld, S. Kempa, J. Thone, S. Demir, D. N. Muller, R. Gold and R. A. Linker (2015). "Dietary Fatty Acids Directly Impact Central Nervous System Autoimmunity via the Small Intestine." *Immunity* **43**(4): 817-829.
- Hayday, A. and D. Gibbons (2008). "Brokering the peace: the origin of intestinal T cells." *Mucosal Immunol* **1**(3): 172-174.
- Hirota, K., J. H. Duarte, M. Veldhoen, E. Hornsby, Y. Li, D. J. Cua, H. Ahlfors, C. Wilhelm, M. Tolaini, U. Menzel, A. Garefalaki, A. J. Potocnik and B. Stockinger (2011). "Fate mapping of IL-17-producing T cells in inflammatory responses." *Nat Immunol* **12**(3): 255-263.
- Honda, K. and D. R. Littman (2016). "The microbiota in adaptive immune homeostasis and disease." *Nature* **535**(7610): 75-84.
- Ivanov, I., K. Atarashi, N. Manel, E. L. Brodie, T. Shima, U. Karaoz, D. Wei, K. C. Goldfarb, C. A. Santee, S. V. Lynch, T. Tanoue, A. Imaoka, K. Itoh, K. Takeda, Y. Umesaki, K. Honda and D. R. Littman (2009). "Induction of intestinal Th17 cells by segmented filamentous bacteria." *Cell* **139**(3): 485-498.
- Ivanov, I., B. S. McKenzie, L. Zhou, C. E. Tadokoro, A. Lepelley, J. J. Lafaille, D. J. Cua and D. R. Littman (2006). "The orphan nuclear receptor ROR γ directs the differentiation program of proinflammatory IL-17+ T helper cells." *Cell* **126**(6): 1121-1133.
- Jager, A., V. Dardalhon, R. A. Sobel, E. Bettelli and V. K. Kuchroo (2009). "Th1, Th17, and Th9 effector cells induce experimental autoimmune encephalomyelitis with different pathological phenotypes." *J Immunol* **183**(11): 7169-7177.
- Jangi, S., R. Gandhi, L. M. Cox, N. Li, F. von Glehn, R. Yan, B. Patel, M. A. Mazzola, S. Liu, B. L. Glanz, S. Cook, S. Tankou, F. Stuart, K. Melo, P. Nejad, K. Smith, B. D. Topcuolu, J. Holden, P. Kivisakk, T.

- Chitnis, P. L. De Jager, F. J. Quintana, G. K. Gerber, L. Bry and H. L. Weiner (2016). "Alterations of the human gut microbiome in multiple sclerosis." *Nat Commun* **7**: 12015.
- Kapoor, R., J. Furby, T. Hayton, K. J. Smith, D. R. Altmann, R. Brenner, J. Chataway, R. A. Hughes and D. H. Miller (2010). "Lamotrigine for neuroprotection in secondary progressive multiple sclerosis: a randomised, double-blind, placebo-controlled, parallel-group trial." *Lancet Neurol* **9**(7): 681-688.
- Kappos, L., B. Weinshenker, C. Pozzilli, A. J. Thompson, F. Dahlke, K. Beckmann, C. Polman, H. McFarland, C. European Interferon beta-1b in Secondary Progressive Multiple Sclerosis Trial Steering, B. Independent Advisory, C. North American Interferon beta-1b in Secondary Progressive Multiple Sclerosis Trial Steering and B. Independent Advisory (2004). "Interferon beta-1b in secondary progressive MS: a combined analysis of the two trials." *Neurology* **63**(10): 1779-1787.
- Kawakami, N., S. Lassmann, Z. Li, F. Odoardi, T. Ritter, T. Ziemssen, W. E. Klinkert, J. W. Ellwart, M. Bradl, K. Krivacic, H. Lassmann, R. M. Ransohoff, H. D. Volk, H. Wekerle, C. Lington and A. Flugel (2004). "The activation status of neuroantigen-specific T cells in the target organ determines the clinical outcome of autoimmune encephalomyelitis." *J Exp Med* **199**(2): 185-197.
- Kebir, H., K. Kreymborg, I. Ifergan, A. Dodelet-Devillers, R. Cayrol, M. Bernard, F. Giuliani, N. Arbour, B. Becher and A. Prat (2007). "Human TH17 lymphocytes promote blood-brain barrier disruption and central nervous system inflammation." *Nat Med* **13**(10): 1173-1175.
- Kidd, D., F. Barkhof, R. McConnell, P. R. Algra, I. V. Allen and T. Revesz (1999). "Cortical lesions in multiple sclerosis." *Brain* **122** (Pt 1): 17-26.
- Kim, K. D., S. Srikanth, Y. V. Tan, M. K. Yee, M. Jew, R. Damoiseaux, M. E. Jung, S. Shimizu, D. S. An, B. Ribalet, J. A. Waschek and Y. Gwack (2014). "Calcium signaling via Orai1 is essential for induction of the nuclear orphan receptor pathway to drive Th17 differentiation." *J Immunol* **192**(1): 110-122.
- Kleinewietfeld, M., A. Manzel, J. Titze, H. Kvakana, N. Yosef, R. A. Linker, D. N. Muller and D. A. Hafler (2013). "Sodium chloride drives autoimmune disease by the induction of pathogenic TH17 cells." *Nature* **496**(7446): 518-522.
- Krishnamoorthy, G., H. Lassmann, H. Wekerle and A. Holz (2006). "Spontaneous opticospinal encephalomyelitis in a double-transgenic mouse model of autoimmune T cell/B cell cooperation." *J Clin Invest* **116**(9): 2385-2392.
- Krishnamoorthy, G., A. Saxena, L. T. Mars, H. S. Domingues, R. Mentele, A. Ben-Nun, H. Lassmann, K. Dornmair, F. C. Kurschus, R. S. Liblau and H. Wekerle (2009). "Myelin-specific T cells also recognize neuronal autoantigen in a transgenic mouse model of multiple sclerosis." *Nat Med* **15**(6): 626-632.
- Krishnamoorthy, G. and H. Wekerle (2009). "EAE: an immunologist's magic eye." *Eur J Immunol* **39**(8): 2031-2035.
- Kyratsous, N. I., I. J. Bauer, G. Zhang, M. Pesic, I. Bartholomaeus, M. Mues, P. Fang, M. Worner, S. Everts, J. W. Ellwart, J. M. Watt, B. V. L. Potter, R. Hohlfeld, H. Wekerle and N. Kawakami (2017). "Visualizing context-dependent calcium signaling in encephalitogenic T cells in vivo by two-photon microscopy." *Proc Natl Acad Sci U S A* **114**(31): E6381-E6389.
- Lassmann, H. (2014). "Multiple sclerosis: lessons from molecular neuropathology." *Exp Neurol* **262** Pt A: 2-7.
- Lecuyer, E., S. Rakotobe, H. Lengline-Garnier, C. Lebreton, M. Picard, C. Juste, R. Fritzen, G. Eberl, K. D. McCoy, A. J. Macpherson, C. A. Reynaud, N. Cerf-Bensussan and V. Gaboriau-Routhiau (2014). "Segmented filamentous bacterium uses secondary and tertiary lymphoid tissues to induce gut IgA and specific T helper 17 cell responses." *Immunity* **40**(4): 608-620.
- Lee, Y. K., J. S. Menezes, Y. Umesaki and S. K. Mazmanian (2011). "Proinflammatory T-cell responses to gut microbiota promote experimental autoimmune encephalomyelitis." *Proc Natl Acad Sci U S A* **108** Suppl 1: 4615-4622.

- Li, D. K., G. J. Zhao, D. W. Paty and M. S. M. R. I. A. R. G. T. S. S. G. University of British Columbia (2001). "Randomized controlled trial of interferon-beta-1a in secondary progressive MS: MRI results." *Neurology* **56**(11): 1505-1513.
- Liang, J., H. I. Huang, F. P. Benzatti, A. B. Karlsson, J. J. Zhang, N. Youssef, A. Ma, L. P. Hale and G. E. Hammer (2016). "Inflammatory Th1 and Th17 in the Intestine Are Each Driven by Functionally Specialized Dendritic Cells with Distinct Requirements for MyD88." *Cell Rep* **17**(5): 1330-1343.
- Lodygin, D., F. Odoardi, C. Schlager, H. Korner, A. Kitz, M. Nosov, J. van den Brandt, H. M. Reichardt, M. Haberl and A. Flugel (2013). "A combination of fluorescent NFAT and H2B sensors uncovers dynamics of T cell activation in real time during CNS autoimmunity." *Nat Med* **19**(6): 784-790.
- Longman, R. S., G. E. Diehl, D. A. Victorio, J. R. Huh, C. Galan, E. R. Miraldi, A. Swaminath, R. Bonneau, E. J. Scherl and D. R. Littman (2014). "CX(3)CR1(+) mononuclear phagocytes support colitis-associated innate lymphoid cell production of IL-22." *J Exp Med* **211**(8): 1571-1583.
- Lublin, F. D. and S. C. Reingold (1996). "Defining the clinical course of multiple sclerosis: results of an international survey. National Multiple Sclerosis Society (USA) Advisory Committee on Clinical Trials of New Agents in Multiple Sclerosis." *Neurology* **46**(4): 907-911.
- Madsen, L. S., E. C. Andersson, L. Jansson, M. Krogsgaard, C. B. Andersen, J. Engberg, J. L. Strominger, A. Svejgaard, J. P. Hjorth, R. Holmdahl, K. W. Wucherpfennig and L. Fugger (1999). "A humanized model for multiple sclerosis using HLA-DR2 and a human T-cell receptor." *Nat Genet* **23**(3): 343-347.
- Mangalam, A., S. K. Shahi, D. Luckey, M. Karau, E. Marietta, N. Luo, R. S. Choung, J. Ju, R. Sompallae, K. Gibson-Corley, R. Patel, M. Rodriguez, C. David, V. Taneja and J. Murray (2017). "Human Gut-Derived Commensal Bacteria Suppress CNS Inflammatory and Demyelinating Disease." *Cell Rep* **20**(6): 1269-1277.
- Mank, M., A. F. Santos, S. Drenberger, T. D. Mrcic-Flogel, S. B. Hofer, V. Stein, T. Hendel, D. F. Reiff, C. Levelt, A. Borst, T. Bonhoeffer, M. Hubener and O. Griesbeck (2008). "A genetically encoded calcium indicator for chronic in vivo two-photon imaging." *Nat Methods* **5**(9): 805-811.
- Masahata, K., E. Umemoto, H. Kayama, M. Kotani, S. Nakamura, T. Kurakawa, J. Kikuta, K. Gotoh, D. Motooka, S. Sato, T. Higuchi, Y. Baba, T. Kurosaki, M. Kinoshita, Y. Shimada, T. Kimura, R. Okumura, A. Takeda, M. Tajima, O. Yoshie, M. Fukuzawa, H. Kiyono, S. Fagarasan, T. Iida, M. Ishii and K. Takeda (2014). "Generation of colonic IgA-secreting cells in the caecal patch." *Nat Commun* **5**: 3704.
- Maynard, C. L., L. E. Harrington, K. M. Janowski, J. R. Oliver, C. L. Zindl, A. Y. Rudensky and C. T. Weaver (2007). "Regulatory T cells expressing interleukin 10 develop from Foxp3+ and Foxp3-precursor cells in the absence of interleukin 10." *Nat Immunol* **8**(9): 931-941.
- Merrill, J. E., D. H. Kono, J. Clayton, D. G. Ando, D. R. Hinton and F. M. Hofman (1992). "Inflammatory leukocytes and cytokines in the peptide-induced disease of experimental allergic encephalomyelitis in SJL and B10.PL mice." *Proc Natl Acad Sci U S A* **89**(2): 574-578.
- Mi, S., R. B. Pepinsky and D. Cadavid (2013). "Blocking LINGO-1 as a therapy to promote CNS repair: from concept to the clinic." *CNS Drugs* **27**(7): 493-503.
- Montes, M., D. McIlroy, A. Hosmalin and A. Trautmann (1999). "Calcium responses elicited in human T cells and dendritic cells by cell-cell interaction and soluble ligands." *Int Immunol* **11**(4): 561-568.
- Mowat, A. M. and W. W. Agace (2014). "Regional specialization within the intestinal immune system." *Nat Rev Immunol* **14**(10): 667-685.
- Mues, M., I. Bartholomaeus, T. Thestrup, O. Griesbeck, H. Wekerle, N. Kawakami and G. Krishnamoorthy (2013). "Real-time in vivo analysis of T cell activation in the central nervous system using a genetically encoded calcium indicator." *Nat Med* **19**(6): 778-783.

- Nojima, T., K. Haniuda, T. Moutai, M. Matsudaira, S. Mizokawa, I. Shiratori, T. Azuma and D. Kitamura (2011). "In-vitro derived germinal centre B cells differentially generate memory B or plasma cells in vivo." *Nat Commun* **2**: 465.
- Ochoa-Reparaz, J., D. W. Mielcarz, L. E. Ditrío, A. R. Burroughs, D. M. Foureau, S. Haque-Begum and L. H. Kasper (2009). "Role of gut commensal microflora in the development of experimental autoimmune encephalomyelitis." *J Immunol* **183**(10): 6041-6050.
- Oh-hora, M. (2009). "Calcium signaling in the development and function of T-lineage cells." *Immunol Rev* **231**(1): 210-224.
- Olsson, T., J. Sun, J. Hillert, B. Hojberg, H. P. Ekre, G. Andersson, O. Olerup and H. Link (1992). "Increased numbers of T cells recognizing multiple myelin basic protein epitopes in multiple sclerosis." *Eur J Immunol* **22**(4): 1083-1087.
- Ontaneda, D., A. J. Thompson, R. J. Fox and J. A. Cohen (2017). "Progressive multiple sclerosis: prospects for disease therapy, repair, and restoration of function." *Lancet* **389**(10076): 1357-1366.
- Panea, C., A. M. Farkas, Y. Goto, S. Abdollahi-Roodsaz, C. Lee, B. Koscsó, K. Gowda, T. M. Hohl, M. Bogunovic and Ivanov, II (2015). "Intestinal Monocyte-Derived Macrophages Control Commensal-Specific Th17 Responses." *Cell Rep* **12**(8): 1314-1324.
- Panitch, H., A. Miller, D. Paty, B. Weinschenker and M. S. North American Study Group on Interferon beta-1b in Secondary Progressive (2004). "Interferon beta-1b in secondary progressive MS: results from a 3-year controlled study." *Neurology* **63**(10): 1788-1795.
- Park, H., Z. Li, X. O. Yang, S. H. Chang, R. Nurieva, Y. H. Wang, Y. Wang, L. Hood, Z. Zhu, Q. Tian and C. Dong (2005). "A distinct lineage of CD4 T cells regulates tissue inflammation by producing interleukin 17." *Nat Immunol* **6**(11): 1133-1141.
- Patejdl, R. and U. K. Zettl (2017). "Spasticity in multiple sclerosis: Contribution of inflammation, autoimmune mediated neuronal damage and therapeutic interventions." *Autoimmun Rev* **16**(9): 925-936.
- Pelfrey, C. M., R. A. Rudick, A. C. Coteleur, J. C. Lee, M. Tary-Lehmann and P. V. Lehmann (2000). "Quantification of self-recognition in multiple sclerosis by single-cell analysis of cytokine production." *J Immunol* **165**(3): 1641-1651.
- Pender, M. P., Z. Tabi, K. B. Nguyen and P. A. McCombe (1995). "The proximal peripheral nervous system is a major site of demyelination in experimental autoimmune encephalomyelitis induced in the Lewis rat by a myelin basic protein-specific T cell clone." *Acta Neuropathol* **89**(6): 527-531.
- Perry, G. A. and J. G. Sharp (1988). "Characterization of proximal colonic lymphoid tissue in the mouse." *Anat Rec* **220**(3): 305-312.
- Pesic, M., I. Bartholomäus, N. I. Kyratsous, V. Heissmeyer, H. Wekerle and N. Kawakami (2013). "2-photon imaging of phagocyte-mediated T cell activation in the CNS." *J Clin Invest* **123**(3): 1192-1201.
- Pette, M., K. Fujita, D. Wilkinson, D. M. Altmann, J. Trowsdale, G. Giegerich, A. Hinkkanen, J. T. Epplen, L. Kappos and H. Wekerle (1990). "Myelin autoreactivity in multiple sclerosis: recognition of myelin basic protein in the context of HLA-DR2 products by T lymphocytes of multiple-sclerosis patients and healthy donors." *Proc Natl Acad Sci U S A* **87**(20): 7968-7972.
- Pierson, E., S. B. Simmons, L. Castelli and J. M. Goverman (2012). "Mechanisms regulating regional localization of inflammation during CNS autoimmunity." *Immunol Rev* **248**(1): 205-215.
- Pilli, D., A. Zou, F. Tea, R. C. Dale and F. Brilot (2017). "Expanding Role of T Cells in Human Autoimmune Diseases of the Central Nervous System." *Front Immunol* **8**: 652.
- Pollinger, B., G. Krishnamoorthy, K. Berer, H. Lassmann, M. R. Bosl, R. Dunn, H. S. Domingues, A. Holz, F. C. Kurschus and H. Wekerle (2009). "Spontaneous relapsing-remitting EAE in the SJL/J mouse: MOG-reactive transgenic T cells recruit endogenous MOG-specific B cells." *J Exp Med* **206**(6): 1303-1316.

- Raftopoulos, R., S. J. Hickman, A. Toosy, B. Sharrack, S. Mallik, D. Paling, D. R. Altmann, M. C. Yiannakas, P. Malladi, R. Sheridan, P. G. Sarrigiannis, N. Hoggard, M. Koltzenburg, C. A. Gandini Wheeler-Kingshott, K. Schmierer, G. Giovannoni, D. H. Miller and R. Kapoor (2016). "Phenytoin for neuroprotection in patients with acute optic neuritis: a randomised, placebo-controlled, phase 2 trial." *Lancet Neurol* **15**(3): 259-269.
- Revy, P., M. Sospedra, B. Barbour and A. Trautmann (2001). "Functional antigen-independent synapses formed between T cells and dendritic cells." *Nat Immunol* **2**(10): 925-931.
- Ridaura, V. K., J. J. Faith, F. E. Rey, J. Cheng, A. E. Duncan, A. L. Kau, N. W. Griffin, V. Lombard, B. Henrissat, J. R. Bain, M. J. Muehlbauer, O. Ilkayeva, C. F. Semenkovich, K. Funai, D. K. Hayashi, B. J. Lyle, M. C. Martini, L. K. Ursell, J. C. Clemente, W. Van Treuren, W. A. Walters, R. Knight, C. B. Newgard, A. C. Heath and J. I. Gordon (2013). "Gut microbiota from twins discordant for obesity modulate metabolism in mice." *Science* **341**(6150): 1241214.
- Rivera, V. M. (2017). "Multiple Sclerosis in Latin Americans: Genetic Aspects." *Curr Neurol Neurosci Rep* **17**(8): 57.
- Rivers, T. M., D. H. Sprunt and G. P. Berry (1933). "Observations on Attempts to Produce Acute Disseminated Encephalomyelitis in Monkeys." *J Exp Med* **58**(1): 39-53.
- Rogier, R., H. Evans-Marin, J. Manasson, P. M. van der Kraan, B. Walgreen, M. M. Helsen, L. A. van den Bersselaar, F. A. van de Loo, P. L. van Lent, S. B. Abramson, W. B. van den Berg, M. I. Koenders, J. U. Scher and S. Abdollahi-Roodsaz (2017). "Alteration of the intestinal microbiome characterizes preclinical inflammatory arthritis in mice and its modulation attenuates established arthritis." *Sci Rep* **7**(1): 15613.
- Sano, T., W. Huang, J. A. Hall, Y. Yang, A. Chen, S. J. Gavzy, J. Y. Lee, J. W. Ziel, E. R. Miraldi, A. I. Domingos, R. Bonneau and D. R. Littman (2015). "An IL-23R/IL-22 Circuit Regulates Epithelial Serum Amyloid A to Promote Local Effector Th17 Responses." *Cell* **163**(2): 381-393.
- Sarrabayrouse, G., C. Bossard, J. M. Chauvin, A. Jarry, G. Meurette, E. Quevrain, C. Bridonneau, L. Preisser, K. Asehnoune, N. Labarriere, F. Altare, H. Sokol and F. Jotereau (2014). "CD4CD8 α lymphocytes, a novel human regulatory T cell subset induced by colonic bacteria and deficient in patients with inflammatory bowel disease." *PLoS Biol* **12**(4): e1001833.
- Sathaliyawala, T., M. Kubota, N. Yudanin, D. Turner, P. Camp, J. J. Thome, K. L. Bickham, H. Lerner, M. Goldstein, M. Sykes, T. Kato and D. L. Farber (2013). "Distribution and compartmentalization of human circulating and tissue-resident memory T cell subsets." *Immunity* **38**(1): 187-197.
- Sawcer, S., R. J. Franklin and M. Ban (2014). "Multiple sclerosis genetics." *Lancet Neurol* **13**(7): 700-709.
- Schuhmann, M. K., D. Stegner, A. Berna-Erro, S. Bittner, A. Braun, C. Kleinschnitz, G. Stoll, H. Wiendl, S. G. Meuth and B. Nieswandt (2010). "Stromal interaction molecules 1 and 2 are key regulators of autoreactive T cell activation in murine autoimmune central nervous system inflammation." *J Immunol* **184**(3): 1536-1542.
- Secher, T., S. Kasseem, M. Benamar, I. Bernard, M. Boury, F. Barreau, E. Oswald and A. Saoudi (2017). "Oral Administration of the Probiotic Strain Escherichia coli Nissle 1917 Reduces Susceptibility to Neuroinflammation and Repairs Experimental Autoimmune Encephalomyelitis-Induced Intestinal Barrier Dysfunction." *Front Immunol* **8**: 1096.
- Shaw, M. H., N. Kamada, Y. G. Kim and G. Nunez (2012). "Microbiota-induced IL-1 β , but not IL-6, is critical for the development of steady-state TH17 cells in the intestine." *J Exp Med* **209**(2): 251-258.
- Sie, C., T. Korn and M. Mitsdoerffer (2014). "Th17 cells in central nervous system autoimmunity." *Exp Neurol* **262 Pt A**: 18-27.
- Soilu-Hanninen, M., M. Laaksonen and A. Hanninen (2005). "Hyaluronate receptor (CD44) and integrin α 4 (CD49d) are up-regulated on T cells during MS relapses." *J Neuroimmunol* **166**(1-2): 189-192.

- Sommer, F. and F. Backhed (2013). "The gut microbiota--masters of host development and physiology." *Nat Rev Microbiol* **11**(4): 227-238.
- Sommer, F., S. Bischof, M. Rollinghoff and M. Lohoff (1994). "Demonstration of organic anion transport in T lymphocytes. L-lactate and fluo-3 are target molecules." *J Immunol* **153**(8): 3523-3532.
- Sospedra, M. and R. Martin (2005). "Immunology of multiple sclerosis." *Annu Rev Immunol* **23**: 683-747.
- Stockinger, B. and S. Omenetti (2017). "The dichotomous nature of T helper 17 cells." *Nat Rev Immunol* **17**(9): 535-544.
- Storch, M. K., A. Stefferl, U. Brehm, R. Weissert, E. Wallstrom, M. Kerschensteiner, T. Olsson, C. Linington and H. Lassmann (1998). "Autoimmunity to myelin oligodendrocyte glycoprotein in rats mimics the spectrum of multiple sclerosis pathology." *Brain Pathol* **8**(4): 681-694.
- Stromnes, I. M. and J. M. Goverman (2006). "Active induction of experimental allergic encephalomyelitis." *Nat Protoc* **1**(4): 1810-1819.
- Takeda, K., B. E. Clausen, T. Kaisho, T. Tsujimura, N. Terada, I. Forster and S. Akira (1999). "Enhanced Th1 activity and development of chronic enterocolitis in mice devoid of Stat3 in macrophages and neutrophils." *Immunity* **10**(1): 39-49.
- Thestrup, T., J. Litzlbauer, I. Bartholomaeus, M. Mues, L. Russo, H. Dana, Y. Kovalchuk, Y. Liang, G. Kalamakis, Y. Laukat, S. Becker, G. Witte, A. Geiger, T. Allen, L. C. Rome, T. W. Chen, D. S. Kim, O. Garaschuk, C. Griesinger and O. Griesbeck (2014). "Optimized ratiometric calcium sensors for functional in vivo imaging of neurons and T lymphocytes." *Nat Methods* **11**(2): 175-182.
- Thompson, A. J., S. E. Baranzini, J. Geurts, B. Hemmer and O. Ciccarelli (2018). "Multiple sclerosis." *Lancet* **391**(10130): 1622-1636.
- Tian, L., S. A. Hires, T. Mao, D. Huber, M. E. Chiappe, S. H. Chalasani, L. Petreanu, J. Akerboom, S. A. McKinney, E. R. Schreiter, C. I. Bargmann, V. Jayaraman, K. Svoboda and L. L. Looger (2009). "Imaging neural activity in worms, flies and mice with improved GCaMP calcium indicators." *Nat Methods* **6**(12): 875-881.
- Tsuji, M., K. Suzuki, H. Kitamura, M. Maruya, K. Kinoshita, Ivanov, I., K. Itoh, D. R. Littman and S. Fagarasan (2008). "Requirement for lymphoid tissue-inducer cells in isolated follicle formation and T cell-independent immunoglobulin A generation in the gut." *Immunity* **29**(2): 261-271.
- Tzartos, J. S., M. A. Friese, M. J. Craner, J. Palace, J. Newcombe, M. M. Esiri and L. Fugger (2008). "Interleukin-17 production in central nervous system-infiltrating T cells and glial cells is associated with active disease in multiple sclerosis." *Am J Pathol* **172**(1): 146-155.
- Valli, A., A. Sette, L. Kappos, C. Oseroff, J. Sidney, G. Miescher, M. Hochberger, E. D. Albert and L. Adorini (1993). "Binding of myelin basic protein peptides to human histocompatibility leukocyte antigen class II molecules and their recognition by T cells from multiple sclerosis patients." *J Clin Invest* **91**(2): 616-628.
- Veenbergen, S. and J. N. Samsom (2012). "Maintenance of small intestinal and colonic tolerance by IL-10-producing regulatory T cell subsets." *Curr Opin Immunol* **24**(3): 269-276.
- Vercellino, M., S. Masera, M. Lorenzatti, C. Condello, A. Merola, A. Mattioda, A. Tribolo, E. Capello, G. L. Mancardi, R. Mutani, M. T. Giordana and P. Cavalla (2009). "Demyelination, inflammation, and neurodegeneration in multiple sclerosis deep gray matter." *J Neuropathol Exp Neurol* **68**(5): 489-502.
- Weaver, C. T., C. O. Elson, L. A. Fouser and J. K. Kolls (2013). "The Th17 pathway and inflammatory diseases of the intestines, lungs, and skin." *Annu Rev Pathol* **8**: 477-512.
- Wei, S. H., O. Safrina, Y. Yu, K. R. Garrod, M. D. Cahalan and I. Parker (2007). "Ca²⁺ signals in CD4⁺ T cells during early contacts with antigen-bearing dendritic cells in lymph node." *J Immunol* **179**(3): 1586-1594.

- Weismann, M., A. H. Guse, L. Sorokin, B. Broker, M. Frieser, R. Hallmann and G. W. Mayr (1997). "Integrin-mediated intracellular Ca²⁺ signaling in Jurkat T lymphocytes." J Immunol **158**(4): 1618-1627.
- Wekerle, H. (2017). "Brain Autoimmunity and Intestinal Microbiota: 100 Trillion Game Changers." Trends Immunol **38**(7): 483-497.
- Windrem, M. S., S. J. Schanz, M. Guo, G. F. Tian, V. Washco, N. Stanwood, M. Rasband, N. S. Roy, M. Nedergaard, L. A. Havton, S. Wang and S. A. Goldman (2008). "Neonatal chimerization with human glial progenitor cells can both remyelinate and rescue the otherwise lethally hypomyelinated shiverer mouse." Cell Stem Cell **2**(6): 553-565.
- Winkler, C. W., S. C. Foster, S. G. Matsumoto, M. A. Preston, R. Xing, B. F. Bebo, F. Banine, M. A. Berny-Lang, A. Itakura, O. J. McCarty and L. S. Sherman (2012). "Hyaluronan anchored to activated CD44 on central nervous system vascular endothelial cells promotes lymphocyte extravasation in experimental autoimmune encephalomyelitis." J Biol Chem **287**(40): 33237-33251.
- Wolff, M. J., J. M. Leung, M. Davenport, M. A. Poles, I. Cho and P. Loke (2012). "TH17, TH22 and Treg cells are enriched in the healthy human cecum." PLoS One **7**(7): e41373.
- Wolinsky, J. S., P. A. Narayana, P. O'Connor, P. K. Coyle, C. Ford, K. Johnson, A. Miller, L. Pardo, S. Kadosh, D. Ladkani and P. R. T. S. Group (2007). "Glatiramer acetate in primary progressive multiple sclerosis: results of a multinational, multicenter, double-blind, placebo-controlled trial." Ann Neurol **61**(1): 14-24.
- Wu, C., N. Yosef, T. Thalhamer, C. Zhu, S. Xiao, Y. Kishi, A. Regev and V. K. Kuchroo (2013). "Induction of pathogenic TH17 cells by inducible salt-sensing kinase SGK1." Nature **496**(7446): 513-517.
- Yadav, S. K., S. Boppana, N. Ito, J. E. Mindur, M. T. Mathay, A. Patel, S. Dhib-Jalbut and K. Ito (2017). "Gut dysbiosis breaks immunological tolerance toward the central nervous system during young adulthood." Proc Natl Acad Sci U S A **114**(44): E9318-E9327.
- Zepp, J., L. Wu and X. Li (2011). "IL-17 receptor signaling and T helper 17-mediated autoimmune demyelinating disease." Trends Immunol **32**(5): 232-239.
- Zhang, J., S. Markovic-Plese, B. Lacet, J. Raus, H. L. Weiner and D. A. Hafler (1994). "Increased frequency of interleukin 2-responsive T cells specific for myelin basic protein and proteolipid protein in peripheral blood and cerebrospinal fluid of patients with multiple sclerosis." J Exp Med **179**(3): 973-984.

ABBREVIATIONS

APC	Antigen Presenting Cell
BBB	Blood Brain Barrier
CaM	Calmodulin
CD	Cluster of Differentiation
CFP	Cyan Fluorescent Protein
CNS	Central Nervous System
CRAC	Calcium-Release-Activated Calcium
DAG	Diacylglycerol
DC	Dendritic Cell
DMEM	Dulbecco's Modified Eagle Medium
DMSO	Dimethyl Sulfoxide
EAE	Experimental Autoimmune Encephalomyelitis
EDTA	Ethylenediaminetetraacetic Acid
EH	Eagle's HEPES
ER	Endoplasmic Reticulum
FACS	Fluorescence-Activated Cell Sorting
FOXP3	Forkhead Box Protein P3
FRET	Förster/Fluorescence Resonance Energy Transfer
G proteins	GTP-binding proteins
GALT	Gut Associated Lymphoid Tissue
GFP	Green Fluorescent Protein
GM-CSF	Granulocyte Macrophage Colony Stimulating Factor

HEPES	4-(2-hydroxyethyl)-1-piperazineethanesulfonic acid
HLA	Human Leukocyte Antigens
IFN γ	Interferon Gamma
Ig	Immunoglobulin
IL	Interleukin
ILC	Innate Lymphoid Cell
i.v.	Intravenous
iGB	<i>in-vitro</i> -induced Germinal Centre B cell
IP3	inositol-1,4,5-trisphosphate
LP	Lamina Propria
MAG	Myelin Associated Glycoprotein
MBP	Myelin Basic Protein
MHC	Major Histocompatibility Complex
MOG	Myelin Oligodendrocyte Glycoprotein
MS	Multiple Sclerosis
NFAT	Nuclear Factor of Activated T cells
NF- κ B	Nuclear Factor kappa B
NS	Not Significant
PBS	Phosphate Buffered Saline
PCR	Polymerase Chain Reaction
pDC	Plasmacytoid Dendritic Cell
PFA	Paraformaldehyde
PLC	Phospholipase C
PLP	Myelin Proteolipid Protein

PMA	Phorbol 12-Myristate 13-Acetate
PP	Peyer's Patch
PPMS	Primary Progressive Multiple Sclerosis
RFP	Red Fluorescent Protein
RRMS	Relapsing Remitting Multiple Sclerosis
SFB	Segmented Filamentous Bacteria
SGK	Serine/threonine-protein Linase
SILT	Solitary Isolated Lymphoid Tissue
SP	Spleen
SPMS	Secondary Progressive Multiple Sclerosis
STIM1	Stromal Interaction Molecule 1
TCM	T Cell Medium
TCR	T Cell Receptor
TGF	Transforming Growth Factor
Th	T helper
TnC	Troponin C
Treg	T Regulatory Cell
YFP	Yellow Fluorescent Protein

CURRICULUM VITAE

PING FANG (房萍)

Education

Ludwig-Maximilians University, Germany, Neuroimmunology Ph.D candidate (Expect to finish on 2018.6)	2013.8 – present
Shantou University, China, Biochemistry and Molecular Biology Master degree	2010.9 – 2013.6
Sun Yat-Sen University (Zhongshan University), China, Bioscience Bachelor degree	2005.9 – 2009.7

Reserch Experiences

<u>Two-photon imaging of encephalitogenic T cells in the small intestine</u> Supervisor: Naoto Kawakami/Hartmut Wekerle	2013.8 – present
The involvements of HMGB1 in neuroregeneration after spinal cord injury Supervisor: Yan-Qin Shen/Melitta Schachner	2010.9 – 2013.6
The function of a short peptide of L1-cam on promoting of neurite outgrowth Supervisor: Wei-Jiang Zhao/Melitta Schachner	2011.3 – 2013.6

Publications

- Ping Fang, Ingo Bartholomäus, Nikolaos I. Kyratsous, Isabel J. Bauer, Hartmut Wekerle and Naoto Kawakami. Two-photon imaging of encephalitogenic T cells in the gut associated lymphoid tissue. *In preparation*
- Nikolaos I. Kyratsous, Isabel J. Bauer, Guokun Zhang, Marija Pesic, Ingo Bartholomäus, Marsilius Mues, **Ping Fang**, Miriam Wörner, Stephanie Everts, Joachim W. Ellwart, Joanna M. Watt, Barry V. L. Potter, Reinhard Hohlfeld, Hartmut Wekerle and Naoto Kawakami. (2017) Visualizing context-dependent calcium signaling in encephalitogenic T cells in vivo by two-photon microscopy, *Proc Natl Acad Sci U S A*, 114(31):E6381-E6389
- **Ping Fang**, Hong-Chao Pan, Stanley Li Lin, Wen-Qing Zhang, Heikki Rauvala, Melitta Schachner and Yan-Qin Shen. (2014) HMGB1 Contributes to Regeneration After Spinal Cord Injury in Adult Zebrafish, *Molecular Neurobiology*, 49(1): 472-483
- **Ping Fang**, Melitta Schachner, Yan-Qin Shen. (2012) HMGB1 in development and diseases

of the central nervous system, *Molecular Neurobiology*, 45(3):499-506

- **Ping Fang**, Jin-Fei Lin, Hong-Chao Pan, Yan-Qin Shen, Melitta Schachner (2012) A Surgery Protocol for Adult Zebrafish Spinal Cord Injury, *Journal of Genetics and Genomics*, 39:481-487
- XIE Lin, **FANG Ping**, LIN Jin-Fei, PAN Hong-Chao, ZHANG Fan, SHEN Yan-Qin (2013) The expression of gdnf and nos in adult zebrafish brain during the regeneration after spinal cord injury, *Yi Chuan*, 35(4):495-501

Experimental Skills

Two photon microscopy	Confocal microscopy
Flow cytometry	Retroviral transduction
Primary lymphocytes culture	Cell line culture
Histology	Plasmid construction
Quantitative-PCR	Western Blotting
In situ hybridization	Cell viability test
Primary culture for rodent hippocampal neurons and granule cells and etc.	
· Animal model:	Experimental autoimmune encephalomyelitis model
	Lymphatic cannulation
	Spinal cord injury
	Other operation of in vivo experiments on mouse and zebrafish

Awards

National scholarship for graduate students	2013.5
Excellent graduate student rewards in Shantou University Medical College	2012.11

Conference Presentations

Midwinter Conference : Advances in Immunobiology, Austria	2017.1
<i>Poster presentation: Intravital imaging of encephalitogenic T cells in the GALT</i>	
Multiple Sclerosis SFB/CRC-TR 128, Germany	2016.3
<i>Poster presentation: Dynamics, local specification and adaptive regulation of phagocyte phenotypes in the course of neuroinflammation</i>	

Languages

Chinese: Native speaker
English: Fluent
German: Basic

ACKNOWLEDGMENTS

First and foremost, I would like to thank my Ph.D. supervisor Dr. Naoto Kawakami for providing me the great opportunity to work on this exciting project in his lab. Not only has he guided me in finishing this Ph.D. project, but also inspired and motivated me to further explore scientific questions. Dr. Naoto Kawakami is an excellent teacher who sets a good example of diligence and perseverance. He is always patient and lent me full support to overcome difficulties. I hereby deeply appreciate his guidance and his efforts.

I also want to express my gratitude to Prof. Hartmut Wekerle for the opportunity of studying in Germany and precious suggestions during the whole course of my Ph.D. study. He is an experienced and venerable scientist.

Additionally, I would like to kindly thank Dr. Marija Pesic for showing me the two-photon microscopy, Dr. Ingo Bartholomäus for helping me establish the setup of intestine imaging, Ms. Isabel Bauer and Ms. Mary Claire Tuohy for correcting the writing of my thesis and being such great friends who make this journey joyful. Besides, I would like to acknowledge former and current colleagues in the institute: Nikos, Michalis, Sabine, Qingqing, Stephan, Caterina, Lian and many others.

Especially, my sincere gratitude goes to my parents in China who are treasures of my life. Thanks for their supports and understanding.

Last but not least, I would like to thank my husband Dr. Kai Li, for sharing this wonderful experience with me in Munich, for his constant support and love.